Observability-Based Approach to Design, Analysis and Optimization of Dynamical Systems

Atiye Alaeddini

A dissertation
submitted in partial fulfilment of the
requirements for the degree of

Doctor of Philosophy

University of Washington

2016

Reading Committee:

Kristi Morgansen, Chair

Bechet Acikmese

Mehran Mesbahi

Juris Vagners

Program Authorized to Offer Degree:
Aeronautics and Astronautics

University of Washington

Abstract

Observability-Based Approach to Design, Analysis and Optimization of Dynamical Systems

Atiye Alaeddini

Chair of the Supervisory Committee:
Kristi Morgansen
William E. Boeing Department of Aeronautics and Astronautics

The present dissertation aims to use the coupling between actuation and sensing in nonlinear systems to alternatively design a set of feasible control policies, to find the minimum number of sensors, or to find an optimal sensors configuration. Feasibility, here, means a combination of sensory system and control policy which guarantees observability. In some cases the optimality of the obtained solution is also considered. In some nonlinear systems, full observability requires active sensing, and will be shown how control policies that guarantee observability can be obtained by considering the geometry of the system dynamics. The observability matrix is used to test observability, whereas for the optimization problem observability Gramian matrix is used. This dissertation also considers the stability in designing controllers. The problem of designing a stabilizing control policy for a control-affine nonlinear system is addressed. The effect of time-varying control on the observability is investigated and shown to potentially improve the system observability.

A particular application of the techniques considered here is the problem of designing network sensing and topology based on the observability criteria. The goal is to develop a protocol for the network which guarantees privacy. Furthermore, given a network of connected agents, we would like to determine which nodes should be observed to maximize information about the entire network. This dissertation begins with theoretical basis then moves towards applications of the theory. The first application is navigation of an autonomous ground robot with limited inertial sensing, motivated by the visuomotor system of insects. The second application is the problem of detecting an epidemic disease, which demonstrates design of an observability-based optimal network.

TABLE OF CONTENTS

LIST OF FIGURES

LIST OF TABLES

ACKNOWLEDGMENTS

Firstly, I would like to express my sincere gratitude to my advisor Professor Kristi Morgansen for the continuous support of my Ph.D. study and related research. Her guidance helped me in all the time of research and writing of this dissertation.

Besides my advisor, I would like to thank the rest of my dissertation committee for their insightful comments and encouragement. In particular, I am grateful to Professor Mehran Mesbahi for his insightful comments and constructive criticisms on my research, valuable discussions and accessibility

I would also like to thank all of the members of NDCL with whom I have interacted during the course of my graduate studies.

Last but not the least, I would like to thank my family: my parents and to my brother and sister for supporting me spiritually throughout writing this thesis and throughout my life in general.

DEDICATION

I dedicated this to my parents without whom it was impossible for me to complete this work.

Chapter 1

INTRODUCTION

Knowing the system state is necessary to solve many control theory problems. In most practical cases, all physical states of the system cannot be determined by direct observation. Instead, indirect effects of the internal states are observed by the sensors. Broadly, the proposed research is concerned with the analysis, design, and optimization of finite-dimensional control-affine nonlinear dynamical systems. A major focus area involves the optimization and qualitative assessment of a well known quality of dynamical systems, called *observability*, from a design point of view. At this point, we need to define this property of the control systems. If a system is observable, it is possible to fully reconstruct the system state from its output measurements. To ensure that the sensor measurements provide enough information for state estimation, the observability of system dynamics must be evaluated. In this dissertation, we are interested in understanding and characterizing the control inputs required to be actuated and the states required to be measured to ensure observability. Particularly, the goal is identifying the critical system locations to be monitored and controlled, and in the case of multi-agent systems, required data exchange topology between the local components.

There are some common tests for determining observability of a system. In the case of linear systems, the system is either perfectly observable or unobservable. There are well defined observability tests working very well for linear systems, but not always for nonlinear systems. To benefit these elegant tools, and for the sake of simplicity, we linearize nonlinear systems to analyze their behaviour. But this linearized model does not always describe all characteristics of the original system. For instance, if the operating conditions of the dynamical system change significantly, the analysis of the linearized model may not adequately capture the input-output behaviour of the system over the whole operating region. An example of such systems are nonholonomic systems. These systems cannot be studied using the usual linear control techniques.

One of the properties of a nonlinear system that might be lost in linearization is observability. Linearisation of a nonlinear system should be done about a fixed point or a nominal trajectory. In

either case, observability of the obtained linearized system does not depend on control input. It is worthy to note, here, that in the case of nonlinear systems, observation and actuation are coupled, which means we might be able to make a system observable by changing control inputs. This coupling makes the problem of control design of nonlinear systems a challenging problem. Besides all other criteria needed to be considered in designing controller, for nonlinear systems, we also need to consider observability of the resulting system.

In this research, we study the observability of dynamical systems in two levels. First, observability of a dynamic system is investigated as a single entity, and at the next step, we study the observability of a group of dynamical systems connected to each other through some type of a network. The problem of observability-based design of a network of dynamical system has two facets. In most cases, a more observable design is desired. Particularly for a large-scale network with some interconnected physical dynamics, identifying the smallest number of sensors required to ensure proper system monitoring is critical. We provide an application of the developed framework on the problem of detecting an epidemic disease outbreak. However, there are some situations in designing a network where increasing observability is undesirable. For instance, when different agents exchange sensitive data, and an intruder tries to steal the information of the network, one of the main concerns is ensuring that privacy is kept. We tackle this issue in this dissertation, and propose a topology of interaction which minimizes observability, that results in minimization of the data being exposed to the foreigner. Examples where this design can be applied include social networks such as Facebook.

1.1 Brief Review of Relevant Literature

As mentioned above, one approach for investigating the observability of a nonlinear system is using a linearized model of the system and implementing the linear observability tests [1]. The most common scalar observability measures for linear systems are described in [2]. The problem of using conventional tests for checking the observability of linear systems is that they do not give any information regarding the effect of control on improving the observability. Unlike conventional linear observability tests, the Lie algebraic tools allow us to investigate the effect of control on observability [3–6].

One place we encounter observability-based design is the problem of optimal sensor location. Some examples of this type of research are [7–10]. In these works, observability evaluation of the system has been done by a measure of observability used for linear systems. Because of the coupling between actuation and sensing in nonlinear systems, observability measures can be used conversely to find either optimal sensor placements for a given set of control inputs, or to find control inputs that guarantee observability for a given sensor location [11]. Localization of a robot in an unknown environment is an example of observability-based controller design. In this case a robot is exploring an unknown unstructured environment, and needs to be able to estimate its own states, or estimate some other parameters, for instance, wind velocity. Some researchers have considered this problem for a specific case. Some examples of observability-based path planning algorithm are developed in [12–15]. In addition, the problem of avoiding poorly observable trajectories has recently been examined by researchers [16], in which the observability of a nominal trajectory are computed as a quantitative measure, and the trajectories with undesired observability quantity are avoided. The goal of this dissertation is developing an algorithm that evaluates a qualitative measure of observability that is applicable to a larger family of dynamical systems.

The author of this dissertation found out that observability and stability often act against each other. When we maximize the observability of a system, we are basically increasing the output energy, which in many cases makes the system unstable. Therefore, in this research, stability of the system is considered in designing of an observability-based optimal control. The study of stabilizing controller design for nonlinear systems has been the subject of intense research; including model predictive control (MPC) [17], feedback passivation [18], nonlinear optimal control [19], time varying Lyapunov methods [20, 21], and stabilizing control of nonholonomic systems [22–25].

Observability-based design of a multi-agent network can be found in some recent works such as [26–29]. The concept of observability has been used in multi-robot localization [30–33], social networks [34], electric power grid management [35], and biological systems [36–38]. We will specifically study the problem of privacy guarantees in networks. Protocols with privacy guarantees have been previously addressed [39–42], where they commonly consider injection of random offsets into the states of the agents. Among the many research efforts aimed at network privacy, the authors of [43] considered the connection between privacy in a network and the observability of the network. Distributed protocols in network design are very critical. In some sensitive applications, agents pre-

fer not to share their data with remote centres because of privacy and secrecy considerations. The authors of [44] argued that distributed optimization methods improves privacy-preserving properties. Decentralized control theory has attracted several researchers, and several methodologies have been proposed, see for instance [45].

The problem of optimal placement of sensors in a network is also studied in this dissertation. Numerous applications including field surveillance, environmental study, and geo-scientific exploration employ distributed sensor networks for wide area monitoring. The notion of an observable distributed sensor network has already been introduced in [46], where necessary conditions to ensure observability of the network are given in terms of graph partitions, though it is assumed that the dynamics of each node in the network are termed linear dynamics. Here, we introduce a method to design most observable multi-agent networks. By observability we mean the property satisfied by a network that we can infer states information about all the agents, where the agents are sharing partial information via a given graph communication topology. The results obtained are illustrated with two examples: the first example considers the virus spreading processes in a network [47], and the second example is a model of a genetic system [48].

1.2 Contribution of this Research

In this dissertation, we bring together control and optimization into a single framework, which allows us to solve the sparsest sensing configuration and control configuration selection efficiently, while empowering us with insights to later characterize other design problems, such as observability-based optimal path planning, and optimal sensor placement. In fact, the insights allows us to bridge from pure theoretical problems towards these applications: privacy guarantees in a networks, most efficient way of an epidemic detection in a community, and optimal trajectory generation for robotic navigation with limited sensing equipment. The present dissertation not only provides us with necessary conditions of having an observable system, but also suggests an optimal design for a considerable class of nonlinear systems.

This dissertation starts with investigation of the coupling between actuation and sensing. We propose the minimum configurations of state variables that needed to be actuated by inputs to achieve observability. At the next step, we introduced an optimal control problem which specif-

ically considers the observability of the obtained solution, while the stability of the closed loop system is guaranteed. The main contribution of this section is presenting a joint solution to the stability of the system, as an asymptotic behaviour, on one hand, and the observability of the system, as a transient behaviour, on the other hand. Later in this dissertation, we provide a systematic method to obtain the minimal sensors placement configuration. The proposed solutions apply under arbitrary nonlinear dynamics of the agents in the network where they only share partial information with their neighbours. This framework is particularly applicable to sensor topology design in large-scale networks, where all states of the individual agents in a network are not diffusive. For instance, we study a biological model of cellular behaviour, where inter-cellular interactions happens through protein concentration, which is the only diffusive quantity in inter-cellular connection. And lastly, we propose an observability-based design of communication topology in the network which improves the privacy in the network whenever the network is threatened by an external agent. This adaptive network responds to this attack by changing the topology of the network online to reduce the information being exposed to the external agent.

The present dissertation can be summarized in four steps as follows:

I Investigate the required control to ensure observability

II Investigate the control to maximize observability

III Investigate the control to maximize observability and ensure stability

IV Observability-based design of a network of a system of connected agents

The study of part I, which mostly relies on obtaining the control required to ensure observability is discussed in Chapter 3. Part II is discussed in Chapter 4, where, a cost function is introduced that consists of a term to maximize observability. Preliminary studies of part III are also discussed in this chapter, where, a recursive algorithm has been proposed to obtain an optimal state feedback control to maximize a non-quadratic cost functional. Until this point, it is assumed that the control is static state feedback ($\mathbf{u} = \mathbf{u}(\mathbf{x})$), which cannot be applied for all nonlinear systems. To solve this optimal control policy for all nonlinear systems, such as nonholonomic systems, Chapter 5 discusses the general case of time varying state feedback control ($\mathbf{u} = \mathbf{u}(\mathbf{x}, t)$). Part IV concerns the nonlinear

observability analysis of a group of dynamical systems. The observability-based design is expanded to multi-agent structure in Chapter 6, to study design of a network considering the observability of network. In Chapter 7, the problem of vision-based navigation of a robot is discussed as the first application. Another application regarding the implementation of the results of the observability-based network design is discussed in Chapter 8.

Chapter 2

BACKGROUND ON OBSERVABILITY

Observability, the feasibility of reconstructing system states from a time history of sensor outputs, is essential in the design of control systems. Technically, if a satisfactory estimator can be constructed, one does not actually need to check the observability of a system. However, in many cases, tests of observability can reveal useful information about system structure that can be leveraged to design more effective or more efficient estimators. For example, some choices of sensor placement may lead to faster estimator convergence times [7].

2.1 Definition of Observability

Consider a nonlinear system given by:

$$\Sigma_1 : \begin{cases} \dot{\mathbf{x}} = \mathbf{f}(\mathbf{x}, \mathbf{u}), \;\; \mathbf{x} \in \mathbb{R}^n, \;\; \mathbf{u} \in \mathbb{R}^p \\ \mathbf{y} = \mathbf{h}(\mathbf{x}), \;\; \mathbf{y} \in \mathbb{R}^m. \end{cases} \tag{2.1}$$

In such systems, $\mathbf{x}$ is referred to as the states of the system, $\mathbf{u}$ is referred to control or input, and $\mathbf{h}(\mathbf{x})$ is termed the observation.

As in [5], points $\mathbf{x}^0$, $\mathbf{x}^1 \in \mathbb{R}^n$ are called indistinguishable ($\mathbf{x}^0 I \mathbf{x}^1$) if the output functions $\mathbf{h}(\mathbf{x}(t, \mathbf{x}^0))$ and $\mathbf{h}(\mathbf{x}(t, \mathbf{x}^1))$ for initial states $\mathbf{x}^0$ and $\mathbf{x}^1$ are identical on their common domain of definition for every admissible input. The system Σ_1 is said to be *observable at* $\mathbf{x}^0$ if $(\mathbf{x}^0 I \mathbf{x}^1) \Rightarrow \mathbf{x}^1 = \mathbf{x}^0$, and the system is *observable* if it is observable at all $\mathbf{x}^0 \in \mathbb{R}^n$. This last definition of observability is a global concept. The system Σ_1 is *locally observable at* $\mathbf{x}^0$ if for every open neighbourhood U of $\mathbf{x}^0$, one can distinguish $\mathbf{x}^0$ from all other $\mathbf{x} \in U$, and it is *locally observable* if it is locally observable at every $\mathbf{x}^0 \in \mathbb{R}^n$. The system is locally observable if the map $\mathbf{x}^0 \rightarrow \mathbf{y}(t), t \in (0, \infty)$ is locally one-to-one. The system is *short time locally observable* if the map $\mathbf{x}^0 \rightarrow \mathbf{y}(t), t \in (0, T)$ is locally one-to-one for any $T > 0$. Intuitively, a system is short time locally observable if one can distinguish each of its states from those of its neighbours using the observation

$\mathbf{h}(\mathbf{x})$ and the time derivatives of $\mathbf{h}(\mathbf{x})$. Notice that this definition of observability does not imply that every input function distinguishes between two points. For linear systems, one can show that if some input distinguishes between two initial states then every input will do so [49].

2.2 Testing Observability

For linear time invariant systems of the form

$$\begin{aligned} \dot{\mathbf{x}} &= A\mathbf{x} + B\mathbf{u} \\ \mathbf{y} &= C\mathbf{x}\,, \end{aligned} \tag{2.2}$$

the observability test can be stated in the following form:

$$\text{rank}(O) = n, \tag{2.3}$$

where

$$O = \begin{bmatrix} C \\ CA \\ \vdots \\ CA^{n-1} \end{bmatrix}, \tag{2.4}$$

is the observability matrix.

Given the nonlinear system, Σ_1 in (2.1), one can linearize the nonlinear system about a given nominal trajectory $\mathbf{x}_d(t)$ with associated nominal controls $\mathbf{u}_d(t)$, the linearization of this system is given by

$$\delta\dot{\mathbf{x}} = F(t)\delta\mathbf{x} + G(t)\delta\mathbf{u}, \;\; \delta y = H(t)\delta\mathbf{x}, \tag{2.5}$$

where

$$F(t) = \left.\frac{\partial \mathbf{f}}{\partial \mathbf{x}}\right|_{\mathbf{x}=\mathbf{x}_d,\mathbf{u}=\mathbf{u}_d}, \;\; G(t) = \left.\frac{\partial \mathbf{f}}{\partial \mathbf{u}}\right|_{\mathbf{x}=\mathbf{x}_d,\mathbf{u}=\mathbf{u}_d}, \;\; H(t) = \left.\frac{\partial \mathbf{h}}{\partial \mathbf{x}}\right|_{\mathbf{x}=\mathbf{x}_d}. \tag{2.6}$$

The Jacobian matrices F, G, and H are evaluated at the points along the nominal trajectory and control, $\mathbf{x}_d$ and $\mathbf{u}_d$. The linearized observability matrix is then given by

$$O(t) = \begin{bmatrix} N_0(t) \\ N_1(t) \\ \vdots \\ N_{n-1}(t) \end{bmatrix}, \tag{2.7}$$

where,

$$N_0(t) = H(t), \;\; N_{m+1}(t) = N_m(t)F(t) + \frac{d}{dt}N_m(t), \;\; m = 0, 1, \cdots, n-1. \tag{2.8}$$

The linearized system is *observable* at t_0 if there exists a finite $t_1 > t_0$ such that the matrix $O(t_1)$ is full rank [50]. Failure to satisfy the linear observability test does not preclude observability for a nonlinear system, but alternative methods must be used to explore nonlinear observability.

In order to determine nonlinear observability without linearization, an observability analysis based on time derivatives of the system output can be used. These time derivatives can be expressed using Lie derivatives of the output for continuous [5] and discrete systems [51].

In this dissertation, the formulation are developed for a specific class of nonlinear systems called control affine form, except otherwise stated. A nonlinear system in control affine form is given by:

$$\Sigma_2 : \begin{cases} \dot{\mathbf{x}} = \mathbf{f}_0(\mathbf{x}) + \sum_{i=1}^{p} \mathbf{f}_i(\mathbf{x})u_i, \;\; \mathbf{x} \in \mathbb{R}^n, \\ \mathbf{y} = \mathbf{h}(\mathbf{x}), \;\; \mathbf{y} \in \mathbb{R}^m. \end{cases} \tag{2.9}$$

In such systems, $\mathbf{f}_0(\mathbf{x})$ is referred to as the drift vector field or simply drift, $\mathbf{f}_i(\mathbf{x})$ are termed control vector fields.

For a nonlinear system in control affine form, by definition, the zeroth order Lie derivative of (scalar) function $h_k = \mathbf{h}[k]$ is the function itself, i.e. $L^0_{\mathbf{f}} h_k = h_k$. The order n Lie derivative of function h_k with respect to $\mathbf{f}_i$ is defined as

$$L^n_{\mathbf{f}_i} h_k = \frac{\partial (L^{n-1}_{\mathbf{f}_i} h_k(\mathbf{x}))}{\partial \mathbf{x}} \mathbf{f}_i.$$

Additionally, mixed Lie derivatives can be constructed. For instance, the second order Lie derivative of h_k with respect to $\mathbf{f}_j$ and $\mathbf{f}_i$ is

$$L^2_{\mathbf{f}_j \mathbf{f}_i} h_k(\mathbf{x}) = L_{\mathbf{f}_j}(L_{\mathbf{f}_i} h_k(\mathbf{x})) = \frac{\partial (L_{\mathbf{f}_i} h_k(\mathbf{x}))}{\partial \mathbf{x}} \mathbf{f}_j(\mathbf{x}).$$

Similar calculations hold for higher order derivatives along mixed vector fields. Given these preliminaries, for a set of piece-wise constant control,

$$u_i(t) = \begin{cases} u_i^1, \;\; t \in [0, t_1) \\ u_i^l, \;\; t \in [t_{l-1}, t_l), \;\; l \geq 2, \end{cases} \tag{2.10}$$

and define the vector fields $\theta_l = \mathbf{f}_0 + \sum_{i=1}^{p} \mathbf{f}_i u_i^l$, then the Lie derivative of the output can be calculated as

$$L_{\mathbf{f}} h_k = L_{\theta_1} \dots L_{\theta_l} h_k(\mathbf{x}). \tag{2.11}$$

Then, the nonlinear observability space is given by

$$\mathcal{O} \equiv \text{span}\left\{ L_{\theta_1} \dots L_{\theta_l} h_k(\mathbf{x}) | l \in \mathbb{N}, 1 \leq k \leq m \right\}. \tag{2.12}$$

Furthermore, the controls can be defined as differentiable functions. In this case, the nonlinear observability space is given by

$$\mathcal{O} \equiv \text{span}\left\{ L_{\mathbf{f}}^l h_k(\mathbf{x}) | l \in \mathbb{N}, 1 \leq k \leq m \right\}. \tag{2.13}$$

The nonlinear observability matrix, or co-distribution, $d\mathcal{O}$ (equation (3.74) in [49]), is then given by

$$d\mathcal{O}(\mathbf{x}) = \text{span}\left\{ d\mathbb{H}(\mathbf{x}) | \mathbb{H} \in \mathcal{O} \right\}, \quad \mathbf{x} \in \mathbb{R}^n. \tag{2.14}$$

Definition 1. *(Observability rank condition [49]) If the nonlinear observability matrix, $d\mathcal{O}$, of the nonlinear system* (2.1) *is full rank at some state $\mathbf{x}^0$, then the system is locally observable at $\mathbf{x}^0$.*

A second type of observability space is introduced by Wang and Sontag in [52] as

$$\mathcal{O} \equiv \text{span}\left\{ \frac{d^l}{dt^l} h_k(\mathbf{x}) | l \geq 0, 1 \leq k \leq m \right\}, \tag{2.15}$$

and proved that (2.13) and (2.15) are equivalent. The second representation (2.15) is in fact the span of all time derivatives of output function $\mathbf{h}$ along all possible trajectories (all possible nominal trajectories corresponding to all possible control policies).

Now, for control inputs given as differentiable functions, let the control $\mathbf{u}$ and its derivative be $\dot{\mathbf{u}}$ with $\dot{\mathbf{u}} \in \mathbb{R}^p$. In this case the Lie derivative operator is defined as

$$L_{\mathbf{f}} = \sum_{i=1}^{n} f_i \frac{\partial}{\partial x_i} + \sum_{i=1}^{p} \dot{u}_i \frac{\partial}{\partial u_i} \tag{2.16}$$

where, $f_i = \mathbf{f}[i]$ is the ith component of vector $\mathbf{f}$. Using the Lie derivative operator defined in (2.16),

the output component, $y_k = \mathbf{h}[k]$, and its time derivatives of nonlinear system (2.9), are given by

$$\begin{aligned}
y_k^{(0)} &= h_k \\
y_k^{(1)} &= L_{\mathbf{f}} h_k = \frac{\partial h_k}{\partial \mathbf{x}} \mathbf{f}_0 + \sum \frac{\partial h_k}{\partial \mathbf{x}} \mathbf{f}_i u_i \\
y_k^{(2)} &= L_{\mathbf{f}} L_{\mathbf{f}} h_k = \frac{\partial}{\partial \mathbf{x}} \left(\frac{\partial h_k}{\partial \mathbf{x}} \mathbf{f}_0 \right) \mathbf{f}_0 + \sum \frac{\partial}{\partial \mathbf{x}} \left(\frac{\partial h_k}{\partial \mathbf{x}} \mathbf{f}_i \right) \mathbf{f}_i u_i + \ldots + \sum \frac{\partial h_k}{\partial \mathbf{x}} \mathbf{f}_i \dot{u}_i \\
y_k^{(3)} &= L_{\mathbf{f}} L_{\mathbf{f}} L_{\mathbf{f}} h_k = \frac{\partial}{\partial \mathbf{x}} \left[\frac{\partial}{\partial \mathbf{x}} \left(\frac{\partial h_k}{\partial \mathbf{x}} \mathbf{f}_0 \right) \mathbf{f}_0 \right] \mathbf{f}_0 + \sum \frac{\partial}{\partial \mathbf{x}} \left[\frac{\partial}{\partial \mathbf{x}} \left(\frac{\partial h_k}{\partial \mathbf{x}} \mathbf{f}_0 \right) \mathbf{f}_0 \right] \mathbf{f}_i u_i + \cdots \\
&\quad \cdots + \sum \frac{\partial}{\partial \mathbf{x}} \left(\frac{\partial h_k}{\partial \mathbf{x}} \mathbf{f}_i \right) \dot{u}_i \\
&\quad \vdots
\end{aligned} \tag{2.17}$$

As it can be seen, the control, $\mathbf{u}$, as well as the derivative of control, $\dot{\mathbf{u}}$, might help to expand the span of the observability space and as a result improve the observability of the system. One example is given here

$$\begin{cases}
\dot{x}_1 = u_1 \\
\dot{x}_2 = u_2 \\
\dot{x}_3 = u_1 x_2 - u_2 x_1 \\
y = x_3.
\end{cases} \tag{2.18}$$

The Jacobian matrix is

$$d\mathcal{O} = \begin{bmatrix} dy \\ d\dot{y} \\ d\ddot{y} \end{bmatrix} = \begin{bmatrix} 0 & 0 & 1 \\ -u_2 & u_1 & 0 \\ -\dot{u}_2 & -\dot{u}_1 & 0 \end{bmatrix}. \tag{2.19}$$

The rank of this matrix depends on the control $\mathbf{u}$ and its time derivative $\dot{\mathbf{u}}$.

The observability Lie algebra, $\mathcal{O}$, includes the Lie derivatives of the output function $\mathbf{h}(\mathbf{x})$ with respect to both the drift vector field and the control vector fields. The spatial derivatives with respect to each vector field generate rows of the matrix $d\mathcal{O}$. If the system satisfies the observability rank condition at every $\mathbf{x} \in \mathbb{R}^n$, then it is short time locally observable. If the system fails to satisfy the observability rank condition on an open subset of $\mathbb{R}^n$, then it is not short time locally observable. More details on the observability of the nonlinear systems can be found in [53].

2.3 Evaluating Observability

Another tool for evaluating the observability is observability Gramian. For a linear system (2.2), the observability Gramian [8],

$$W_{o,L} = \int_0^{t_f} e^{A^T t} C^T C e^{At} \mathrm{d}t \,, \tag{2.20}$$

can be computed to evaluate the observability of a linear system. A linear system is fully observable if and only if the corresponding observability Gramian is full rank [2]. If the observability Gramian is rank deficient, some of the states (or directions in the state space) cannot be reconstructed from the sensors data, regardless of the control policy being applied.

As it was explained, we can use the local linear approximation system around the state trajectory $\mathbf{x}_d(t)$ and output trajectory $\mathbf{y}_d(t)$. To measure the observability, the local observability Gramian, $W_o(\mathbf{x}_d)$, is computed, which is the observability Gramian over $[0, t_f]$ of the linear approximation of (2.5). If $\Phi(t)$ is the state transition matrix of the linearized system, then the local observability Gramian is

$$W_o(\mathbf{x}_d) = \int_0^{t_f} \Phi^T(t) H^T(t) H(t) \Phi(t) \mathrm{d}t \,. \tag{2.21}$$

This formulation requires computation of Jacobian matrices. The observability Gramian for nonlinear systems can also be obtained from the solution of the Lyapunov measure equation [54].

Theorem 1. *Maximizing a norm of the observability Gramian matrix is equivalent to minimizing the error of the estimation for a linear system, which is independent from the estimation method.*

Proof. Assume that the measurement vector is a linear combination of the states, with the addition of zero mean Gaussian noise given by $\tilde{\mathbf{y}} = C\mathbf{x} + \mathbf{v}$, where, $\mathbf{v} \in \mathbb{R}^m$ is a vector of zero mean Gaussian random variables with covariance $\mathbb{E}\left[\mathbf{v}\mathbf{v}^T\right] = \sigma I$. It is assumed that errors are independent and identically distributed. To find the optimal estimation of the initial state $\mathbf{x}_0$ from noisy measurements $\tilde{\mathbf{y}}$, $t(0) \leq t \leq t(N), N > n$, the following least squares optimization problem should be solved [55]:

$$\begin{aligned} &\underset{\mathbf{x}_0}{\text{minimize}} \quad \|\mathbf{e}\|_{L^2}^2 \\ &\text{subject to} \quad \tilde{\mathbf{y}}(t(i)) = Ce^{At(i)}\hat{\mathbf{x}}_0 + \mathbf{e}(t(i)), \;\; i = 0, ..., N \,, \end{aligned} \tag{2.22}$$

where $\|X\|_{L^2} = \left(\int_0^{t_f} |X(t)|^2 \, \mathrm{d}t \right)^{\frac{1}{2}}$. Using measurements $\tilde{\mathbf{y}}(t(i))$, $t(0) \leq t \leq t(N)$ and a least

squares approach, the optimal initial state estimate, $\hat{\mathbf{x}}_0^*$, is given by

$$\left(\begin{bmatrix} e^{A^T t(0)} C^T & \dots & e^{A^T t(N)} C^T \end{bmatrix} \begin{bmatrix} Ce^{At(0)} \\ \vdots \\ Ce^{At(N)} \end{bmatrix} \right)^{-1} \begin{bmatrix} e^{A^T t(0)} C^T & \dots & e^{A^T t(N)} C^T \end{bmatrix} \begin{bmatrix} \tilde{\mathbf{y}}(t(0)) \\ \vdots \\ \tilde{\mathbf{y}}(t(N)) \end{bmatrix}. \tag{2.23}$$

Using the definition of the observability Gramian for the linear systems, given in (2.20), the minimum variance estimate is given by

$$\hat{\mathbf{x}}_0^* = (W_{o,L})^{-1} \left(\sum_{i=1}^{N} e^{A^T t(i)} C^T \tilde{\mathbf{y}}(t(i)) \right). \tag{2.24}$$

Considering that the errors are independent, computing the estimation covariance results in

$$E\left\{ (\hat{\mathbf{x}}_0^* - \mathbf{x}_0)(\hat{\mathbf{x}}_0^* - \mathbf{x}_0)^T \right\} = \sigma W_{o,L}^{-1}. \tag{2.25}$$

Therefore, it is clear that by maximizing a norm of $W_{o,L}$, we would be able to minimize the estimation covariance. □

Consider a smooth nonlinear system (2.1). Given $\epsilon > 0$, let E be the minimum value from the following minimization problem

$$\begin{aligned} E = \min_{\hat{\mathbf{x}}} \quad & \|\mathbf{h}(\hat{\mathbf{x}}) - \mathbf{h}(\mathbf{x})\|_{L^2} \\ \text{subject to} \quad & \|\hat{\mathbf{x}}_0 - \mathbf{x}_0\|_2 = \epsilon \end{aligned} \tag{2.26}$$

The ratio $\dfrac{\epsilon}{E}$ measures the unobservability of initial state $\mathbf{x}_0$. This measure is independent of the estimation method. Note that E can be infinite if the system is unstable.

Theorem 2. *Minimization of the measure the unobservability,* $\dfrac{\epsilon}{E}$ *as defined in* (2.26)*, for a linear system* (2.2) *is equivalent to maximization of the minimum eigenvalue of the observability Gramian.*

Proof. Without loss of generality, assume $\mathbf{h}(0) = \mathbf{0}$. The amount of output energy generated by $\hat{\mathbf{x}}_0$, where $\|\hat{\mathbf{x}}_0\|_2 = \epsilon$, is defined as

$$E(\hat{\mathbf{x}}_0)^2 = \int_0^\infty \|\mathbf{y}(t)\|^2 \, \mathrm{d}t, \;\; \mathbf{x}(0) = \hat{\mathbf{x}}_0. \tag{2.27}$$

Consider $W_{o,L}$ be the observability Gramian given by (2.20), then the output energy is given by

$$E(\hat{\mathbf{x}}_0)^2 = \hat{\mathbf{x}}_0^T W_{o,L} \hat{\mathbf{x}}_0. \tag{2.28}$$

Since $\|\hat{\mathbf{x}}_0\|_2 = \epsilon$, then the measure of unobservability can be written as

$$\frac{\epsilon}{E} = \frac{\epsilon}{\min\limits_{\hat{\mathbf{x}}} \; E(\hat{\mathbf{x}}_0)} = \frac{\epsilon}{\epsilon\sqrt{\lambda_{min}\{W_{o,L}\}}} = \frac{1}{\sqrt{\lambda_{min}\{W_{o,L}\}}}\,. \tag{2.29}$$

therefore, by minimizing the measure of unobservability, we are able to maximize the minimum eigenvalue of the observability Gramian. □

2.3.1 Empirical Observability Gramian

While observability Gramian works very well for determining the observability of the linear system, it may not be very useful for nonlinear system. Calculation of observability Gramian using (2.21) requires computation of Jacobian matrices, and only gives an approximation of the local observability for a specific given trajectory. One alternative method to evaluate observability of a nonlinear system is using the relatively new concepts of the observability covariance or the empirical observability Gramian has been used here [8]. This tool provides a more accurate description of a nonlinear system's observability, while it is much less computationally expensive than some other tools such as Lie algebra based approaches.

For a given small perturbation $\epsilon > 0$ of the state, let $\mathbf{x}_0^{\pm i} = \mathbf{x}_0 \pm \epsilon e^i$ be the initial condition and $\mathbf{y}^{\pm i}(t)$ be the corresponding output, with e^i is the i^{th} unit vector in $\mathbb{R}^n$. For system (2.1), the *empirical observability gramian*, W_o is an $n \times n$ matrix, whose (i, j) component is

$$W_{o_{ij}} = \frac{1}{4\epsilon^2} \int_0^\infty \left(\mathbf{y}^{+i}(t) - \mathbf{y}^{-i}(t)\right)^T \left(\mathbf{y}^{+j}(t) - \mathbf{y}^{-j}(t)\right) \mathrm{d}t. \tag{2.30}$$

It can be shown that if the system is smooth then the empirical observability Gramian converges to the local observability gramian as $\epsilon \to 0$. Note that the perturbation, ϵ, should always be chosen such that system stays in the region of attraction of the equilibrium point of the system.

The largest singular value [7], smallest eigenvalue [8], the determinant [9, 14], and the trace of the inverse [14] of the observability Gramian have been used as measures for observability.

One of the most important applications of the empirical observability Gramian is model reduction of nonlinear systems [56]. The purpose of model reduction is to identify the states (modes) of the system which most affects the sensors and to search for a reduced order state space model in which the dynamics of the original system are contained as much as possible. That is, for a class of input $\mathbf{u}$, we would like the output $\mathbf{y}$ of the original and the reduced order systems to be as close

as possible. Model reduction has been used in several different problems in nonlinear systems optimization to simplify computations or eliminate some numerical problems arise from unobservable, uncontrollable, or marginally observable states [9, 57]. For a controlled nonlinear system, we need to study input-state and state-output behaviours of the system. The method presented here relies heavily on the work of Lall *et al.* [58].

First, the input-state behaviour of the original system is extracted using the empirical controllability gramian. For a given small perturbation $\epsilon > 0$, and the i^{th} unit vector e^i in $\mathbb{R}^p$, let $\mathbf{u}^{\pm i}(t) = \pm\epsilon e^i \delta(t)$ be an impulsive input and $\mathbf{x}^{\pm i}(t)$ be the corresponding trajectory. For system (2.1), define the *empirical controllability gramian* W_c by

$$W_c = \sum_{i=1}^{p} \frac{1}{4\epsilon^2} \int_0^\infty \left(\mathbf{x}^{+i}(t) - \mathbf{x}^{-i}(t)\right) \left(\mathbf{x}^{+i}(t) - \mathbf{x}^{-i}(t)\right)^T \mathrm{d}t. \tag{2.31}$$

Note that the empirical controllability gramian W_c of the stable linear system (2.2) is equal to the exact value of controllability gramian. For linear systems, the controllability gramian measures to what degree each state is excited by an input. For two states $\mathbf{x}_1$ and $\mathbf{x}_2$ with $\|\mathbf{x}_1\| = \|\mathbf{x}_2\|$, if $\mathbf{x}_1^T W_c \mathbf{x}_1 > \mathbf{x}_2^T W_c \mathbf{x}_2$, then state $\mathbf{x}_1$ is more controllable than $\mathbf{x}_2$ (i.e. it takes a smaller input to drive the system from rest to $\mathbf{x}_1$ than to $\mathbf{x}_2$). The eigenvectors of W_c corresponding to non-zero eigenvalues span a subspace which contains a set of states reachable using the chosen initial impulsive inputs. Now, we can eliminate those states corresponding to small eigenvalues of W_c. To obtain the reduced order model, one might perform a projection onto the subspace spanned by the eigenvectors corresponding to the largest eigenvalues.

Now, we need to study the state-output behaviour of the system. The definition of the empirical observability Gramian was given in (2.30). The only difference here is that in this case, the input is $\mathbf{u} = 0$. The empirical observability gramian W_o of the stable linear system (2.2) is equal to the exact value observability gramian. The observability gramian measures to what degree each state can excite the outputs. States which excite larger output signals are more observable, and in this sense they are less likely to be truncated than states that are less observable.

The method used here for calculating the Gramians is inspired by the method introduced by Krener and Ide for the empirical observability gramian [8]. Also, Lall, Marsden, and Glavski [58] calculated the empirical controllability and observability gramian for a nonlinear system around an equilibrium state in a very similar fashion.

These two tools can help us to find modes of the nonlinear system which preserve the most input-output behaviour of the system. The purpose here is to find a linear change of coordinates and perform a projection onto a subspace. The *empirical balanced truncation* method, which has been presented in [58], is as follows.

Let T be the change of coordinates such that the system is balanced, that is

$$TW_cT^T = T^{-1^T}W_oT^{-1} = \Sigma\,,$$

and let $P = \begin{bmatrix} I_{r\times r} & 0_{r\times(n-r)} \end{bmatrix}$ be an $r \times n$ projection matrix. Applying the transformation leads to a reduced-order model given by

$$\begin{aligned} \dot{\mathbf{x}}_r(t) &= PT\mathbf{f}\left(T^{-1}P^T\mathbf{x}_r(t), \mathbf{u}(t)\right) \\ \mathbf{y}(t) &= \mathbf{h}\left(T^{-1}P^T\mathbf{x}_r(t)\right)\,. \end{aligned} \tag{2.32}$$

The numerical technique for finding T from the empirical Gramians is as follows:

- Apply a Cholesky factorization to W_c so that $W_c = ZZ^T$, where Z is lower triangular with non-negative diagonal entries.
- Let $U\Sigma^2U^T$ be a singular value decomposition of Z^TW_oZ.
- The change of coordinates is given by $T = \Sigma^{\frac{1}{2}}U^TZ^{-1}$.

The resulting transformed system is the reduced order model.

Chapter 3

ACTIVE SENSING IN NONLINEAR SYSTEMS

In linear systems, while the ability to build an efficient estimator may be influenced by the sensor locations, the ability to estimate system states is completely decoupled from the particular choice of actuation. In nonlinear systems, however, the choice of controller can have significant impact not only on whether or not estimation is feasible but also on how well it can be accomplished.

One approach for investigating the observability of a nonlinear system is using a linearized model of the system and implementing the common linear observability tests; one example of this approach can be found in [1]. But a linearized model does not always retain all of the characteristics of interest for the original system. For instance, if the operating conditions of the dynamical system change significantly, the analysis of the linearized model may not adequately capture the input-output behaviour of the system over the entire operating region. An example is a nonholonomic system. These systems generally cannot be studied using the usual linear control techniques, as the linearization of this type of system about an equilibrium is degenerate [59]. Furthermore, the feedback linearization method fails for such systems. Perhaps most importantly, the use of linearized models does not allow for the consideration of effects of control on estimation that can be present in nonlinear systems but not in linear systems. The idea here is to let the controller have dual goals. A large number of dual controllers have been developed over the years. A good review of dual controllers is given in [60].

In the case of linear systems, the system is either completely observable or unobservable with the control inputs not affecting the observability results (the separation principle). For nonlinear systems, observability is not necessarily decoupled from control, and a particular choice of inputs might make a system observable while another choice is not. For some specific forms of nonlinear systems the nonlinear observation problem can be disconnected from the control synthesis problem [61]. However, in general, observation and actuation are coupled for nonlinear systems. An example of this coupling can be found in [62], which demonstrates a bio-inspired ground robot and

how control can be used to improve state observability. Another example is the mobile rover model considered in [12], which is a driftless nonlinear system, and for which the linear approximation of the system is unobservable, but for the nonlinear system some inputs allow reconstruction while other inputs do not. To address the issue of constructing controls that support observability in certain classes of nonlinear systems, a methodology based upon the Lie-algebra observability characterization is used. Unlike conventional linear observability tests, the Lie algebraic tools allow us to investigate the effect of control on observability.

Observability criteria have been used in a number of cases to determine optimal sensor location for nonlinear systems [7–9]. In these works, a measure of complete observability for linear systems was used (a set of scalar observability measures for linear systems can be found in [2]). Because of the coupling between actuation and observation for nonlinear systems, observability measures can be used conversely to find either optimal sensor placements for a given set of control inputs, or as we explore in this chapter, to find control inputs that guarantee observability for given sensor locations.

The aim of this chapter of the dissertation is to use the coupling between actuation and observation in certain nonlinear systems to design a control policy which guarantees observability.

3.1 Control Dependent Structure in Nonlinear Observability

In this chapter, a nonlinear system in control affine form with scalar measurement is considered. While we specifically consider scalar observations, all results can be generalized to vector observations. The dynamics is given by:

$$\Sigma_3 : \begin{cases} \dot{\mathbf{x}} = \mathbf{f}_0(\mathbf{x}) + \sum_{i=1}^{p} \mathbf{f}_i(\mathbf{x}) u_i, \;\; \mathbf{x} \in \mathbb{R}^n, \;\; \mathbf{u} \in \mathbb{R}^p \\ y = h(\mathbf{x}), \;\; y \in \mathbb{R}. \end{cases} \tag{3.1}$$

Given nonlinear system (3.1), define an accessibility distribution, $\widetilde{D}$, by

$$\widetilde{D} \triangleq \text{span} \left\{ \text{ad}^k_{\mathbf{f}_0} \mathbf{f}_i : 0 \leq k \leq n-1, 1 \leq i \leq p \right\}, \tag{3.2}$$

where, $\text{ad}^k_{\mathbf{f}_0} \mathbf{f}_i$ is the repeated Lie bracket operation [63]. If the distribution, $\widetilde{D}$, spans $\mathbb{R}^n$, where n equals the number of states, then, the nonlinear system in the control-affine form (3.1) is locally controllable about $\mathbf{x}_0$. For a control system, the direction of $\mathbf{f}$ at each point $\mathbf{x}$ is determined by

the choice of input $\mathbf{u}$, and if the system satisfies the local accessibility condition, then at least one $\mathbf{u}(\mathbf{x}, t)$ always exists such that the set of admissible values of $\mathbf{f}$ span $\mathbb{R}^n$. Here, local accessibility of the system of the form (3.2) is assumed, which means the ability to move a system around in its entire configuration space using admissible control inputs. The construction of controls for nonlinear systems that satisfy the local controllability condition (3.2) can be found in literature, e.g. [64] and [65]. Below, the observability Lie algebra is used to find controls from among those guaranteed by local controllability that ensure full state observability.

As (2.13) indicates, the set $\mathcal{O}$ is the set of all finite linear combinations of the Lie derivatives of h with respect to all possible vector fields, $\mathbf{f}$, and $d\mathcal{O}$ is the set of all their gradients. If one can find n linearly independent vectors within $d\mathcal{O}$, then the system is locally observable. The functional form of the terms in the observability Lie algebra (2.15) depends on the trajectory chosen. For example, the term $\dot{y} = L_{\mathbf{f}}h$ is the rate at which h changes with respect to time as one moves along the vector field $\mathbf{f}$. If the system state always changes in a direction such that the output remains constant, one can show that the system is unobservable. Here, we will find the requirements for vector field $\mathbf{f}$, and consequently $\mathbf{u}$, that guarantee local observability of the system.

Assumption 1. *Consider a control affine nonlinear system as given in* (3.1)*, assume that the first* $n-1$ *Lie derivatives of the output function* $h(\mathbf{x})$ *determine the observability of the system with* n *states.*

Let $\mathcal{O}'$ be formed of the first $n-1$ Lie derivatives as

$$\mathcal{O}' = \begin{bmatrix} h(\mathbf{x}) \\ L_{\mathbf{f}}h(\mathbf{x}) \\ \vdots \\ L_{\mathbf{f}}^{(n-1)}h(\mathbf{x}) \end{bmatrix}. \tag{3.3}$$

In the work by Sontag [66] it has been shown that if the entries of $\mathbf{f}_i(\mathbf{x})$ and $h(\mathbf{x})$ are rational functions with no poles, then the first $n-1$ Lie derivatives of the output function of the rational system (3.1) are polynomial functions with coefficients that are analytic functions. Sontag [66] showed that for rational systems with n states, only the first $n-1$ Lie derivatives have to be considered in the rank test. The validity of this result has been investigated in [67] for a broader class of control systems. Anguelova [67] derived the same upper bound for the number of Lie-derivatives of the output

functions for analytical systems affine in the input variables. Typical examples of analytic functions are polynomial, exponential, trigonometric, logarithm, and power functions.

Therefore, the necessary and sufficient condition for local observability at a point is having a full rank matrix $d\mathcal{O}'$ at that point, which means the rows of matrix $d\mathcal{O}'$ should be non-zero and linearly independent.

For the simple case where the number of states is $n = 2$, we can graphically illustrate how the control $\mathbf{u}$ and the vector field $\mathbf{f}$ can affect the observability of the system. Let the first element of $\mathcal{O}'$ be $h(\mathbf{x})$, so that the first row of $d\mathcal{O}'$ is $dL^0_{\mathbf{f}}h = \frac{\partial h}{\partial \mathbf{x}} = \mathbf{h_x}$. In the rest of this chapter, the short-hand notation $\frac{\partial h}{\partial \mathbf{x}} = \mathbf{h_x}$ will be used. In this case, if the second row of $d\mathcal{O}'$ is independent from the first row, the system is observable. If the output function $h(\mathbf{x})$ is twice continuously differentiable, and the second element of $\mathcal{O}'$ is $L_{\mathbf{f}}h(\mathbf{x})$, the second row is given by

$$dL_{\mathbf{f}}h = \left[\underbrace{\mathbf{h_x}\frac{\partial \mathbf{f}}{\partial x_1}}_{\zeta_1} + \underbrace{\frac{\partial}{\partial \mathbf{x}}(\frac{\partial h}{\partial x_1})\mathbf{f}}_{\zeta_2} \qquad \underbrace{\mathbf{h_x}\frac{\partial \mathbf{f}}{\partial x_2}}_{\zeta_3} + \underbrace{\frac{\partial}{\partial \mathbf{x}}(\frac{\partial h}{\partial x_2})\mathbf{f}}_{\zeta_4}\right]. \tag{3.4}$$

Hypothetically, if a mechanism can be found to assign an arbitrary value to the terms $\zeta_i, \quad i = 1, \ldots, 4$ in (3.4) at each state $\mathbf{x}$, then local observability can be guaranteed at $\mathbf{x}$. Specifically, finding these ζ_i values is equivalent to choosing $\mathbf{f}$ via construction of $\mathbf{u}$. Since the systems considered here are assumed to satisfy local accessibility condition, a controller, $\mathbf{u}$, always exists to produce a desired vector field. A schematic view of these vector fields is shown in Fig. 3.1. For a hypothetical example, the contours of h, $\frac{\partial h}{\partial x_1}$, and $\frac{\partial h}{\partial x_2}$ are shown in Figs. 3.1a to 3.1c. By selecting $\mathbf{f}$, $\frac{\partial \mathbf{f}}{\partial x_1}$ and $\frac{\partial \mathbf{f}}{\partial x_2}$, the value of $\frac{\partial}{\partial \mathbf{x}}(\frac{\partial h}{\partial x_i})\mathbf{f}, i = 1, 2$ (Figs. 3.1b and 3.1c) and $\mathbf{h_x}\frac{\partial \mathbf{f}}{\partial x_i}, \quad i = 1, 2$ (Fig. 3.1a) can be specified. For instance, for ζ_2 to be non-zero, the vector $\mathbf{f}$ should not be aligned with the tangents to the curves shown in Fig. 3.1b.

3.2 Observability-Based Control Policies

Here, we utilize three approaches to construct controllers, when they exist, that guarantee observability by maximizing particular observability measures. Specifically, we consider this observability optimization through the use of determinant (Section 3.2.1), condition number (Section 3.2.2) and row orthogonality (Section 3.2.3) of the Jacobian of the matrix $\mathcal{O}'$ given by (3.3) to ensure that the Jacobian is full rank. We begin by expressing the observability conditions in a particular

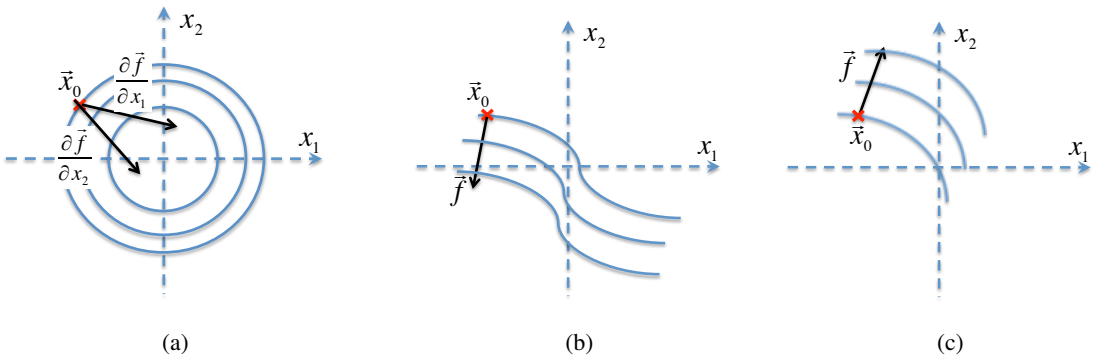

Figure 3.1: Contours of the output function h and its gradients. (a) Given h contours, choice of $\frac{\partial \mathbf{f}}{\partial x_1}$ and $\frac{\partial \mathbf{f}}{\partial x_2}$ determines $\mathbf{h_x}\frac{\partial \mathbf{f}}{\partial x_1}$ and $\mathbf{h_x}\frac{\partial \mathbf{f}}{\partial x_2}$ (ζ_1 and ζ_3 in (3.4)). (b) Given $\frac{\partial h}{\partial x_1}$ contours, the choice of $\mathbf{f}$ determines $\frac{\partial}{\partial \mathbf{x}}(\frac{\partial h}{\partial x_1})\mathbf{f}$ (ζ_2 in (3.4)). (c) Given $\frac{\partial h}{\partial x_2}$ contours, the choice of $\mathbf{f}$ determines $\frac{\partial}{\partial \mathbf{x}}(\frac{\partial h}{\partial x_2})\mathbf{f}$ (ζ_4 in (3.4)).

parametrized form to facilitate construction of controls. The first row of $d\mathcal{O}'$ is $dh = \mathbf{h_x}$, and the second row, $dL_\mathbf{f}h$, in case of $\mathbf{u}(\mathbf{x})$ can be written as

$$dL_\mathbf{f}h = \mathbf{h_x}\frac{\partial \mathbf{f}}{\partial \mathbf{x}} + \mathbf{f}^T\frac{\partial^2 h}{\partial \mathbf{x}^2} = \mathbf{h_x}\frac{\partial \mathbf{f}_0}{\partial \mathbf{x}} + \mathbf{f}_0^T\frac{\partial^2 h}{\partial \mathbf{x}^2} + \sum_{j=1}^{p}\left[\mathbf{h_x}\frac{\partial \mathbf{f}_j}{\partial \mathbf{x}} + \mathbf{f}_j^T\frac{\partial^2 h}{\partial \mathbf{x}^2}\right]u_j + \sum_{j=1}^{p}\mathbf{h_x}\mathbf{f}_j\frac{\partial u_j}{\partial \mathbf{x}}. \quad (3.5)$$

If we assume that the control, $\mathbf{u}$, is state-independent then $dL_\mathbf{f}h$ can be written in control affine form as

$$dL_\mathbf{f}h = \underbrace{\left[\mathbf{h_x}\frac{\partial \mathbf{f}_0}{\partial \mathbf{x}} + \mathbf{f}_0^T\frac{\partial^2 h}{\partial \mathbf{x}^2}\right]}_{\mathbf{g}_0(\mathbf{x})} + \sum_{j=1}^{p}\underbrace{\left[\mathbf{h_x}\frac{\partial \mathbf{f}_j}{\partial \mathbf{x}} + \mathbf{f}_j^T\frac{\partial^2 h}{\partial \mathbf{x}^2}\right]}_{\mathbf{g}_j(\mathbf{x})}u_j = \mathbf{g}_0(\mathbf{x}) + \sum_{j=1}^{p}\mathbf{g}_j(\mathbf{x})u_j. \quad (3.6)$$

Lemma 1. *The kth row of the Lie algebra observability matrix $d\mathcal{O}'$ is an order k polynomial function, $\eta_k(\mathbf{x}, \mathbf{u})$, of the controls, $u_1, \cdots u_p$.*

Proof. As it was mentioned above, the first row of $d\mathcal{O}'$ is dh, which is a zero order polynomial function with respect to controls. Now, let assume $dL_\mathbf{f}^k h$ is an order k polynomial function, η_k. And we also know that

$$dL_\mathbf{f}^{k+1}h = d\left(L_\mathbf{f}L_\mathbf{f}^k h\right) = d\left(\left(dL_\mathbf{f}^k h\right)\mathbf{f}\right) = d\left(\eta_k \cdot \mathbf{f}\right). \quad (3.7)$$

Since $\mathbf{f}$ is an affine function of control, and we assumed that η_k is an order k polynomial, then we can conclude that $d\left(\eta_k \cdot \mathbf{f}\right)$ is an order $k+1$ polynomial of the controls. Therefore, the $(k+1)$th row of the Lie algebra observability matrix can be written as a polynomial of order $k+1$. By the principle of induction, the lemma is proved. □

In order for the system to be observable, all rows of $d\mathcal{O}'$ must be nonzero, and they must be linearly independent. The conditions for non-zero rows are $dL_{\mathbf{f}}^{i}h = \eta_i(\mathbf{x},\mathbf{u}) \neq \mathbf{0},\ \ i = 0,\cdots,n-1$. These conditions at each $\mathbf{x}_0$ is a set of n inequalities. According to Lemma 1, each $\eta_k(\mathbf{x},\mathbf{u}),\ \ k = 0,...,n-1$ is a degree-k polynomial with respect to $u_j,\ \ j = 1,..,p$, which form hyper-surfaces in $p-$dimensional space. Each inequality. Therefore, the conditions $\eta_i(\mathbf{x},\mathbf{u}) \neq \mathbf{0}$ for $i = 0,\cdots,n-1$ is obtained by intersection of n hyperplanes, which determines a forbidden region. The acceptable region for controls is obtained by removing these forbidden regions from the entire $p-$dimensional space.

In the rest of this section, for the sake of simplicity, it is often assumed that the system has two states, $n = 2$, as given by

$$\begin{cases} \dot{\mathbf{x}} = \mathbf{f}_0(\mathbf{x}) + \sum_{i=1}^{p} \mathbf{f}_i(\mathbf{x})u_i,\ \ \mathbf{x} \in \mathbb{R}^2,\ \ \mathbf{u} \in \mathbb{R}^p \\ y = h(\mathbf{x}),\ \ y \in \mathbb{R}\,. \end{cases} \tag{3.8}$$

In this case, the Lie algebra observability matrix is spanned by h and $L_{\mathbf{f}}h$, and $d\mathcal{O}'$ can be written as

$$d\mathcal{O}' = \begin{bmatrix} dh \\ dL_{\mathbf{f}}h \end{bmatrix}. \tag{3.9}$$

In order for the system to be observable, both rows of $d\mathcal{O}'$ must be nonzero, and they must be linearly independent. The conditions for non-zero rows are

$$\begin{aligned} dh &= \begin{bmatrix} \left(\frac{\partial h}{\partial x_1}\right) & \left(\frac{\partial h}{\partial x_2}\right) \end{bmatrix} \neq \mathbf{0}, \\ dL_{\mathbf{f}}h &= \mathbf{g}_0(\mathbf{x}) + \sum_{j=1}^{p} \mathbf{g}_j(\mathbf{x})u_j \neq \mathbf{0}. \end{aligned} \tag{3.10}$$

Each u_j should be chosen such that the linear inequality equations given in (3.10) is satisfied. Since in real systems, $p \leq n$, the largest forbidden region obtained from inequality (3.10) is a single point in one-dimensional space (single input) and a line in two-dimensional space (two inputs).

To have full state local observability, the Lie algebra observability matrix, $d\mathcal{O}'$, must be full rank. Three approaches are used to find an admissible control that satisfies the Lie algebra observability condition. These approaches are non-zero determinant, finite condition number of Lie algebra observability matrix, and the third approach concerns with building an observability matrix with orthogonal rows.

3.2.1 Non-Singular Determinant of $d\mathcal{O}'$

Here, a control policy is constructed to ensure that the determinant of $d\mathcal{O}'$ is non-zero. The determinant of $d\mathcal{O}'$ is non-zero if and only if the rows of the matrix are independent. The rows of $d\mathcal{O}'$ are linearly independent if and only if the n-volume of the parallelepiped defined by the rows of the matrix is non-zero. In this case, the absolute value of the determinant of $d\mathcal{O}'$ ($|\det(d\mathcal{O}')|$) is equal to the n-volume of this parallelepiped, $Vol(dL_{\mathbf{f}}^0 h, ..., dL_{\mathbf{f}}^{n-1} h)$. For $n = 2$ or $n = 3$, the calculation of the volume is straightforward. For the higher dimensions, we have the following result.

Proposition 1. *Given system* (3.1)*, the system is locally observable at a given point* $(\mathbf{x}^0, \mathbf{u}^0)$ *if and only if* $\det(M) \neq 0$*, where* $M[i,j] = \left\langle dL_{\mathbf{f}}^{i-1} h, dL_{\mathbf{f}}^{j-1} h \right\rangle \Big|_{(\mathbf{x}^0, \mathbf{u}^0)}$ [1].

Proof. It has been proved in [68] that the volume of the parallelepiped defined by vectors $\mathbf{v}_1, ..., \mathbf{v}_n$ is equal to $\sqrt{\det(M)}$, where $M[i,j] = \langle \mathbf{v}_i, \mathbf{v}_j \rangle$. On the other hand, the volume of the parallelepiped defined by $dL_{\mathbf{f}}^i h$ is equal to $|\det(d\mathcal{O}')|$. Therefore, the Jacobian matrix is non-singular if and only if $\det(M) \neq 0$, where $M[i,j] = \left\langle dL_{\mathbf{f}}^{i-1} h, dL_{\mathbf{f}}^{j-1} h \right\rangle$. Finally, the system is locally observable at a given point if and only if the Jacobian matrix is non-singular at that point. □

Proposition 2. *Given system* (3.8)*, let the values of* u_j *be chosen such that* $\sum_{j=1}^{p} \mathbf{g}_j(\mathbf{x}^0) u_j$ *and* $\mathbf{g}_0(\mathbf{x}^0)$ *satisfy*

$$\left\langle \Big(\mathbf{h}_{\mathbf{x}} \times \mathbf{g}_0\Big), \Big(\mathbf{h}_{\mathbf{x}} \times \sum_{j=1}^{p} \mathbf{g}_j u_j\Big) \right\rangle \Bigg|_{\mathbf{x}^0} > 0. \tag{3.11}$$

Then the system is locally observable at $\mathbf{x}^0$.

Proof. Assume that u_j are chosen such that (3.11) is satisfied and that the observability matrix is not full rank. Note that in the case of $n = 2$, to have non-singular $d\mathcal{O}'$, $\mathbf{g}_0(\mathbf{x}) + \sum_{j=1}^{p} \mathbf{g}_j(\mathbf{x}) u_j$

[1] $M[i,j]$ is the (i,j) index of matrix M

should be independent of $\mathbf{h_x}$. Since the matrix is not full rank, the rows are not linearly independent which means that there exists a constant $\alpha \in \mathbb{R}$ such that $\mathbf{g}_0(\mathbf{x}) + \sum_{j=1}^{p} \mathbf{g}_j(\mathbf{x})u_j = \alpha \mathbf{h_x}$. With the substitution $\sum_{j=1}^{p} \mathbf{g}_j(\mathbf{x})u_j = \alpha \mathbf{h_x} - \mathbf{g}_0(\mathbf{x})$ and knowing that $\mathbf{h_x} \times \alpha \mathbf{h_x} = 0$, we have

$$\langle (\mathbf{h_x} \times \mathbf{g}_0), (\mathbf{h_x} \times -\mathbf{g}_0) \rangle = -\|\mathbf{h_x} \times \mathbf{g}_0\|^2 < 0, \tag{3.12}$$

which is a contradiction to (3.11). Therefore, the rows are independent, and the observability matrix is full rank. Based on Proposition 1, the system is locally observable. □

In the special case of a linear output function ($\frac{\partial^2 h}{\partial \mathbf{x}^2} = 0$), the drift and control vectors should satisfy some necessary conditions for local observability. The following proposition gives necessary conditions, which are independent of the choice of control inputs for the case of $n = 2$.

Proposition 3. *In the case of* $\frac{\partial^2 h}{\partial \mathbf{x}^2} = 0$*, if the system* (3.8) *is observable, then* $\exists j, \;\; j = 0, \cdots, p$*, such that* $(\mathbf{h_x})^T \notin Null(\frac{\partial \mathbf{f}_j}{\partial \mathbf{x}})^T$.

Proof. If $\frac{\partial^2 h}{\partial \mathbf{x}^2} = 0$ and $\forall j, \;\; j = 0, \ldots, p, \;\; (\mathbf{h_x})^T \in Null(\frac{\partial \mathbf{f}_j}{\partial \mathbf{x}})^T$, then $\forall j, \;\; j = 0, \ldots, p, \;\; \mathbf{h_x} \frac{\partial \mathbf{f}_j}{\partial \mathbf{x}} = \mathbf{g}_j = 0$, which means $dL_{\mathbf{f}} h = 0$, and the system is unobservable. □

Now consider the case of $\mathbf{u} = \mathbf{u}(\mathbf{x})$. The objective here is to find a linear state feedback control to guarantee a full observability.

Theorem 3. *Given a nonlinear system in control affine form* (3.8) *and linear state feedback control,* $\mathbf{u} = K\mathbf{x}$*, the determinant of the Jacobian matrix can be expressed as an affine function of the feedback gains,* $K[i, j]$.

Proof. From (3.5), the second row of $d\mathcal{O}'$ in this case is given as follows:

$$dL_{\mathbf{f}} h = \underbrace{\mathbf{h_x} \frac{\partial \mathbf{f}_0}{\partial \mathbf{x}} + \mathbf{f}_0^T \frac{\partial^2 h}{\partial \mathbf{x}^2}}_{dL_{\mathbf{f}_0} h} + \sum_{j=1}^{p} \mathbf{k}_j^T \mathbf{x} \underbrace{\left[\mathbf{h_x} \frac{\partial \mathbf{f}_j}{\partial \mathbf{x}} + \mathbf{f}_j^T \frac{\partial^2 h}{\partial \mathbf{x}^2} \right]}_{dL_{\mathbf{f}_j} h} + \sum_{j=1}^{p} \underbrace{[\mathbf{h_x} \mathbf{f}_j]}_{L_{\mathbf{f}_j} h} \mathbf{k}_j^T, \tag{3.13}$$

where $\mathbf{k}_j^T$ is the jth row of matrix K. We know that $\det(d\mathcal{O}') = \langle e_3, \mathbf{h_x} \times dL_{\mathbf{f}} h \rangle^2$. Computation

[2]The vector e_3 is the standard basis vector, which is given by $\begin{bmatrix} 0 & 0 & 1 \end{bmatrix}$.

of the cross product for two-dimensional vectors is straightforward, giving

$$\det(d\mathcal{O}') = \underbrace{\langle e_3, \mathbf{h}_{\mathbf{x}} \times dL_{\mathbf{f}_0} h \rangle}_{\xi_0} + \sum_{j=1}^{p} \mathbf{k}_j^T \underbrace{\begin{bmatrix} x_1 \left\langle e_3, \left(\mathbf{h}_{\mathbf{x}} \times dL_{\mathbf{f}_j} h\right)\right\rangle - \left(L_{\mathbf{f}_j} h\right)\left(\frac{\partial h}{\partial x_2}\right) \\ x_2 \left\langle e_3, \left(\mathbf{h}_{\mathbf{x}} \times dL_{\mathbf{f}_j} h\right)\right\rangle + \left(L_{\mathbf{f}_j} h\right)\left(\frac{\partial h}{\partial x_1}\right) \end{bmatrix}}_{\xi_j} \tag{3.14}$$

$$= \xi_0(\mathbf{x}) + \operatorname{trace}(K\Xi)\,,$$

where

$$\Xi = \begin{bmatrix} \xi_1(\mathbf{x}) & \xi_2(\mathbf{x}) & \cdots & \xi_p(\mathbf{x}) \end{bmatrix}. \tag{3.15}$$

Therefore, the determinant can be written as an affine function of control gains. □

Theorem 4. *Consider a nonlinear system in control affine form, as given in* (3.8)*. For any given nominal trajectory and nominal control such that*

$$|\xi_0(t)| + \|\Xi(t)\|_1 > 0\,, \quad \forall t\,, \tag{3.16}$$

there exists an additive control in the form of a linear state feedback control, $\mathbf{u} = K(t)\mathbf{x}$*, that guarantees non-zero determinant of the Jacobian matrix,* $d\mathcal{O}'$*.*

Proof. Assume that the nominal given control is incorporated in (3.8), and a new set of drift and control vectors are obtained. By considering an additive control as the new input, then the new system obtained from utilizing the nominal control can be written in a control affine form, as:

$$\dot{\mathbf{x}} = \underbrace{\mathbf{f}_0(\mathbf{x}) + \sum \mathbf{f}_j(\mathbf{x}) u_j^{nom}(\mathbf{x})}_{\bar{\mathbf{f}}_0(\mathbf{x})} + \sum \mathbf{f}_j(\mathbf{x}) u_j\,. \tag{3.17}$$

Assume the nominal trajectory is given as $\mathbf{x}^0(t)$ in $[t_i, t_f]$. Consider the additive control is given by $\mathbf{u} = K(t)\mathbf{x}$, Based upon Theorem 3, the determinant of the matrix $d\mathcal{O}'$ for the given nominal trajectory can be expressed as $\det(d\mathcal{O}') = \xi_0(t) + \operatorname{trace}(K\Xi(t)) = \xi_0(t) + \sum_{i,j} K[i,j]\,\Xi(t)[i,j]$. The non-zero determinant condition can be written as

$$\xi_0(t) + \sum_{i,j} K[i,j]\,\Xi(t)[i,j] \neq 0\,. \tag{3.18}$$

We have to find K, such that $|\det(d\mathcal{O}')| > 0$ for all $t \in [t_i, t_f]$. In the case of $|\xi_0(t)| > 0, \ \ \forall t \in [t_i, t_f]$, the inequality (3.18) is satisfied with no need of control input, and to impose minimum

deviation from the given nominal trajectory, we set the control to zero ($K = 0$). Now assume that $\exists \tau \in [t_i, t_f]$ s.t. $|\xi_0(\tau)| = 0$. Consider the following two optimization problems:

$$\begin{aligned} \underset{K[i,j]}{\text{minimize}} \quad & \|K\|_E^2 \\ \text{subject to} \quad & \sum_{i,j} K[i,j]\, \Xi(\tau)[i,j] \geq \epsilon_o \,, \end{aligned} \tag{3.19}$$

and

$$\begin{aligned} \underset{K[i,j]}{\text{minimize}} \quad & \|K\|_E^2 \\ \text{subject to} \quad & \sum_{i,j} K[i,j]\, \Xi(\tau)[i,j] \leq -\epsilon_o \,, \end{aligned} \tag{3.20}$$

where $\|K\|_E$ is the Euclidean norm of the matrix K, and ϵ_o is the minimum acceptable value for the determinant of the observability matrix. Because of condition (3.16) we have $\Xi \neq 0$. Thus as long as $0 < \epsilon_o < \|\Xi(t)\|_1$, one of the optimization problems (3.19) or (3.20) must have feasible solution. The solution of either one of the two optimization problems guarantees (3.18) and provides the minimal deviation from the nominal trajectory. □

3.2.2 Minimization of Condition Number

The second approach to maximizing observability that we consider is based on optimal condition number of a matrix. The condition number, κ, of a matrix is the ratio of the largest singular value to its smallest. The condition number of the observability matrix can be used as a criterion to maximize the observability with a goal of having the eigenvalues of the observability matrix as close together as possible:

$$\begin{aligned} \underset{u_1,\ldots u_p}{\text{minimize}} \quad & \kappa(d\mathcal{O}') = \frac{\lambda_{max}(M)}{\lambda_{min}(M)} \\ \text{subject to} \quad & |u_j| < u_j^{max}, j = 1 \ldots p, \end{aligned} \tag{3.21}$$

where

$$M = (d\mathcal{O}')^T (d\mathcal{O}'). \tag{3.22}$$

This optimization problem is highly nonlinear and cannot, in general, be solved. However, in the case of control-affine second-order system (3.8), we have

$$M = \begin{bmatrix} \|\mathbf{h_x}\|^2 & \left\langle \mathbf{h_x}, dL_\mathbf{f}^1 h \right\rangle \\ \left\langle \mathbf{h_x}, dL_\mathbf{f}^1 h \right\rangle & \left\| dL_\mathbf{f}^1 h \right\|^2 \end{bmatrix},$$

and the following theorem gives a control function that minimizes the condition number of $d\mathcal{O}'$.

Theorem 5. *Given system* (3.8)*, if* $\langle \mathbf{g}_0, \mathbf{h}_\mathbf{x} \rangle = 0$ *and* $\forall j, \langle \mathbf{g}_j, \mathbf{h}_\mathbf{x} \rangle = 0$*, then the system is observable with no need of any control. Selecting control inputs* u_j *which give* $\left\| \mathbf{g}_0 + \sum_{j=1}^{p} \mathbf{g}_j u_j \right\| = \|\mathbf{h}_\mathbf{x}\|$ *will minimize the condition number of the observability matrix.*

Proof. If $\langle \mathbf{g}_0, \mathbf{h}_\mathbf{x} \rangle = 0$ and $\forall j, \langle \mathbf{g}_j, \mathbf{h}_\mathbf{x} \rangle = 0$, then

$$\left\langle \mathbf{h}_\mathbf{x}, dL_\mathbf{f}^1 h \right\rangle = \langle \mathbf{g}_0, \mathbf{h}_\mathbf{x} \rangle + \sum_{j=1}^{p} \langle \mathbf{g}_j, \mathbf{h}_\mathbf{x} \rangle u_j = 0\,. \tag{3.23}$$

In this case, the rows of M are orthogonal. Therefore, the system is observable $\forall \mathbf{u}$. The solution to (3.21) is given by

$$\begin{aligned} \underset{u_1,\ldots u_p}{\text{minimize}} \quad & \frac{\max\left(\|\mathbf{h}_\mathbf{x}\|^2, \left\|dL_\mathbf{f}^1 h\right\|^2\right)}{\min\left(\|\mathbf{h}_\mathbf{x}\|^2, \left\|dL_\mathbf{f}^1 h\right\|^2\right)} \\ \text{subject to} \quad & |u_j| < u_j^{max}, j = 1 \ldots p. \end{aligned} \tag{3.24}$$

If the control input is chosen such that it minimizes $\left\| \mathbf{g}_0 + \sum_{j=1}^{p} \mathbf{g}_j u_j \right\|^2 - \|\mathbf{h}_\mathbf{x}\|^2$, then $M \approx \|\mathbf{h}_\mathbf{x}\|^2 I_2$, where I_2 is a 2×2 identity matrix. Therefore, $\lambda_{min}(M) = \lambda_{max}(M) = \|\mathbf{h}_\mathbf{x}\|^2$, and $\kappa(d\mathcal{O}') = 1$, which is the minimum value for the condition number of a matrix. □

3.2.3 Row Orthogonality

The third approach to guarantee observability that is considered here is based on row orthogonality. Because an orthogonal matrix always has full rank, one approach to guaranteeing local observability is to construct an orthogonal or nearly orthogonal Lie algebra observability matrix. To have orthogonal rows, we want

$$\left\langle dL_\mathbf{f}^i h, dL_\mathbf{f}^j h \right\rangle = \langle \eta_i(\mathbf{x}, \mathbf{u}), \eta_j(\mathbf{x}, \mathbf{u}) \rangle = 0, \;\; 0 \le i, j \le n-1, \;\; i \ne j. \tag{3.25}$$

The purpose here is to minimize $\left\langle dL_\mathbf{f}^i h, dL_\mathbf{f}^j h \right\rangle^2$, which makes the rows of the observability Jacobian matrix being independent. As was explained in Section 3.2.2, the minimization of the condition number is a highly nonlinear optimization problem, and hence is difficult to solve. In this section a new observability criterion is introduced which is close to the concept of the condition number of the observability matrix. The following theorem illustrates how the condition number of a matrix is related to the row orthogonality condition introduced here.

Theorem 6. *For a nonlinear system given in* (3.8) *the control that minimizes the orthogonality condition, as given by*

$$\begin{aligned} &\underset{\mathbf{u}}{\textit{minimize}} \quad \left\langle dL_{\mathbf{f}}^{0}h, dL_{\mathbf{f}}^{1}h \right\rangle^{2} \\ &\textit{subject to} \quad \|dL_{\mathbf{f}}^{j}h\| = c_j\,, \;\; j = 0, 1\,, \end{aligned} \tag{3.26}$$

also minimizes the condition number of the observability matrix, $\kappa(d\mathcal{O}')$.

Proof. Assume $\mathbf{u}_1$ is the optimal control obtained from the optimization problem (3.26). Therefore,

$$\left\langle dL_{\mathbf{f}}^{0}h(\mathbf{u}), dL_{\mathbf{f}}^{1}h(\mathbf{u}) \right\rangle^{2} > \left\langle dL_{\mathbf{f}}^{0}h(\mathbf{u}_1), dL_{\mathbf{f}}^{1}h(\mathbf{u}_1) \right\rangle^{2}, \;\; \forall \mathbf{u}\,. \tag{3.27}$$

Now, assume there exists a control $\mathbf{u}_2 \neq \mathbf{u}_1$ for which $\|dL_{\mathbf{f}}^{j}h(\mathbf{u}_2)\| = c_j, j = 0, 1$ and minimizes the condition number of the observability matrix. Define M_1 and M_2 as:

$$\begin{aligned} M_1 &= (d\mathcal{O}'(\mathbf{u}_1))^T (d\mathcal{O}'(\mathbf{u}_1)) \\ M_2 &= (d\mathcal{O}'(\mathbf{u}_2))^T (d\mathcal{O}'(\mathbf{u}_2))\,. \end{aligned} \tag{3.28}$$

Since $\|dL_{\mathbf{f}}^{j}h(\mathbf{u}_1)\| = \|dL_{\mathbf{f}}^{j}h(\mathbf{u}_2)\|, j = 0, 1$, then $\operatorname{trace}(M_1) = \operatorname{trace}(M_2)$. The determinant of the matrix M_i is given by

$$\det(M_i) = \left(\|dL_{\mathbf{f}}^{0}h(\mathbf{u}_i)\|\|dL_{\mathbf{f}}^{1}h(\mathbf{u}_i)\|\right)^2 - \left\langle dL_{\mathbf{f}}^{0}h(\mathbf{u}_i), dL_{\mathbf{f}}^{1}h(\mathbf{u}_i) \right\rangle^{2} \tag{3.29}$$

Considering condition (3.27), we can conclude that $\det(M_1) > \det(M_2)$. Therefore,

$$\kappa(d\mathcal{O}'(\mathbf{u}_1)) < \kappa(d\mathcal{O}'(\mathbf{u}_2))$$

which contradicts our assumption that $\mathbf{u}_2$ minimizes the condition number of the observability matrix. Hence, $\mathbf{u}_2 = \mathbf{u}_1$, and the statement of the theorem is true. □

Lemma 2. *Given system* (3.1)*, and constant control,* $\mathbf{u}$*, the minimum number of control inputs to have an orthogonal observability matrix is* $\frac{n(n-1)}{2}$.

Proof. For observability of the system, we need the rows of the observability matrix to be independent, so the number of independent equations from (3.25) for all pairs of i and j is $\frac{n(n-1)}{2}$, while we have p unknowns. Therefore, in order to have a solution for the controls, we should have $p \geq \frac{n(n-1)}{2}$. □

In most real systems, we have $p \leq n$. Therefore, we cannot be certain about finding an orthogonal Jacobian matrix if $n > 3$.

Proposition 4. *Given system* (3.8) *and constant control,* $\mathbf{u}$*, define*

$$\mu_j(\mathbf{x}) = \langle \mathbf{g}_j, \mathbf{h}_\mathbf{x} \rangle \,, \;\; j = 0, \cdots, p \,. \tag{3.30}$$

Then, in order to have an orthogonal observability matrix, one should be able to write the function $\mu_0(\mathbf{x})$ *as* $\mu_0(\mathbf{x}) = \sum_j \alpha_j \mu_j(\mathbf{x}), \;\; j = 1, \cdots, p, \;\; \alpha_j \in \mathbb{R}$.

Proof. The condition of an orthogonal Jacobian matrix was given by (3.25). In the case of $n = 2$, we need to have $\left\langle dL^0_\mathbf{f} h, dL^1_\mathbf{f} h \right\rangle = 0$. This requirement means

$$\langle \mathbf{g}_0, \mathbf{h}_\mathbf{x} \rangle + \sum_{j=1}^{p} \langle \mathbf{g}_j, \mathbf{h}_\mathbf{x} \rangle \, u_j = 0, \;\; \forall \mathbf{x} \in \mathbb{R}^n \,. \tag{3.31}$$

Since the control inputs, u_j, have to be constant ($\frac{\partial u_j}{\partial \mathbf{x}} = \mathbf{0}$), (3.31) can be solved only if the the condition of Proposition 4 is satisfied. □

It seems that finding a control policy which gives an orthogonal observability over is hardly possible. The objective of the next section is to find a control policy which gives observability matrix as close as possible to an orthogonal matrix.

3.3 Tuning Control for a Given Trajectory

Here, a nominal trajectory is given, but there is no guarantee that the system is observable over the entire trajectory. The purpose, here, is to fine-tune the given nominal trajectory to find the closest trajectory to the nominal trajectory while satisfies observability condition. Let assume $\mathbf{u}^{nom}$, and its corresponding nominal trajectory $\mathbf{x}^{nom}$ are given. A small tuning term $\mathbf{w}(t)$ is added to the nominal control as

$$\mathbf{u} = \mathbf{u}^{nom}(\mathbf{x}) + \mathbf{w}(t). \tag{3.32}$$

If the modified control given in (3.32) is substituted in (3.1), then

$$\left\langle dL^i_\mathbf{f} h, dL^j_\mathbf{f} h \right\rangle = P^{ij}(\mathbf{w}), \tag{3.33}$$

where $P^{ij}(\mathbf{w})$ is a polynomial of order $\leq (i+j)$. The optimization problem can be written as

$$\begin{aligned} \underset{\mathbf{w}(\tau)}{\text{minimize}} \quad & \sum_{i=0}^{n-2} \sum_{j=i+1}^{n-1} \left[P^{ij}(\mathbf{w}(\tau))\right]^2 \\ \text{subject to} \quad & \|\mathbf{w}(\tau)\|^2 < \epsilon, \end{aligned} \tag{3.34}$$

where, ϵ is a small value, determines the maximum allowable perturbation size of the nominal control. One can also write this optimization problem in the form of regularization problem which is minimization of the weighted sum of the objectives:

$$\underset{\mathbf{w}(\tau)}{\text{minimize}} \quad \sum_{i=0}^{n-2} \sum_{j=i+1}^{n-1} \left[P^{ij}(\mathbf{w}(\tau))\right]^2 + \delta \|\mathbf{w}(\tau)\|^2, \tag{3.35}$$

where, $\delta > 0$ is a parameter which varies over $(0, \infty)$. The regularized approximation problem given by (3.35), solves a bi-criterion problem of making both terms small.

If the nonlinear system is simplified in the form of (3.8), the optimization problem can be written as

$$\underset{\mathbf{w}}{\text{minimize}} \quad \|A\mathbf{w} - \mathbf{b}\|^2 + \delta \|\mathbf{w}(\tau)\|^2, \tag{3.36}$$

where,

$$\begin{aligned} A &= \frac{\partial h}{\partial \mathbf{x}} \frac{\partial}{\partial \mathbf{x}} \left(\frac{\partial h}{\partial \mathbf{x}} \begin{bmatrix} \mathbf{f}_1 & \dots & \mathbf{f}_p \end{bmatrix} \right) \Bigg|_{\mathbf{x}=\mathbf{x}^{nom}, \mathbf{u}=\mathbf{u}^{nom}} \\ \mathbf{b} &= -\frac{\partial}{\partial \mathbf{x}} \left(\frac{\partial h}{\partial \mathbf{x}} \mathbf{f}_0 \right) \left(\frac{\partial h}{\partial \mathbf{x}} \right)^T \Bigg|_{\mathbf{x}=\mathbf{x}^{nom}, \mathbf{u}=\mathbf{u}^{nom}}. \end{aligned} \tag{3.37}$$

If the norms are Euclidean norms, the optimization problem is a form of the most common regularization, which results in a convex quadratic optimization problem, called *Tikhonov* regularization problem [69]. This problem has analytical solution as

$$\mathbf{w} = \left(A^T A + \delta I\right)^{-1} A^T \mathbf{b}. \tag{3.38}$$

Since $A^T A + \delta I \succ 0$ for any $\delta > 0$, the Tikhonov least square solution requires no rank (or dimension) assumption on the matrix A.

3.4 Feedback Control To Generate Nearly Orthogonal Observability Matrix

Finding a set of constant value controls that give an orthogonal matrix is almost impossible. Consider relaxing the condition of $\frac{\partial u_j}{\partial \mathbf{x}} = \mathbf{0}$, and find a control input $\mathbf{u}(\mathbf{x})$ which is not necessarily

constant. Even in this case, there is not necessarily an analytical solution, however, the following algorithm introduces a heuristic to generate an orthogonal Lie algebra observability matrix. Consider a single-input nonlinear system given by:

$$\begin{aligned} \dot{\mathbf{x}} &= \mathbf{f}(\mathbf{x}, u) = \mathbf{f}_0(\mathbf{x}) + \mathbf{f}_1(\mathbf{x})u \\ y &= h(\mathbf{x})\,, \quad \mathbf{x} \in \mathbb{R}^2 \;\; y\,, u \in \mathbb{R}\,. \end{aligned} \tag{3.39}$$

The purpose here is to find control u and trajectory $\mathbf{x}$ which maximize the observability in the sense of finding the minimum value of $\left\langle dL_{\mathbf{f}}^0 h, dL_{\mathbf{f}}^1 h \right\rangle$, which is close zero. In this case with (3.5), the orthogonality condition can be expressed as

$$\left\langle dL_{\mathbf{f}}^0 h, dL_{\mathbf{f}}^1 h \right\rangle = \langle dL_{\mathbf{f}_0} h, \mathbf{h}_{\mathbf{x}} \rangle + \frac{\partial u}{\partial \mathbf{x}} (m(\mathbf{x})\mathbf{h}_{\mathbf{x}})^T + l(\mathbf{x})u(\mathbf{x}) = 0, \tag{3.40}$$

where

$$m(\mathbf{x}) = \mathbf{h}_{\mathbf{x}}\mathbf{f}_1, \;\; l(\mathbf{x}) = \mathbf{h}_{\mathbf{x}} \frac{\partial \mathbf{f}_1}{\partial \mathbf{x}} \mathbf{h}_{\mathbf{x}}^T + \mathbf{f}_1^T \frac{\partial^2 h}{\partial \mathbf{x}^2} \mathbf{h}_{\mathbf{x}}^T. \tag{3.41}$$

The relation (3.40) is a linear partial differential equation of order one in the form of $F\left(\mathbf{x}, u, \nabla u\right) = 0$, which does not always have a unique solution. We would like to solve for u directly from the PDE, if possible. In the case that we cannot solve for $\mathbf{u}$ directly, a heuristic has been developed to find an approximated solution of the PDE. Let pre-multiply (3.40) by $\frac{\mathbf{f}(\mathbf{x},u)}{m(\mathbf{x})}$, then

$$\begin{bmatrix} \frac{\partial u}{\partial x_1}\dot{x}_1 & \frac{\partial u}{\partial x_2}\dot{x}_1 \\ \frac{\partial u}{\partial x_1}\dot{x}_2 & \frac{\partial u}{\partial x_2}\dot{x}_2 \end{bmatrix} \mathbf{h}_{\mathbf{x}}^T = \frac{-\mathbf{f}(\mathbf{x}, u)}{m(\mathbf{x})} \left[l(\mathbf{x})u(\mathbf{x}) + \langle dL_{\mathbf{f}_0} h, \mathbf{h}_{\mathbf{x}} \rangle \right]. \tag{3.42}$$

Now, post-multiply both sides by $\mathbf{h}_{\mathbf{x}} \left(\mathbf{h}_{\mathbf{x}}^T \mathbf{h}_{\mathbf{x}} + \delta I \right)^{-1}$, where δ is a small value to ensure that $\left(\mathbf{h}_{\mathbf{x}}^T \mathbf{h}_{\mathbf{x}} + \delta I \right)$ is invertible. Here, it is assumed that $\left(\mathbf{h}_{\mathbf{x}}^T \mathbf{h}_{\mathbf{x}} \right) \left(\mathbf{h}_{\mathbf{x}}^T \mathbf{h}_{\mathbf{x}} + \delta I \right)^{-1} \approx I$. Then, we have

$$\dot{u} = \frac{-1}{m(\mathbf{x})} \left[l(\mathbf{x})u(\mathbf{x}) + \langle dL_{\mathbf{f}_0} h, \mathbf{h}_{\mathbf{x}} \rangle \right] \operatorname{trace} \left(\mathbf{f}(\mathbf{x}, u) \mathbf{h}_{\mathbf{x}} \left(\mathbf{h}_{\mathbf{x}}^T \mathbf{h}_{\mathbf{x}} + \delta I \right)^{-1} \right). \tag{3.43}$$

Since $\mathbf{f}(\mathbf{x}, u)$ is a first order affine function with respect to u, the following ordinary differential equation is obtained:

$$\dot{u} = \zeta_2(\mathbf{x})u^2 + \zeta_1(\mathbf{x})u + \zeta_0(\mathbf{x}). \tag{3.44}$$

Solution of the system of ODE equations given by (3.39) and (3.44) gives an optimal control u^* and a corresponding optimal trajectory $\mathbf{x}^*$ in the sense of the orthogonal observability matrix. This

system of ODEs can be expressed as

$$\begin{aligned}\dot{\mathbf{x}} &= \mathbf{f}_0(\mathbf{x}) + \mathbf{f}_1(\mathbf{x})u \\ \dot{u} &= \zeta_2(\mathbf{x})u^2 + \zeta_1(\mathbf{x})u + \zeta_0(\mathbf{x}),\end{aligned} \tag{3.45}$$

with initial conditions:

$$\begin{aligned}\mathbf{x}(0) &= \mathbf{x}_0 \\ u(0) &= \left.\frac{-\langle dL_{\mathbf{f}_0}h, \mathbf{h}_{\mathbf{x}}\rangle}{l(\mathbf{x})}\right|_{\mathbf{x}=\mathbf{x}_0}.\end{aligned} \tag{3.46}$$

Although, the initial condition for u can be chosen to be any desired value, here, it is assumed that $\frac{\partial u}{\partial \mathbf{x}}\big|_{t=0} = 0$, and then $u(0)$ is chosen to satisfy (3.40). Note that this algorithm fails when $l(\mathbf{x})$ is zero. The situation of $l(\mathbf{x}) = 0$ happens when the control input of the system does not have any effect on the observability of the system. In this case, any change in the control input does not change the value of the observability matrix.

Theorem 7. *Given system* (3.39)*, if there exists a constant control, $u = c$, that generates an orthogonal observability matrix, then the solution of the system of ODEs given by* (3.45) *with initial conditions* (3.46) *gives the exact solution for an orthogonal observability matrix.*

Proof. If there exists a constant control, $u = c$, that generates an orthogonal observability matrix, then there exists a unique c that satisfies

$$\left\langle dL^0_{\mathbf{f}}h, dL^1_{\mathbf{f}}h\right\rangle = \langle dL_{\mathbf{f}_0}h, \mathbf{h}_{\mathbf{x}}\rangle + \langle dL_{\mathbf{f}_1}h, \mathbf{h}_{\mathbf{x}}\rangle\, c = \langle dL_{\mathbf{f}_0}h, \mathbf{h}_{\mathbf{x}}\rangle + l(\mathbf{x})c = 0, \;\; \forall \mathbf{x}\,. \tag{3.47}$$

If $\mathbf{x}(0) = \mathbf{x}_0$ is substituted into (3.47), then

$$\left.\frac{-\langle dL_{\mathbf{f}_0}h, \mathbf{h}_{\mathbf{x}}\rangle}{l(\mathbf{x})}\right|_{\mathbf{x}=\mathbf{x}_0} = c. \tag{3.48}$$

Therefore, $u(0) = c$. For these values of $\mathbf{x}_0$ and $u(0)$, the ODE for solving the control, given in (3.43), at time zero can be written as

$$\dot{u}(0) = \frac{-1}{m(\mathbf{x}_0)}\left[l(\mathbf{x}_0)c + \langle dL_{\mathbf{f}_0}h, \mathbf{h}_{\mathbf{x}}\rangle|_{\mathbf{x}=\mathbf{x}_0}\right] \operatorname{trace}\left(\mathbf{f}(\mathbf{x}, c)\mathbf{h}_{\mathbf{x}}\left(\mathbf{h}_{\mathbf{x}}^T\mathbf{h}_{\mathbf{x}} + \delta I\right)^{-1}\right)\Big|_{\mathbf{x}=\mathbf{x}_0}. \tag{3.49}$$

From (3.48) we have:

$$\left[l(\mathbf{x}_0)c + \langle dL_{\mathbf{f}_0}h, \mathbf{h}_{\mathbf{x}}\rangle|_{\mathbf{x}=\mathbf{x}_0}\right] = 0\,, \tag{3.50}$$

Thus, $\dot{u}(0) = 0$, which the control u remains unchanged at time zero. Because of the orthogonality condition in this case, given by (3.47), we have $\dot{u}(t) = 0 \ \ \forall t$, and the control remains at its initial condition which is equal to $u = c$, which is the exact solution of the optimal control in the sense of the orthogonal observability matrix. □

3.5 Illustrative Examples

In this section, the control policies obtained from the algorithms presented in this chapter are compared for some systems with different types of nonlinearities. The first example is a system with linear dynamics and nonlinear range-only measurement. Conversely, the second example has nonlinear dynamics and linear measurement. The last example is a nonholonomic system.

3.5.1 Linear Dynamics with Nonlinear Measurement

Consider the following system with linear dynamics and nonlinear observation:

$$\begin{aligned} \dot{\mathbf{x}} = \mathbf{f}(\mathbf{x}, u) = \begin{bmatrix} u_1 \\ x_1 \end{bmatrix} = \begin{bmatrix} 0 \\ x_1 \end{bmatrix} + \begin{bmatrix} 1 \\ 0 \end{bmatrix} u_1 \\ h(\mathbf{x}) = ||\mathbf{x}||_2^2 = x_1^2 + x_2^2. \end{aligned} \tag{3.51}$$

This system is marginally stable, and the controllability matrix is full rank, so the system is locally controllable. Linearizing the system about any point $(a, 0)$:

$$F = \begin{bmatrix} 0 & 0 \\ 1 & 0 \end{bmatrix}, \ \ G = \begin{bmatrix} 1 \\ 0 \end{bmatrix}, \ \ H = \begin{bmatrix} 2a & 0 \end{bmatrix}. \tag{3.52}$$

The observability matrix for the linearized system is then given by

$$O = \begin{bmatrix} H \\ HF \end{bmatrix} = \begin{bmatrix} 2a & 0 \\ 0 & 0 \end{bmatrix} \tag{3.53}$$

Therefore, the system does not satisfy the linear observability rank condition. Furthermore, the linearized observability matrix, O, is close to singular for any point close to origin, will cause the linear observability condition to fail for nominal trajectories that pass through origin. Since the system is locally controllable, one might be able to find a control policy which improves the observability of the system. Here, the system is analytic with $n = 2$, so only the first two terms in

the observability Lie algebra are required for evaluating the observability of the system [67]. The Lie algebra observability matrix for the system (3.51) is then given by

$$d\mathcal{O}' = \begin{bmatrix} dL_{\mathbf{f}}^0 h \\ dL_{\mathbf{f}}^1 h \end{bmatrix} = 2 \begin{bmatrix} x_1 & x_2 \\ u_1 + x_2 & x_1 \end{bmatrix}. \tag{3.54}$$

In this example $\mathbf{g}_0 = \begin{bmatrix} 2x_2 & 2x_1 \end{bmatrix}$, $\mathbf{g}_1 = \begin{bmatrix} 2 & 0 \end{bmatrix}$, and $\mathbf{h_x} = \begin{bmatrix} 2x_1 & 2x_2 \end{bmatrix}$. The system is not observable at the origin, no matter the control input. Along the line $x_1 = 0$ except for the origin, $\langle \mathbf{g}_0, \mathbf{h_x} \rangle = 0$ and $\langle \mathbf{g}_1, \mathbf{h_x} \rangle = 0$, so $\forall u_1$ the Lie algebra observability matrix, $d\mathcal{O}'$, is orthogonal. Along the line $x_2 = 0$ except at the origin, $\langle \mathbf{g}_0, \mathbf{h_x} \rangle = 0$ and $\mathbf{g}_1 \times \mathbf{h_x} = \mathbf{0}$, so the rows of $d\mathcal{O}'$ are independent $\forall u_1$, and the rows are orthogonal with zero control. Along the lines $x_1 = \pm x_2$ except at the origin, $\mathbf{g}_0 \times \mathbf{h_x} = \mathbf{0}$, so the control is needed for observability at all points.

We first consider the non-zero determinant approach, given in Section 3.2.1, to determine controls for this system. Here, assume a nominal control is given as $u^{nom} = -2x_2$. This control is implemented on the system given by (3.51) for a randomly chosen initial condition. The calculation of the determinant of the observability matrix for all point along the nominal given trajectory shows that the nominal given control policy does not guarantee non-zero determinant (see Fig. 3.2b). Now, consider adding a state feedback control to the given control using the methods of Section 3.2.1 to modify the given trajectory in order to guarantee local observability using the non-zero determinant condition. In this example, (3.18) is written as $\left(x_2^2(\tau) - x_1^2(\tau)\right) + \left(-2x_1(\tau)x_2(\tau)\right) k_1 + \left(x_1^2(\tau) - x_2^2(\tau)\right) k_2 \neq 0$. Then, problems (3.19) and (3.20) are summarized as

$$\begin{aligned} &\underset{k_1,k_2}{\text{minimize}} \quad k_1^2 + k_2^2 \\ &\text{subject to} \quad \left| -2x_1(\tau)x_2(\tau)k_1 + \left(x_1^2(\tau) - x_2^2(\tau)\right)(k_2 - 1) \right| \geq \epsilon_o. \end{aligned} \tag{3.55}$$

The nominal given trajectory and the modified trajectory are given by the solid blue line and black dashed line, respectively, in Fig. 3.2a. The value of $|\det(d\mathcal{O}')|^2$ for the nominal trajectory is shown in Fig. 3.2b. The red circles in this figure indicate two points where the non-zero determinant condition fails. The values of $|\det(d\mathcal{O}')|^2$ of the modified trajectory are also given in Fig. 3.2b. As can be seen, the modified trajectory satisfies the Lie algebra observability condition.

Note that for this example there does not exist any control that satisfies the condition of Proposition 4. Here, $\mu_0(\mathbf{x}) = 8x_1x_2$, and $\mu_1(\mathbf{x}) = 4x_1$. Therefore, there does not exist any constant control that generates an orthogonal observability matrix.

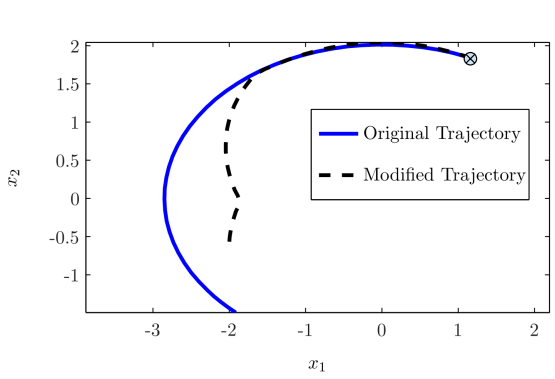

(a) The initial point of the trajectory is also shown by a small cross.

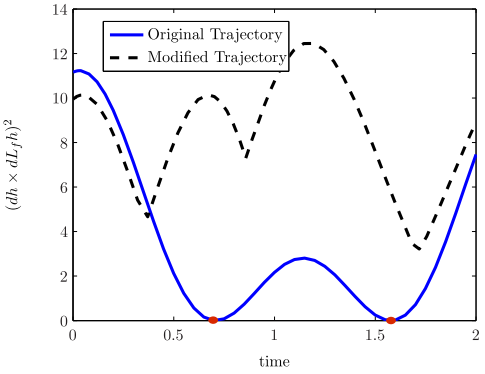

(b) The red circles indicate two points for which the non-zero determinant condition fails.

Figure 3.2: The blue solid line indicates the original trajectory for the example (3.51) after implementing $u_1 = -2x_2$. The black dashed line indicates the modified trajectory. The value of $(dh \times dL_{\mathbf{f}} h)^2$ for the original trajectory and the modified trajectory are given in figure (b).

3.5.2 Nonlinear Dynamics with Linear Measurement

Consider the system

$$\dot{\mathbf{x}} = \begin{bmatrix} \frac{1}{2}x_1^2 + x_2 + e^{x_2}u_1 \\ x_1^2 \end{bmatrix} = \begin{bmatrix} \frac{1}{2}x_1^2 + x_2 \\ x_1^2 \end{bmatrix} + \begin{bmatrix} e^{x_2} \\ 0 \end{bmatrix} u_1$$
$$h(\mathbf{x}) = x_1. \tag{3.56}$$

In this example, a control is obtained that guarantees observability in the sense of generating orthogonal rows of the Jacobian of the Lie algebra observability matrix, as in Section 3.2.3. The orthogonality condition, shown in (3.40), gives $x_1 + e^{x_2}\frac{\partial u_1}{\partial x_1} = 0$. One solution of this partial differential equation is $u_1(x_1, x_2) = -\frac{x_1^2}{2e^{x_2}}$. This control is shown in Fig. 3.3, and the system trajectory resulting from this control is given in Fig. 3.4. The rows of the Lie algebra observability matrix are also shown as vectors at a number of points along the trajectory. As can be seen by the orthogonality of the rows of the observability matrix as shown in Fig. 3.4, the obtained input drives the system to be locally observable at all points along the nominal trajectory. A limitation of this method is that no guarantee is given for stability of the system. In fact, the nominal control obtained for this

example drives the system toward instability.

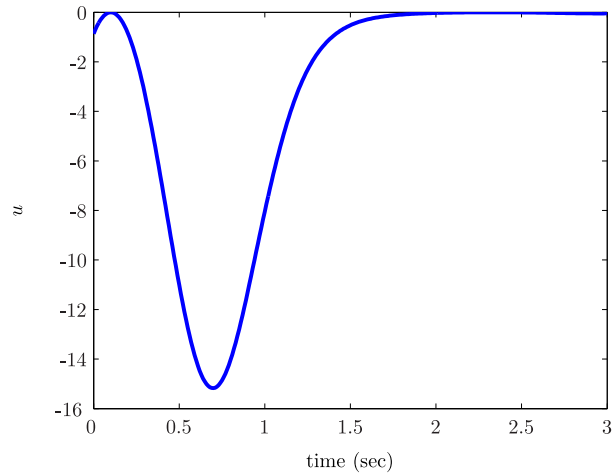

Figure 3.3: The nominal control policy for the example (3.56) obtained by solving the PDE (3.40).

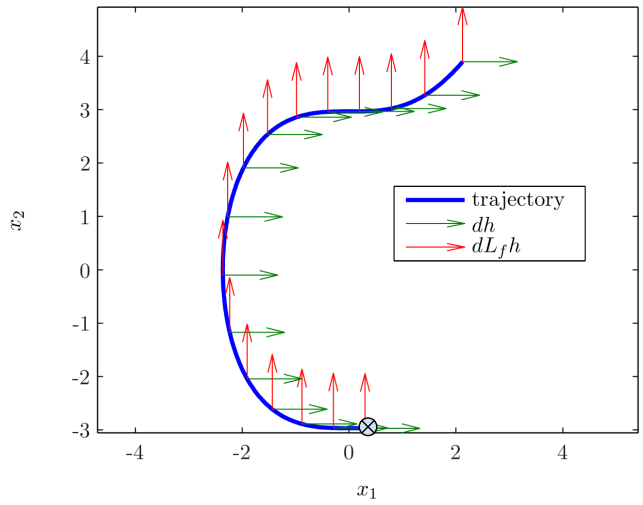

Figure 3.4: The nominal trajectory for the example (3.56) resulting from the control shown in Fig. 3.3. The rows of the Jacobian of the observability Lie algebra, vectors dh (green) and $dL_{\mathbf{f}}h$ (red), are plotted for some points along the nominal trajectory. The initial point of the trajectory is also shown by a small cross.

Since we do not have any limit on maximum value of the control inputs, the control obtained

above is also the solution for the minimum condition number of the observability matrix, given in Section 3.2.2. The condition number of the observability matrix for system (3.56) is given by

$$\kappa(d\mathcal{O}') = \frac{\lambda_{max}(M)}{\lambda_{min}(M)}\,, \tag{3.57}$$

where

$$M = \begin{bmatrix} 1 & x_1 + e^{x_2}\frac{\partial u_1}{\partial x_1} \\ x_1 + e^{x_2}\frac{\partial u_1}{\partial x_1} & \left(x_1 + e^{x_2}\frac{\partial u_1}{\partial x_1}\right)^2 + \left(1 + e^{x_2}\left(u_1 + \frac{\partial u_1}{\partial x_2}\right)\right)^2 \end{bmatrix}. \tag{3.58}$$

If we substitute the control given for the orthogonality condition from method Section 3.2.3,

$$u_1(x_1, x_2) = -\frac{x_1^2}{2e^{x_2}}\,,$$

in (3.58), then we have $M = \begin{bmatrix} 1 & 0 \\ 0 & 1 \end{bmatrix}$. Therefore, we have $\kappa(d\mathcal{O}') = 1$, which is the minimum value for the condition number of any matrix and we can see that the result from either method Section 3.2.3 or Section 3.2.2 is the same in this case.

3.5.3 Nonholonomic System

The next example is a first order nonholonomic system given by

$$\begin{aligned} \dot{x}_1 &= u_1 \\ \dot{x}_2 &= u_2 \\ \dot{x}_3 &= x_1 u_2 - x_2 u_1 \\ h(\mathbf{x}) &= x_3. \end{aligned} \tag{3.59}$$

The observability of this system is studied in [70]. This example does not satisfy the local accessibility condition, but based on the observability analysis in [70], we know that this system is observable if and only if measurements of the nonholonomic states (x_3 here) are available, and the actuation in at least two control channels is utilized. Let assume that the nominal controls are given as

$$\begin{aligned} u_1^{nom} &= -x_1 \\ u_2^{nom} &= 0. \end{aligned} \tag{3.60}$$

The initial condition is $\mathbf{x}_0 = \begin{bmatrix} 1 & 1 & -1 \end{bmatrix}^T$. Based on the theorem in [70], the system (3.59) is not observable by utilizing the set of nominal controls given in (3.60). Now we add tuning term to the nominal control as

$$\mathbf{u} = \mathbf{u}^{nom} + \mathbf{w}(t) = \begin{bmatrix} -x_1 \\ 0 \end{bmatrix} + \begin{bmatrix} 0 \\ w(t) \end{bmatrix}. \tag{3.61}$$

The Jacobian of the Lie algebra observability matrix is

$$dO = \begin{bmatrix} dh \\ dL_{\mathbf{f}}h \\ dL_{\mathbf{f}}^2 h \end{bmatrix} = \begin{bmatrix} 0 & 0 & 1 \\ x_2 + w & x_1 & 0 \\ -x_2 & -x_1 & 0 \end{bmatrix}. \tag{3.62}$$

As it can be seen, the first row of the matrix is orthogonal to the second and third rows of the matrix. Furthermore, $w \neq 0$ is required for observability. If $w = 0$, then $\det dO = 0$, which results in unobservable system. The optimal $w^*(\tau)$, $\tau \in [0 \;\; t_f]$ can be computed as

$$w^*(\tau) = \text{argmin} \left\| x_2(\tau) w(\tau) + \left(x_1^2(\tau) + x_2^2(\tau) \right) \right\|_2^2 + \delta \left\| \mathbf{w}(\tau) \right\|_2^2. \tag{3.63}$$

The Tikhonov least square solution for this problem is

$$w^*(\tau) = -\frac{x_2 \left(x_1^2 + x_2^2 \right)}{\left(\delta + x_2^2 \right)} \Bigg|_{\mathbf{x}=\mathbf{x}^{nom}}. \tag{3.64}$$

The tuning term, $w^*(t)$, for $t \in [0 \;\; 10]$ sec for two values of $\delta = 10$ and $\delta = 100$ are given in Fig. 3.5. The original nominal trajectory and the modified trajectories for those two values of δ are given in Fig. 3.6.

A state estimator is simulated to demonstrate the usefulness of this tuning control for observability. A Unscented Kalman Filter is implemented with measurement noise $R = 10^{-2} I$. Estimates are initialized at $\hat{\mathbf{x}} = \mathbf{0}$ with an initial covariance matrix of $P = 10^{-1} I$. Simulation result is shown in Fig. 3.7. As it is shown in this figure, in case of $w = 0$, the estimator does not converge to the true value. For both values of $\delta = 10$ and $\delta = 100$, the covariance converges to zero.

3.6 Conclusion

This chapter concerned with obtaining sufficient conditions for observability of a class of nonlinear systems which are linear with respect to the controls. An admissible control for a nonlinear system

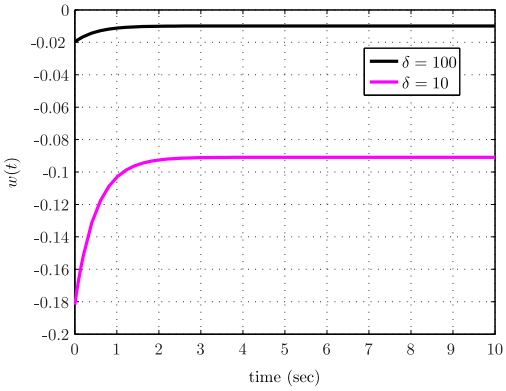

Figure 3.5: The tuning control given in (3.61) for two values of $\delta = 10$ and $\delta = 100$.

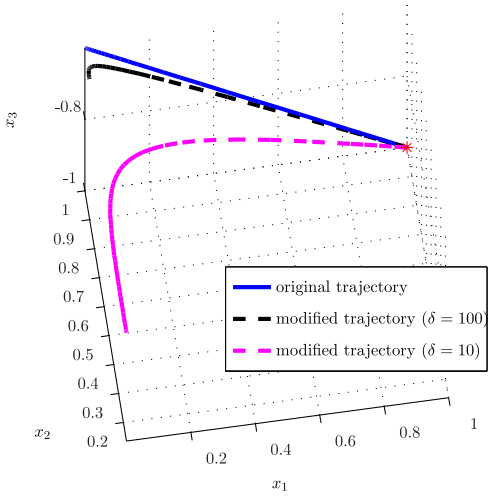

Figure 3.6: The nominal trajectory and the modified trajectories for $\delta = 10$ and $\delta = 100$.

was computed using three methods: Non-zero determinant of $d\mathcal{O}'$, finite condition number of $d\mathcal{O}'$ and generating orthogonal $d\mathcal{O}'$ matrix.

Determinant of $d\mathcal{O}'$ is one index of observability considered here. A value of the determinant of zero indicates that the matrix is rank deficient, corresponding to a system that is not observable. The determinant advantageously includes all of the terms in the matrix. Most scalar functions other than the determinant do not include all of the observability information from the matrix as they

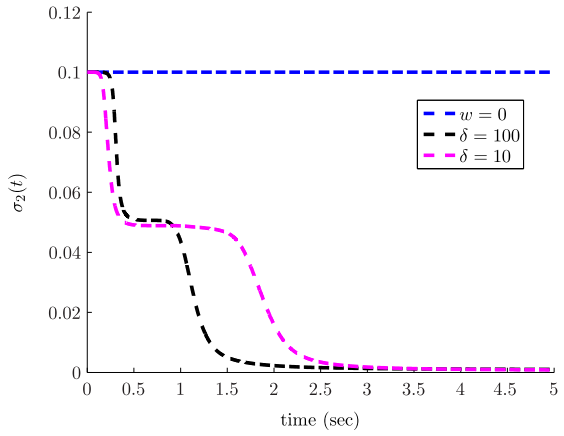

Figure 3.7: State estimate covariance of state x_2 for two values of $\delta = 10$ and $\delta = 100$.

only operate on certain terms in the matrix. However, the determinant of the observability matrix is mentioned as useful, but often not incorporated into the final approach. This may be due to the complexity that the determinant causes in the final problem formulation. It should also be pointed out that for systems that are marginally observable, this metric creates numerical problems. This occurs often in systems with many states, in situations where few are being measured.

Another index of interest was the condition number of $d\mathcal{O}'$, which provides a measure of the difference of the quality of observability of the state components, where $\kappa(d\mathcal{O}') = 1$ if all the state components have the same quality of observability. This observability index quantifies the closeness to singularity of the mapping created by the measurement function and its higher Lie derivatives used to observe the system. Singularities in the map cause observability to decrease and information about the system to be lost. The calculation of a matrix condition number, compared to the determinant index, would provide a more robust determination of the ill-conditioning inherent in a given observability matrix. However, similar to the determinant index, the high complexity in the final problem formulation is a drawback of this observability index.

Finally we proposed an index of observability based on orthogonality of $d\mathcal{O}'$. As it was discussed above, the determinant and the condition number measures are difficult to implement. Compared to two other measures, constructing an admissible control in sense that the observability matrix, $d\mathcal{O}'$, is as close as possible to an orthogonal matrix was easier to implement.

The next step is obtaining an algorithm to stabilize the system and optimize the observability of the system at the same time. Addressing system stability while improving observability is the subject of Chapter 4. In addition, some types of nonlinear systems, such as nonholonomic systems, are not stabilizable by time invariant state feedback control. The either discontinuous or time varying oscillatory control is a way to stabilize these kinds of nonlinear systems. Utilizing an oscillatory control to improve the observability of these types of nonlinear systems is the subject of Chapter 5.

Chapter 4

TIME-INVARIANT STATE FEEDBACK CONTROL

In this chapter, designing a feedback controller using optimal control problem is investigated. The fundamental idea in optimal control is to formulate the goal of control as the long-term optimization of a scalar cost function. In order to formulate this control design problem using optimal control, we must define a scalar objective which scores the long-term performance of running each candidate control policy, $\mathbf{u}(\mathbf{x})$, from each initial condition, $\mathbf{x}_0$, and a list of constraints that must be satisfied. Optimal control has a long history in robotics. For instance, there has been a great deal of work on the minimum-time problem for pick-and-place robotic manipulators, and the linear quadratic regulator (LQR) and linear quadratic regulator with Gaussian noise (LQG) have become essential tools for any controls engineer. With increasingly powerful computers and algorithms, the popularity of numerical optimal control has grown at an incredible pace over the last few years.

For linear systems, Linear Quadratic Regulation (LQR) is a well known and commonly used method for designing an optimal control law given a quadratic cost function of state and control. For nonlinear systems, optimal state feedback can be obtained from the solution of the Hamilton-Jacobi-Bellman (HJB) equation. This equation is usually hard to solve analytically, therefore different approximation methods have been used to obtain suboptimal feedback control policies for quadratic [71, 72] or non-quadratic [19, 73] cost functionals. Most of these solution methods involve solving Riccati equations and a series of linear algebraic or differential equations.

It was shown in the previous chapters that one might be able to make a system more observable by changing the control inputs. However, nonlinear observability analysis is computationally expensive. Several measures have been discussed in Section 2.1 to evaluate the observability of a system. In the case of the observability-based optimization problem, the observability Gramian has been the most popular observability notion. In order to perform an optimization on the observability Gramian matrix, a scalar function of the matrix must be chosen. The smallest singular value, the determinant, the trace of the inverse of the Gramian, and the spectral norm of the observability Gramian are some

of the criteria have been used for observability optimization. The notion of observability used in this chapter is the trace of the empirical observability Gramian. This quantity was used as a measure of the level of observability for nonlinear systems (e.g. Kang and Xu in [74]). The equivalence between the measure of output energy as an observability index and the observability Gramian for linear systems is explored in [75].

The problem of deriving controls that maximize the observability characteristics is important, for example, in the case of exploring unknown unstructured environments. The robot can use the path that maximizes observability to localize itself or construct a map of the environment [12, 14]. In [12], an optimal path is given for a specific type of nonlinear system ($\dot{\mathbf{x}} = G(\mathbf{x})\mathbf{u}$, where $G(\mathbf{x})$ is invertible) and triangulation measurements. Yu *et al.* in [13] developed a path planning algorithm based on dynamic programming for navigation of an MAV using bearing-only measurements. In this algorithm, at each time step one of three possible choices of roll command is selected by solving an optimization problem based on an observability criterion for the chosen path. In [14], sampling trajectories for autonomous vehicles are selected to maximize observability of an environmental flow field. In that work, an iteration technique was used on a finite number of sampling parameters rather than over all possible sampling trajectories. The optimized path was computed by exhaustive search. Each of these approaches are applicable for a specific type of nonlinear system; solving the problem of choosing controls to improve the observability of an arbitrary nonlinear system is a difficult problem. In comparison with the above-mentioned observability-based path planning algorithms, the state feedback obtained in this chapter can be applied to a larger family of nonlinear systems, and it also ensures the stability of the nonlinear system. A recursive algorithm is used to find a solution to our optimization problem which maximizes the observability while ensuring stability.

4.1 Control Design as An Optimization

The long-term cost for a trajectory can be written as

$$\int_0^{t_f} l(\mathbf{x}(t), \mathbf{u}(t))\mathrm{d}t\,, \tag{4.1}$$

where $l(\cdot)$ is the instantaneous cost, and t_f can be either a finite real number or ∞. Thus the optimal cost-to-go for an initial point $\mathbf{x}_0$ is given by

$$J^*(\mathbf{x}_0) = \min_{\mathbf{u}} \quad \int_0^{t_f} l(\mathbf{x}(t), \mathbf{u}(t)) \mathrm{d}t \,. \tag{4.2}$$

For a system $\dot{\mathbf{x}} = \mathbf{f}(\mathbf{x}, \mathbf{u})$ and an infinite-horizon additive cost $\int_0^{\infty} l(\mathbf{x}(t), \mathbf{u}(t)) \mathrm{d}t$, we have:

$$0 = \min_{\mathbf{u}} \quad \left[l(\mathbf{x}, \mathbf{u}) + \frac{\partial J^*}{\partial \mathbf{x}} \mathbf{f}(\mathbf{x}, \mathbf{u}) \right] , \tag{4.3}$$

$$\mathbf{u}^*(\mathbf{x}) = \operatorname*{argmin}_{\mathbf{u}} \quad \left[l(\mathbf{x}, \mathbf{u}) + \frac{\partial J^*}{\partial \mathbf{x}} \mathbf{f}(\mathbf{x}, \mathbf{u}) \right] . \tag{4.4}$$

Equation (4.3) is known as the Hamilton-Jacobi-Bellman (HJB) equation, and gives sufficient condition for optimality.

Now, assume a nonlinear system in control affine form as given by (2.9). Let also assume that we only restrict ourselves to instantaneous cost functions of the form

$$l(\mathbf{x}, \mathbf{u}) = l_0(\mathbf{x}) + \mathbf{u}^T R \mathbf{u} \,, \;\; R = R^T \succ 0 \,. \tag{4.5}$$

Given these assumptions, we can write the HJB (4.3) as

$$0 = \min_{\mathbf{u}} \quad \left[l_0(\mathbf{x}) + + \mathbf{u}^T R \mathbf{u} + \frac{\partial J}{\partial \mathbf{x}} \Big(\mathbf{f}_0(\mathbf{x}) + F(\mathbf{x}) \mathbf{u} \Big) \right] , \tag{4.6}$$

where $F(\mathbf{x}) = \begin{bmatrix} \mathbf{f}_1(\mathbf{x}) & \mathbf{f}_2(\mathbf{x}) & \dots & \mathbf{f}_p(\mathbf{x}) \end{bmatrix}$. Since (4.6) is a quadratic function in $\mathbf{u}$, if the system does not have any constraints on $\mathbf{u}$, then we can solve in closed-form for the minimizing $\mathbf{u}$ by taking the gradient of the right-hand side, and setting it equal to zero, as:

$$2\mathbf{u}^T R + \frac{\partial J}{\partial \mathbf{x}} F(\mathbf{x}) = 0 \,, \;\; R = R^T \succ 0 \,, \tag{4.7}$$

to obtain

$$\mathbf{u}^* = -\frac{1}{2} R^{-1} F^T(\mathbf{x}) \frac{\partial J}{\partial \mathbf{x}}^T \,. \tag{4.8}$$

Now, we can substitute (4.8) in (4.6) to obtain

$$-\frac{1}{4} \frac{\partial J^*}{\partial \mathbf{x}} F(\mathbf{x}) R^{-1} F^T(\mathbf{x}) + \frac{\partial J^*}{\partial \mathbf{x}}^T + \frac{\partial J^*}{\partial \mathbf{x}} \mathbf{f}_0(\mathbf{x}) + l_0(\mathbf{x}) = 0 \,. \tag{4.9}$$

These partial differential equations can be solved to obtain the optimal cost-to-go, J^*, and the optimal control, $\mathbf{u}^*$ using (4.8).

It was shown, here, that for a nonlinear system in control affine form, and an instantaneous cost in the form of (4.5), there exists an optimal control given as (4.8). The major barrier of using the HJB equation to obtain the optimal control is finding an analytic solution for the cost-to-go, J^*. In the next section, a numerical algorithm is developed to find the optimal control.

The formulation in this section mainly obtained from [76].

4.2 A Quantitative Measure of Observability

Empirical observability gramian, introduced in Section 2.3.1, is used to introduce an index to measure the level of observability. This index is called *observability index*. Here, this index is introduced. The trace of the empirical observability Gramian is used as a measure of observability, which is given by

$$\mathrm{trace}(\bar{W}) = \frac{1}{4\epsilon^2}\int_0^\infty \sum_{i=1}^{n} \left\|\mathbf{h}(\mathbf{x}^{+i}(t)) - \mathbf{h}(\mathbf{x}^{-i}(t))\right\|^2 \mathrm{d}t. \tag{4.10}$$

In order to preserve the asymptotic convergence property of the closed loop state trajectory, the influence of the observability measure on the behaviour of the controlled system is designed to fade. An admissible function for the observability index, $l_2(t, \mathbf{x}, \mathbf{x}^1, \cdots, \mathbf{x}^n)$, is

$$l_2(t, \mathbf{x}, \mathbf{x}^1, \cdots, \mathbf{x}^n) = e^{-t}\mathrm{sat}_\zeta\left(\frac{1}{4\epsilon^2}\sum_{i=1}^{n}\left\|\mathbf{h}(\mathbf{x}^{+i}) - \mathbf{h}(\mathbf{x}^{-i})\right\|^2\right), \tag{4.11}$$

where, $\mathrm{sat}_\zeta(x)$ is given by

$$\mathrm{sat}_\zeta(x) = \begin{cases} \zeta & \text{if } x > \zeta \\ x & \text{if } x \leq \zeta \end{cases} \tag{4.12}$$

where $\zeta > 0$ is chosen to be a value to make sure that the optimization problem is feasible and meaningful. The optimization problem is introduced in the next section.

4.3 Optimal Linear State Feedback

The cost function has two parts: 1) $l_1(\mathbf{x}, \mathbf{u})$ which takes into account the input energy and the distance to the desired steady state trajectory, and 2) an observability index $l_2(t, \mathbf{x}, \mathbf{x}^{\pm 1}, \cdots, \mathbf{x}^{\pm n})$ which is a transient term takes into account the local observability of the system. The cost function is given by:

$$\min_{\mathbf{x},\mathbf{u}} \quad J = \int_0^\infty \left\{l_1(\mathbf{x}, \mathbf{u}) - l_2(t, \mathbf{x}, \mathbf{x}^{\pm 1}, \cdots, \mathbf{x}^{\pm n})\right\} \mathrm{d}t\,, \tag{4.13}$$

where, $l_1(\mathbf{x},\mathbf{u}) = \mathbf{x}^T Q\mathbf{x} + \mathbf{u}^T R\mathbf{u}$ and $l_2(\mathbf{x},\mathbf{x}^{\pm 1},\cdots,\mathbf{x}^{\pm n},t)$ was introduced in (4.11). In this cost functional, the integral of control effort (i.e., the $\mathbf{u}^T R\mathbf{u}$ term) plus the square of a norm of the states (i.e., the $\mathbf{x}^T Q\mathbf{x}$ term), and the observability criterion is minimized.

The idea, here, is to design a piece-wise linear state feedback. Assume we have $0 = t_0 < t_1 < \cdots < t_j < t_{j+1} < \cdots < t_f$, then the optimal linear state feedback control for $t \in [t_j \;\; t_{j+1})$ is given by

$$\mathbf{u}^*(t) = \underset{\mathbf{x},\mathbf{u}}{\operatorname{argmin}} \quad \int_{t_j}^{t_{j+1}} \left\{ l_1(\mathbf{x},\mathbf{u}) - l_2(t,\mathbf{x},\mathbf{x}^{\pm 1},\cdots,\mathbf{x}^{\pm n}) \right\} \mathrm{d}t + L(\mathbf{x}(t_{j+1}),t_{j+1}) \,, \tag{4.14}$$

$L(\mathbf{x}(t_{j+1}),t_{j+1})$ is the cost-to-go at the final time of the interval $[t_j \;\; t_{j+1}]$.

To have a meaningful optimization problem, it is desired to have $\mathbf{x}^T Q\mathbf{x} - l_2(\cdot) \geq 0$. The saturation limit, ζ, can be chosen equal to $\mathbf{x}^T Q\mathbf{x}$ to insure $\mathbf{x}^T Q\mathbf{x} - l_2(\cdot)$ remains a positive semi-definite function.

The saturation limit can be set to a constant number, in case we have information on the rate of convergence of the system. Given a nonlinear system $\dot{\mathbf{x}} = \mathbf{f}(\mathbf{x},\mathbf{u})$, assume that there is a lower-bound, β, on the rate of decay of the nonlinear system, such that

$$\|\mathbf{x}(t)\|_Q \geq e^{-\beta t} \|\mathbf{x}(t_j)\|_Q \,, \quad \forall t \in [t_j, t_{j+1}], \tag{4.15}$$

where $\|\cdot\|_Q$ is norm of a vector associated with positive semi-definite matrix Q. In this case, the saturation parameter, ζ, could be set to

$$\zeta = \begin{cases} \|\mathbf{x}(t_j)\|_Q^2 & \text{if} \quad 0 < \beta \leq \dfrac{1}{2}, \\ e^{(1-2\beta)t_f} \|\mathbf{x}(t_j)\|_Q^2 & \text{if} \qquad \beta > \dfrac{1}{2} \,. \end{cases} \tag{4.16}$$

Theorem 8. *Given a nonlinear system* $\dot{\mathbf{x}} = \mathbf{f}(\mathbf{x},\mathbf{u})$*, if condition* (4.15) *is satisfied. Then the saturation parameter,* ζ*, given by* (4.16) *guarantees* $l_0(\mathbf{x}) = \mathbf{x}^T Q\mathbf{x} - l_2(\cdot) \geq 0$.

Proof. From (4.16) we have

$$\zeta \leq e^{(1-2\beta)t} \|\mathbf{x}(t_j)\|_Q^2 \,. \tag{4.17}$$

Now using (4.15), one can conclude that

$$\zeta \leq e^t \|\mathbf{x}(t)\|_Q^2, \;\; \forall t \in [t_j, t_{j+1}] \,. \tag{4.18}$$

From definition of saturation function, given by (4.12), we have $\text{sat}_\zeta(\cdot) \leq \zeta$. Then

$$\begin{aligned} &\|\mathbf{x}\|_Q^2 - l_2(\cdot) \geq 0\,, \\ &\mathbf{x}^T Q \mathbf{x} - l_2(\cdot) \geq 0\,, \;\; \forall t \in [t_j, t_{j+1}]\,. \end{aligned} \tag{4.19}$$

□

The cost function given in (4.14) does not directly maximize the observability notion, but the observability term, $l_2(t, \mathbf{x}, \mathbf{x}^{\pm 1}, \cdots, \mathbf{x}^{\pm n})$, tunes the cost function so that the obtained optimal control drives the system to be more observable. Maximizing the observability notion while ignoring the remaining terms makes the system unstable in many cases. Therefore, Q should be chosen to be non-zero. In this case, $l_1(\mathbf{x}, \mathbf{u})$ index determines the asymptotic behaviour of the closed loop system, while $l_2(t, \mathbf{x}, \mathbf{x}^{\pm 1}, \cdots, \mathbf{x}^{\pm n})$ specifies the desired transient behaviour of the system.

The governing equation of motion is nonlinear. Finding the optimal control is obtained by solving partial differential equation (4.9). There is no analytical solution of this PDE, and solving this PDE is hardly possible in general case. To simplify the problem, the problem of obtaining optimal control over the entire time interval is divided to some smaller problems of finding an optimal control in the form of a linear feedback control policy $\mathbf{u} = K\mathbf{x}$ for small time intervals. Without loss of generality, consider the first time interval, $[0 \;\; t_1]$. By substitution of $\mathbf{u} = K\mathbf{x}$ into (4.14), the cost functional can be approximated as:

$$J(K) = \int_0^{t_f} \Gamma(t, \mathbf{x}, \mathbf{x}^{\pm 1}, \cdots, \mathbf{x}^{\pm n}, K) \mathrm{d}t + L(\mathbf{x}(t_1), t_1)\,, \tag{4.20}$$

where,

$$\Gamma(t, \mathbf{x}, \mathbf{x}^{\pm 1}, \cdots, \mathbf{x}^{\pm n}, K) = \mathbf{x}^T \left(K^T R K + Q\right) \mathbf{x} - l_2(t, \mathbf{x}, \mathbf{x}^{\pm 1}, \cdots, \mathbf{x}^{\pm n})\,. \tag{4.21}$$

Now, considering the dynamics of the nonlinear system, the optimization problem can be expressed as

$$\begin{aligned} \underset{K}{\text{minimize}} \quad & J(K) = \int_0^{t_1} \Gamma(t, \mathbf{x}, \mathbf{x}^{\pm 1}, \cdots, \mathbf{x}^{\pm n}, K) \mathrm{d}t + L(\mathbf{x}(t_1), t_1) \\ \text{subject to} \quad & \dot{\mathbf{x}} = \mathbf{f}(\mathbf{x}, \mathbf{u}), \;\; \mathbf{x}(0) = \mathbf{x}_0, \\ & \dot{\mathbf{x}}^{\pm k} = \mathbf{f}(\mathbf{x}^{\pm k}, \mathbf{u}), \;\; \mathbf{x}^{\pm k}(0) = \mathbf{x}_0 \pm \epsilon \mathbf{e}_k\,, \;\; k = 0, \cdots, n\,. \end{aligned} \tag{4.22}$$

The optimal K should be found to minimize cost-to-go, J.

4.3.1 Optimization Algorithm

In this section, an algorithm will be presented to find an optimal control policy in the sense of observability that optimizes a cost function with additional performance index, which improves observability. Here, a recursive gradient-based algorithm will be use to find a solution of this optimization problem.

First, define a new variable

$$x_{n+1}(t) = \int_0^t \Gamma(\tau, \mathbf{x}(\tau), \mathbf{x}^{\pm 1}(\tau), \cdots, \mathbf{x}^{\pm n}(\tau), K) d\tau + L(\mathbf{x}(t), t). \tag{4.23}$$

It is obvious that $x_{n+1}(0) = L(\mathbf{x}_0, 0)$ and $x_{n+1}(t_1) = J$. Define a new state vector as

$$\bar{\mathbf{x}} = \begin{bmatrix} \mathbf{x} \\ \mathbf{x}^{\pm 1} \\ \vdots \\ \mathbf{x}^{\pm n} \\ x_{n+1} \end{bmatrix}.$$

Then,

$$\dot{\bar{\mathbf{x}}} = \begin{bmatrix} \dot{\mathbf{x}} \\ \dot{\mathbf{x}}^{\pm 1} \\ \vdots \\ \dot{\mathbf{x}}^{\pm n} \\ \dot{x}_{n+1} \end{bmatrix} = \mathbb{H}(t, \bar{\mathbf{x}}, K)\,; \;\; \bar{\mathbf{x}}(0) = \begin{bmatrix} \mathbf{x}(0) \\ \mathbf{x}(0) \pm \epsilon \mathbf{e}_1 \\ \vdots \\ \mathbf{x}(0) \pm \epsilon \mathbf{e}_n \\ L(\mathbf{x}_0, 0) \end{bmatrix}, \tag{4.24}$$

where,

$$\mathbb{H}(t, \bar{\mathbf{x}}, K) = \begin{bmatrix} \mathbf{f}(\mathbf{x}, K) \\ \mathbf{f}(\mathbf{x}^{\pm 1}, K) \\ \vdots \\ \mathbf{f}(\mathbf{x}^{\pm n}, K) \\ \Gamma(t, \mathbf{x}, \mathbf{x}^{\pm 1}, \cdots, \mathbf{x}^{\pm n}, K) + \dot{L}(\mathbf{x}, t) \end{bmatrix}, \tag{4.25}$$

and, $\mathbf{f}(\mathbf{x}, K)$ is given in (2.9) substituting $\mathbf{u} = K\mathbf{x}$. The optimization problem can now be summarized as

$$\begin{aligned} \underset{K}{\text{minimize}} \quad & J = x_{n+1}(t_1) \\ \text{subject to} \quad & \dot{\bar{\mathbf{x}}} = \mathbb{H}(t, \bar{\mathbf{x}}, K). \end{aligned} \tag{4.26}$$

To solve this optimization problem, the gradient vector, $\frac{\partial J}{\partial K} = \left.\frac{\partial x_{n+1}}{\partial K}\right|_{t=t_1}$, is required. In [73], a method is demonstrated for solving a similar problem. By defining $\bar{X}_K = \frac{\partial \bar{\mathbf{x}}}{\partial K}$, and applying the chain rule, we have

$$\dot{\bar{X}}_K = \frac{\partial \mathbb{H}}{\partial \bar{\mathbf{x}}}\frac{\partial \bar{\mathbf{x}}}{\partial K} + \frac{\partial \mathbb{H}}{\partial K} = \frac{\partial \mathbb{H}}{\partial \bar{\mathbf{x}}}\bar{X}_K + \frac{\partial \mathbb{H}}{\partial K},$$
$$\bar{X}_K(0) = \mathbf{0}. \tag{4.27}$$

Notice that if the system is multi-input, K is a matrix, and the term $\frac{\partial \bar{\mathbf{x}}}{\partial K}$ is the derivative of a vector with respect to a matrix, which results in a higher order tensor. To include multi-input as well as single-input control problems, using conventional algebra with vectors and matrices, we need to have separate equations for $\bar{X}_{\mathbf{k}_i} = \frac{\partial \bar{\mathbf{x}}}{\partial \mathbf{k}_i}, i = 1 \dots p$, where $\mathbf{k}_i$ is the i^{th} row of matrix K.

Now (4.24) and (4.27) should be solved together for $0 < t < t_1$. The last row of $\bar{X}_K$ at $t = t_1$ are the gradient vectors which can be used for improving the optimal value of K. Based on these observations, an iterative algorithm for obtaining the optimal feedback gain, K^*, is presented here.

The iteration stops when the gradient vector becomes small enough or remains almost unchanged. The algorithm also checks the convexity at the obtained solution to insure that the solution is a local minimum. The value of K is updated based upon the gradient descent rule. The step size Θ_i is a positive definite matrix, which should be chosen with a norm small enough that stability is guaranteed. Section 4.5 presents discussion on the relation between step size and stability.

4.4 Convergence

The gradient method is very popular mainly because of its simplicity. It requires the calculation of a gradient, but not the second derivatives. One of the parameters that must be chosen in this method is step size. The step size can be chosen in a variety of ways [77]. Stability of the system for a sufficiently small step size will be proved in section 4.5.

Proposition 5. *Any direction that makes an angle of strictly less than $\frac{\pi}{2}$ with $-\nabla J$ is guaranteed to produce a decrease in J provided that the step size is sufficiently small [77].*

Proof. Suppose that the cost function J, given in (4.20), is continuously differentiable. Then Taylor's theorem can be used to prove this proposition. The details of this proof can be found in Wright

Choose step size $\Theta_0 \succeq 0$;

Choose K_0, an initial value for K that stabilizes the system;

cvxCheck : = TRUE;

Choose a convergence tolerance ϵ_t;

repeat

Solve (4.24) and (4.27) together for $0 < t < t_1$;

$\mathbf{g}_i$:= the last row of $\bar{X}_K$ at $t = t_1$;

$K_{i+1} = K_i - \Theta_i \mathbf{g}_i$;

Calculate H such that $H[mn] = \frac{\mathbf{g}_i[m] - \mathbf{g}_{i-1}[m]}{K_{i+1}[n] - K_i[n]}$;

if $H \succeq 0$ **then**

cvxCheck := TRUE ;

else

cvxCheck := FALSE ;

end

if *cvxCheck is TRUE* **then**

Update step size Θ_i;

else

Do not change step size;

end

until $\|\mathbf{g}_i\| \leq \epsilon_t$ *AND cvxCheck is TRUE*;

Algorithm 1: Iterative algorithm to find K^*

and Nocedal [77]. □

The suggested rule for step size selection here is

$$\mu_i = \frac{\mu_0}{i}, \tag{4.28}$$

where, $0 < \mu_0 < \infty$ is constant, and i is the iteration counter. This step size policy, which is called

Square summable but not summable, satisfies

$$\begin{aligned}\sum_{i=1}^{\infty}\mu_i &= \sum_{i=1}^{\infty}\frac{\mu_0}{i} = \mu_0\sum_{i=1}^{\infty}\frac{1}{i} = \infty \\ \sum_{i=1}^{\infty}\mu_i^2 &= \sum_{i=1}^{\infty}\frac{\mu_0^2}{i^2} = \mu_0^2\sum_{i=1}^{\infty}\frac{1}{i^2} < \infty.\end{aligned} \tag{4.29}$$

It is worthy to note that because of the transient term (l_2) the cost functional $J(K)$ is not convex. But since the transient term is bounded, the cost functional is bounded by two convex functions as shown in Fig. 4.1. The lower and upper bounds are given by

$$\begin{aligned}\underline{J} &= \int_{t_j}^{t_{j+1}} \{l_1(\mathbf{x},\mathbf{u}) - \zeta\}\,\mathrm{d}t + L(\mathbf{x}(t_f), t_f) \\ \bar{J} &= \int_{t_j}^{t_{j+1}} l_1(\mathbf{x},\mathbf{u})\mathrm{d}t + L(\mathbf{x}(t_f), t_f)\,.\end{aligned} \tag{4.30}$$

Both of lower and upper bounds ($\underline{J}$ and $\bar{J}$) are convex functions. Therefore, the cost function cannot be concave over the entire search space and there should exist some regions over which the cost function is locally convex. We assume, here, that after a finite number of iterations, the algorithm ends up at a locally convex point and after that remains at convex region around that point until the algorithm converges to a local minimum.

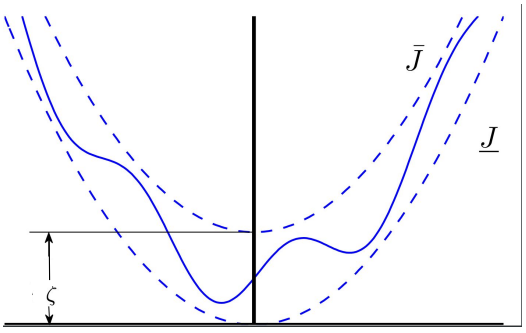

Figure 4.1: Illustrative figure of the upper and lower bounds of the cost function.

Here, a proof of convergence is given. It is assumed that K^* is a local minimum of J, and also it is assumed that the norm of the gradient vectors, $\mathbf{g}_i$, are bounded, i.e., there is a G such that $\|\mathbf{g}_i\|_2 \leq G$ for all i. This is the case if $J(K)$ satisfies the Lipschitz condition,

$$|J(K_{i_1}) - J(K_{i_2})| \leq G\|K_{i_1} - K_{i_2}\|_2, \tag{4.31}$$

for all i_1 and i_2. Recall that K^* is a local minimum of J, so there is a neighbourhood U containing K^* such that the function is convex on this neighbourhood. It is assumed here that $K_j \in U, j = 0, ..., i+1$, so we have

$$\begin{aligned} \|K_{i+1} - K^*\|_2^2 = \|K_i - \mu_i \mathbf{g}_i - K^*\|_2^2 = \|K_i - K^*\|_2^2 - 2\mu_i \mathbf{g}_i (K_i - K^*) + \mu_i^2 \|\mathbf{g}_i\|_2^2 \\ \leq \|K_i - K^*\|_2^2 - 2\mu_i \left(J(K_i) - J^*\right) + \mu_i^2 \|\mathbf{g}_i\|_2^2, \end{aligned} \tag{4.32}$$

where, $J^* = J(K^*)$. The inequality above comes from the property of the gradient vector of a convex function which is

$$J(K^*) \geq J(K_i) + \mathbf{g}_i (K^* - K_i). \tag{4.33}$$

Applying the inequality above recursively, we have

$$\|K_{i+1} - K^*\|_2^2 \leq \|K_0 - K^*\|_2^2 - 2 \sum_{j=0}^{i} \mu_j \left(J(K_j) - J^*\right) + \sum_{j=0}^{i} \mu_j^2 \|\mathbf{g}_j\|_2^2, \tag{4.34}$$

then

$$2 \sum_{j=0}^{i} \mu_j \left(J(K_j) - J^*\right) \leq \|K_0 - K^*\|_2^2 + \sum_{j=0}^{i} \mu_j^2 \|\mathbf{g}_j\|_2^2. \tag{4.35}$$

If we define $J_{sol}^{(i)} = \min\limits_{j=0,...,i} J(K_j)$ as the solution of the algorithm after i iterations, then we have

$$J_{sol}^{(i)} - J^* \leq \frac{\|K_0 - K^*\|_2^2 + \sum_{j=0}^{i} \mu_j^2 \|\mathbf{g}_j\|_2^2}{2 \sum_{j=0}^{i} \mu_j}. \tag{4.36}$$

Finally, using the assumption $\|\mathbf{g}_i\|_2 \leq G$, we obtain the inequality

$$J_{sol}^{(i)} - J^* \leq \frac{\|K_0 - K^*\|_2^2 + G^2 \sum_{j=0}^{i} \mu_j^2}{2 \sum_{j=0}^{i} \mu_j}. \tag{4.37}$$

If $K_i \in U$ when $i \to \infty$, then by applying the conditions given in (4.29)

$$\lim_{i \to \infty} J_{sol}^{(i)} - J^* \leq \lim_{i \to \infty} \frac{\|K_0 - K^*\|_2^2 + G^2 \sum_{j=0}^{i} \mu_j^2}{2 \sum_{j=0}^{i} \mu_j} = 0. \tag{4.38}$$

Therefore, the gradient method proposed above converges to the local minimum K^*. Otherwise, if at an iteration, say $k < \infty$, $K_k \notin U$, then there is always a finite number of iterations, say k', such that $K_{k+k'} \in U'$, where U' is also a neighbourhood over which the function is convex and it contains a local minimum. We can use the same proof given above for this local minimum. Finally it can be shown that the algorithm converges to a local minimum.

The discussion above shows the convergence of the algorithm. Other methods, such as Newton's method, can be used to improve the rate of convergence. But these methods require the calculation of the Hessian matrix $\nabla^2 J$ or an approximation of this matrix. Explicit computation of the Hessian matrix is often an expensive process. Some approaches such as the quasi-Newton method can be used to estimate the Hessian matrix. However, any of these higher order methods that can be used to achieve higher rate of convergence do so at the cost of increased complexity. Improving the rate of convergence is not the main focus here. More discussion on different methods can be found in Wright and Nocedal [77].

4.5 Stability of Closed Loop System

4.5.1 Local Stability in Case of Control-Affine Form

Here, it will be shown that Algorithm 1 maintains the local stability about an equilibrium point, if the initial choice for K_0 satisfies local stability condition and the step size is small enough. Here, control affine nonlinear system of the following form is considered

$$\dot{\mathbf{x}} = \mathbf{f}(\mathbf{x}, \mathbf{u}) = \mathbf{f}_0(\mathbf{x}) + \sum_{j=1}^{p} \mathbf{f_j}(\mathbf{x}) u_j. \tag{4.39}$$

In this section we will assume $\Theta_i = \mu_i I_p$, where, μ_i is a positive scalar and I_p is $p \times p$ identity matrix. Here, it will be shown that the proper selection of μ_i can ensure the local stability of the closed loop nonlinear system. The proof is based on induction. Let us assume K_i drives the system to be locally stable about an equilibrium point $\mathbf{x}_{ss}$:

$$\dot{\mathbf{x}} = \mathbf{f}(\mathbf{x}, K_i)\,, \;\; \mathbf{f}(\mathbf{x}_{ss}) = \mathbf{0}\,, \;\; F^i = \left.\frac{\partial \mathbf{f}(\mathbf{x}, K_i)}{\partial \mathbf{x}}\right|_{\mathbf{x}_{ss}}. \tag{4.40}$$

Consider the perturbations about this equilibrium point:

$$\begin{aligned} \mathbf{x} &= \mathbf{x}_{ss} + \delta\mathbf{x} \\ \delta\dot{\mathbf{x}} &= F^i \delta\mathbf{x} + h.o.t. \end{aligned} \tag{4.41}$$

Since it is assumed that K_i maintains the local stability, then

$$\Re\{\lambda(F^i)\} < 0, \tag{4.42}$$

where, $\Re\{.\}$ and $\lambda(.)$ are the real part of a complex number and the set of eigenvalues respectively. The objective is to show there always exists an upper bound, $\mu_0 > 0$, such that for all $0 < \mu_i < \mu_0$ the nonlinear system at iteration $i+1$ is locally stable. At iteration $i+1$:

$$\dot{\mathbf{x}} = \mathbf{f}(\mathbf{x}, K_{i+1}) = \mathbf{f}(\mathbf{x}, K_i) + \mu_i \sum_{j=1}^{p} -\mathbf{f}_j(\mathbf{x}) e^j \mathbf{g}_i \mathbf{x}, \tag{4.43}$$

where, the row vector e^j is the j^{th} unit vector in $\mathbb{R}^p$. Linearising about the equilibrium point, , gives us

$$\begin{aligned} \delta\dot{\mathbf{x}} &= F^{i+1}\delta\mathbf{x} + h.o.t\,, \\ F^{i+1} &= F^i + \mu_i \sum_{j=1}^{p} \left.\frac{\partial\big(-\mathbf{f}_j(\mathbf{x}) e^j \mathbf{g}_i \mathbf{x}\big)}{\partial \mathbf{x}}\right|_{\mathbf{x}_{ss}}. \end{aligned} \tag{4.44}$$

The eigenvalues of matrix F^{i+1} at iteration $i+1$ can be given as:

$$\lambda\left(F^{i+1}\right) = \lambda\left(F^i + \mu_i \sum_{j=1}^{p} \left.\frac{\partial\left(-\mathbf{f}_j(\mathbf{x}) e^j \mathbf{g}_i \mathbf{x}\right)}{\partial \mathbf{x}}\right|_{\mathbf{x}_{ss}}\right), \tag{4.45}$$

where,

$$\left.\frac{\partial\left(-\mathbf{f}_j(\mathbf{x}) e^j \mathbf{g}_i \mathbf{x}\right)}{\partial \mathbf{x}}\right|_{\mathbf{x}_{ss}} = -\mathbf{f}_j(\mathbf{x}_{ss}) e^j \mathbf{g}_i - \left(e^j \mathbf{g}_i \mathbf{x}_{ss}\right) \left.\frac{\partial \mathbf{f}_j}{\partial \mathbf{x}}\right|_{\mathbf{x}_{ss}}. \tag{4.46}$$

Here, it is assumed that the matrix given by (4.46) has finite value indices, which is a valid assumption, because in real systems, it is rare that the control vector, $\mathbf{f}_j(\mathbf{x}_{ss})$, has any infinite values or infinite-valued derivatives. The eigenvalues of a matrix are a continuous function of the elements of that matrix, therefore, the eigenvalues of F^{i+1} at iteration $i+1$ are a continuous function of μ_i. Since it is assumed that the system is locally stable at iteration i, then $\Re\{\lambda(F^{i+1})\} < 0$ for $\mu_i = 0$. Therefore, if $\mu_i \to 0$, the eigenvalues of F^{i+1} continuously move toward the eigenvalues of F^i. Thus, there is always $\mu_0 > 0$, such that for all $0 < \mu_i < \mu_0$, the local stability is guaranteed.

4.5.2 Lyapunov Stability

Here, stability of the system in the sense of Lyapunov is investigated. The observability term is a transient term. Here we assume that this term is upper bounded by an integrable function $b(t)$:

$$\begin{aligned} &l_2(t, \mathbf{x}) \le b(t), \;\; \forall t \ge 0, \mathbf{x} \in \mathbb{R}^n, \mathbf{u} \in \mathbb{R}^p \\ &\mathcal{L}(t) = \int_t^{\infty} b(\tau)\mathrm{d}\tau < \infty, \;\; \forall t \ge 0. \end{aligned} \tag{4.47}$$

In section 4.3, an admissible function for l_2 was introduced, which satisfies the conditions given in (4.47). We also need to have a condition on the terminal cost, $L(t, \mathbf{x})$. The effect of terminal cost on the stability of the closed loop system has been studied for linear systems as well as nonlinear systems [17]. The terminal cost function should be positive semi-definite, continuously differentiable, and decrease faster than the value of the function $l_1(\mathbf{x}, \mathbf{u})$ along all admissible control inputs $\mathbf{u}$ and the corresponding trajectories $\mathbf{x}$. This condition is given as:

$$\dot{L}(t, \mathbf{x}) = L_t + L_{\mathbf{x}}\mathbf{f}(\mathbf{x}, \mathbf{u}) \leq -l_1(\mathbf{x}, \mathbf{u}). \tag{4.48}$$

By replacing l_1 with $l_1 + l_2$ in (4.48), we obtain the well known condition on the final cost for convergence to the origin of the finite-horizon optimal control problem. The idea of this replacement is from Alessandretti *et al.* [78].

Now, suppose $\mathbf{u}^*$ and $\mathbf{x}^*$ are the optimal control and its corresponding trajectory obtained from optimization problem (4.14) for $t \in [t_j \;\; t_{j+1})$. To show the stability of this control, a Lyapunov function is defined as:

$$\begin{aligned} V(t) = &\int_t^{t+\Delta t} \{l_1(\mathbf{x}^*, \mathbf{u}^*) - l_2(t, \mathbf{x}^*) + b(t)\}\, \mathrm{d}t + \mathcal{L}(t + \Delta t) + L(\mathbf{x}(t + \Delta t), t + \Delta t)\,, \\ &\forall t \in [t_i \;\; t_{i+1} - \Delta t]\,. \end{aligned} \tag{4.49}$$

Note that all terms in (4.49) are positive, therefore, $V(t) > 0$. Now we need to show that the Lyapunov function (4.49) is decreasing. In fact, the inequality $V(t+\delta) < V(t)$ should hold for any $\delta > 0$, such that $t + \delta \in [t_j \;\; t_{j+1} - \Delta t]$. At time $t + \delta$:

$$\begin{aligned} V(t+\delta) = &\int_{t+\delta}^{t+\delta+\Delta t} \{l_1(\mathbf{x}^*, \mathbf{u}^*) - l_2(t, \mathbf{x}^*) + b(t)\}\, \mathrm{d}t + \mathcal{L}(t + \delta + \Delta t) \\ &+ L(\mathbf{x}(t + \delta + \Delta t), t + \delta + \Delta t) = V(t) - \int_t^{t+\delta} \{l_1(\mathbf{x}^*, \mathbf{u}^*) - l_2(t, \mathbf{x}^*) + b(t)\}\, \mathrm{d}t \\ &+ \int_{t+\Delta t}^{t+\delta+\Delta t} \{l_1(\mathbf{x}^*, \mathbf{u}^*)\}\, \mathrm{d}t + \int_{t+\Delta t}^{t+\delta+\Delta t} \{-l_2(t, \mathbf{x}^*) + b(t)\}\, \mathrm{d}t + \mathcal{L}(t + \delta + \Delta t) - \mathcal{L}(t + \Delta t) \\ &+ L(\mathbf{x}(t + \delta + \Delta t), t + \delta + \Delta t) - L(\mathbf{x}(t + \Delta t), t + \Delta t). \end{aligned} \tag{4.50}$$

Based on the assumptions (4.47), we have

$$\int_{t+\Delta t}^{t+\delta+\Delta t} \{-l_2(t, \mathbf{x}^*) + b(t)\}\, \mathrm{d}t \leq \int_{t+\Delta t}^{t+\delta+\Delta t} b(t)\mathrm{d}t = \mathcal{L}(t + \Delta t) - \mathcal{L}(t + \delta + \Delta t), \tag{4.51}$$

and from assumption (4.48), one can conclude

$$-\int_{t+\Delta t}^{t+\delta+\Delta t} l_1(\mathbf{x}^*,\mathbf{u}^*)\mathrm{d}t \geq \int_{t+\Delta t}^{t+\delta+\Delta t} \dot{L}\mathrm{d}t = L(\mathbf{x}(t+\delta+\Delta t), t+\delta+\Delta t) - L(\mathbf{x}(t+\Delta t), t+\Delta t). \tag{4.52}$$

Therefore,

$$V(t+\delta) \leq V(t) - \int_t^{t+\delta} \{l_1(\mathbf{x}^*,\mathbf{u}^*) - l_2(t,\mathbf{x}^*) + b(t)\}\,\mathrm{d}t < V(t). \tag{4.53}$$

This proof guarantees the convergence of the closed loop state trajectory $\mathbf{x}(t)$ to origin.

The stability in the sense of Lyapunov can be proved for all intervals $[t_j \;\; t_{j+1})$. The stability of the closed loop system has been proved using Lyapunov approach. The basin of attraction obtained from Lyapunov function in $[t_j \;\; t_{j+1})$ contains the goal state of the previous interval ($\mathbf{x}(t_j)$). Therefore, the optimal control obtained here will stabilize the closed loop system. The idea of consecutive design of stabilizing control using Lyapunov function is very much inspired by LQR-Trees presented in [79].

4.6 Illustrative Examples

The control policies and the algorithms presented in this chapter are illustrated by implementing the results on two systems with different types of nonlinearities.

4.6.1 Linear Dynamics with Nonlinear Measurement

Assume our state space equations are given by the following linear dynamics and nonlinear observation:

$$\begin{aligned}\dot{\mathbf{x}} &= \mathbf{f}(\mathbf{x},u) = \begin{bmatrix}0\\ x_1\end{bmatrix} + \begin{bmatrix}1\\ 0\end{bmatrix} u = A\mathbf{x} + Bu\,,\\ h(\mathbf{x}) &= ||\mathbf{x}||_2 = \sqrt{x_1^2 + x_2^2}\,.\end{aligned} \tag{4.54}$$

First assume that we have a quadratic linear cost function $l(t) = 5x_1^2(t) + 5x_2^2(t) + u^2(t)$. In this case the optimal linear state feedback can be easily obtained by solving the LQR problem. The optimal feedback control in case of $l_2 = 0$ is $u = K\mathbf{x} = -3.08x_1 - 2.24x_2$. Now let add the

observability index to the optimization problem. Assume the instantaneous cost is given by:

$$l(t) = 5\left(x_1^2(t) + x_2^2(t)\right) + u^2(t) - e^{-t}\text{sat}_\zeta\left(\frac{1}{\epsilon^2}\sum_{i=1}^{2}\left(\left\|\mathbf{x}^i(t)\right\| - \left\|\mathbf{x}(t)\right\|\right)^2\right). \tag{4.55}$$

Let assume $t_f = 10$. The final cost needs to be chosen to meet the condition (4.48). The final cost can be set to $L(\mathbf{x}) = \mathbf{x}^T P\mathbf{x}$, where P is obtained from solving the following Lyapunov equation:

$$(A+BK)^T P + P(A+BK) + \left(5\begin{bmatrix}1 & 0\\ 0 & 1\end{bmatrix} + K^T K\right). \tag{4.56}$$

Now, to obtain a suboptimal state feedback control, the equations (4.24) and (4.27) are solved together for $0 < t < 10$ sec. The resulting trajectory for randomly chosen initial conditions can be seen in Fig. 4.2.

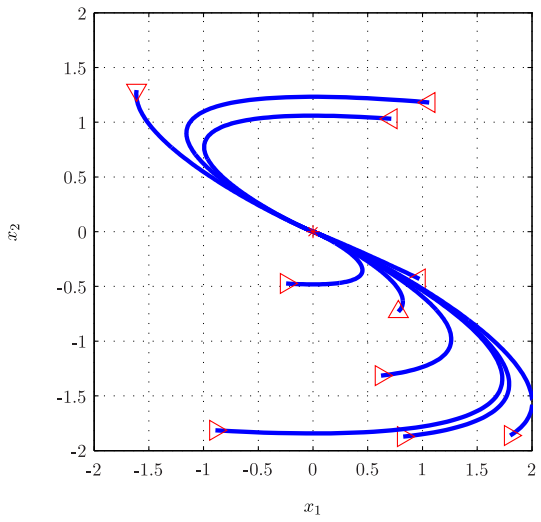

Figure 4.2: Sample Trajectories for the example (4.54) using optimal state feedback method.

4.6.2 Nonlinear Dynamics with Linear Measurement

The system we consider here contains two states and one control variable. This system, which has quadratic non-linearity, is given by

$$\begin{aligned}\dot{\mathbf{x}} &= \begin{bmatrix} -x_1 + x_2 + e^{x_2}u \\ x_1 x_2 - 1 \end{bmatrix} = \begin{bmatrix} -x_1 + x_2 \\ x_1 x_2 - 1 \end{bmatrix} + \begin{bmatrix} e^{x_2} \\ 0 \end{bmatrix} u \\ h(\mathbf{x}) &= x_1 = C\mathbf{x}\,. \end{aligned} \tag{4.57}$$

This system has two equilibria, one stable equilibrium at $\begin{bmatrix} -1 & -1 \end{bmatrix}$ and one unstable equilibrium at $\begin{bmatrix} 1 & 1 \end{bmatrix}$ (saddle point). It can be shown that the state space is divided into two regions; every initial point in the stable region is attracted to the stable point, and every initial point in the other region goes off to infinity. To investigate the effect of the suboptimal control on the observability of this nonlinear system, the optimal trajectory is obtained for two cases. In the first simulation, the observability term in cost function is set to zero. In the second simulation, the observability term is added. The empirical observability gramian is computed for these two cases ($t \in [0 \;\; 10]$ sec). In case one ($l_2 = 0$), we have $\det(W_o) = 23.7$ with singular values $\sigma_1 = 97.2, \;\; \sigma_2 = 0.24$. In the second case ($l_2 \neq 0$), we have $\det(W_o) = 54.1$ with singular values $\sigma_1 = 151.5, \;\; \sigma_2 = 0.36$. As can be seen, the determinant, the minimum singular value, and the maximum singular value of the observability gramian has increased.

Chapter 5

TIME-VARYING STATE FEEDBACK CONTROL

One of the primary goals of control theory is to guarantee stability of a system. The study of stabilizing controller design for nonlinear systems has been the subject of intense research with resulting methods including model predictive control (MPC) [17], nonlinear optimal control [19] and time varying Lyapunov methods [20,21]. An important point to note is that many nonlinear systems, most notably nonholonomic systems, cannot be asymptotically stabilized by smooth feedback control [22, 24, 25]. The authors of [24] presented sufficient conditions under which a nonlinear system is asymptotically stabilizable by smooth state feedback. In the case where smooth state feedback is not sufficient, either discontinuous or time-varying oscillatory controls have been shown to stabilize these kinds of nonlinear systems [23].

In many practical problems, nonlinearities come from the system measurements. An example of this type of system is a simplified particle model of a vehicle with camera or sonar with range-only/bearing-only measurement, such as an autonomous underwater vehicle (AUV). The measurements for these vehicles are usually based on acoustic localization [80]. In this case, acoustic transducers are installed on the AUV and on a set of other beacons. The AUV has the exact global location of the beacons and can determine its range to one (Single Beacon Navigation [81]), three (Long-Baseline Localization [82]), or more separate beacons to determine its position. Another example is an omnidirectional (holonomic) vehicle with bearing-only observation. A system is holonomic if the kinematic constraints restrict the motion of the system to a manifold [23]. A holonomic vehicle model which is given by $\dot{\mathbf{x}} = \mathbf{u}, \;\; \mathbf{x} \in \mathbb{R}^2$ was investigated in [12, 78] among others. In this case, the vehicle only has information about the direction of the vehicle but not about the distance from reference points. A modelling of a vehicle with azimuth bearing, conical bearing, and depth/elevation angle measurements can be found in [83].

Another type of non-linearity is nonlinear state dynamics. The most well known and challenging type of nonlinear system are those subject to nonholonomic constraints. Many vehicles have

nonholonomic constraints in their dynamics, e.g. ground, air, or underwater vehicles. Here, we specifically consider nonholonomic systems in chained form. Systems in chain form have in recent years been used to model the kinematic equations of nonholonomic mechanical systems (e.g., for nonholonomic wheeled vehicle). A two-input system with a single chain has the form:

$$\begin{aligned}
\dot{\zeta}_1 &= u_1 \\
\dot{\zeta}_2 &= u_2 \\
\dot{\zeta}_3 &= \zeta_2 u_1 \\
\dot{\zeta}_4 &= \zeta_3 u_1 \\
&\vdots \\
\dot{\zeta}_n &= \zeta_{n-1} u_1 \,.
\end{aligned} \tag{5.1}$$

Some classical examples of this type of system are a rolling disk [84], a hopping robot [23], a simple kinematic model of a car [23, 84, 85], a car with multiple number of trailers [23, 84], under-actuated symmetric rigid spacecraft [84], and many others.

The purpose of this chapter is construction of transient time-varying state feedback designed to stabilize certain classes of nonlinear systems. By changing some parameters of the time-varying control, we can enhance the performance of the system when it is required. In some cases, we can avoid unobservable trajectories by superimposing some oscillatory terms onto smooth state feedback, with no effect on the asymptotic stability behaviour. An important point about these results is that with the insight obtained in this chapter, we are able to construct schemes capable of dealing with some particularly challenging types of nonlinear systems including certain classes of nonholonomic systems. In this chapter, the asymptotic stability of nonlinear systems is investigated via designing a control policy which is a combination of a smooth state feedback and a transient sinusoidal term. Furthermore, a specific set of stabilizing controls will be introduced for nonholonomic systems in chained form. Here, Lyapunov approach will be used for stability analysis of the obtained control.

5.1 Time-Varying Oscillatory Control

For the stability analysis of nonlinear time-varying system, we must work with the following stability theorem.

Proposition 6. *(Theorem 4.8 from [86]) Let* $\mathbf{x} = 0$ *be an equilibrium point for a nonlinear system* $\dot{\mathbf{x}} = \mathbf{f}(\mathbf{x}, t)$*, and* $D \subset \mathbb{R}^n$ *be a domain containing* $\mathbf{x} = 0$*. Let* $V : [0, \infty) \times D \to \mathbb{R}$ *be a continuously differentiable function such that*

$$\begin{aligned} W_1(\mathbf{x}) \leq V(t, \mathbf{x}) \leq W_2(\mathbf{x}) \\ \frac{\partial V}{\partial t} + \frac{\partial V}{\partial \mathbf{x}} \mathbf{f}(\mathbf{x}, t) \leq 0 \,. \end{aligned} \tag{5.2}$$

$\forall t \geq 0$*, and* $\forall \mathbf{x} \in D$*, where* $W_1(\mathbf{x})$ *and* $W_2(\mathbf{x})$ *are continuous positive definite functions on* D*. Then,* $\mathbf{x} = 0$ *is uniformly stable.*

Here, a nonlinear system in control affine form, termed as Σ_2 in (2.9) is considered. The problem of stabilization of this type of nonlinear systems via smooth state feedback has been investigated in the previous chapter. Here, designing a time-varying oscillatory control is considered, such that the asymptotic stability behaviour does not violate. The following theorem presents the main result of this chapter.

Theorem 9. *Given a nonlinear system in control-affine form* (2.9)*, if there exists a positive definite, radially unbounded smooth function* $V(\mathbf{x})$*, such that* $L_{\mathbf{f}_0} V(\mathbf{x}) = 0$*, and*

$$\dim \tilde{D} \triangleq \dim \ \textit{span} \left\{ ad_{\mathbf{f}_0}^k \mathbf{f}_i : 0 \leq k \leq n-1, 1 \leq i \leq m \right\} = n, \ \ \forall \mathbf{x} \in \mathbb{R}^n - \{0\}, \tag{5.3}$$

then the control given by

$$\begin{aligned} \mathbf{u}(\mathbf{x}, t) &= -\left[I + S(t) \right] \left(L_G V(\mathbf{x}) \right)^T , \\ G &= \begin{bmatrix} \mathbf{f}_1 & \mathbf{f}_2 & \cdots & \mathbf{f}_p \end{bmatrix} , \end{aligned} \tag{5.4}$$

where, $S(t)$ *is a diagonal matrix with diagonal elements* $S[i,i] = \alpha_i e^{-t} \sin(\omega_i t + \phi_i), \ \ 0 < |\alpha_i| < 1, \ \ \phi_i \in [0, \pi), i = 1, \ldots, p$*, asymptotically stabilizes the system.*

Proof. In [24], It has been proved that if the condition (5.3) is satisfied, and there exists $V(\mathbf{x}) > 0$ such that $L_{\mathbf{f}_0} V(\mathbf{x}) = 0$, then the control $\mathbf{u}_0(\mathbf{x}) = -\left(L_G V(\mathbf{x}) \right)^T$ asymptotically stabilizes the system. Now, consider the Lyapunov function $V(\mathbf{x})$ with the control $\mathbf{u}(\mathbf{x}, t)$. Then

$$\begin{aligned} W_1(\mathbf{x}) = \frac{1}{2} V(\mathbf{x}) \leq V(\mathbf{x}) \leq 2V(\mathbf{x}) = W_2(\mathbf{x}), \\ \dot{V} = \frac{\partial V}{\partial \mathbf{x}} \dot{\mathbf{x}} = \frac{\partial V}{\partial \mathbf{x}} \left[\mathbf{f}_0(\mathbf{x}) + G(\mathbf{x}) \mathbf{u} \right] \\ = -\left(\frac{\partial V}{\partial \mathbf{x}} \right) G(\mathbf{x}) \left[I + S(t) \right] G^T(\mathbf{x}) \left(\frac{\partial V}{\partial \mathbf{x}} \right)^T . \end{aligned} \tag{5.5}$$

Since $-1 < S[i,i] < 1,\ \ i = 1, \cdots, p$, then $[I + S(t)]$ is a positive semi-definite matrix. Therefore, $\dot{V} \leq 0,\ \ \forall (t, \mathbf{x}) \in \mathbb{R}^{>0} \times \mathbb{R}^n - \{0\}$. Now, let M be a positive invariant subset of $\{\mathbf{x} \in \mathbb{R}^n : \dot{V}(\mathbf{x}) = 0\}$, and $\mathbf{x}_0 \neq 0 \in M$, then

$$\dot{V}(\mathbf{x}_0) = -\sum_{i=1}^{p} (1 + S[i,i]) \left(L_{\mathbf{f}_i} V(\mathbf{x}_0)\right)^2 = 0. \tag{5.6}$$

Since $1 + S[i,i] > 0$, one can conclude that $L_{\mathbf{f}_i} V(\mathbf{x}_0) = 0$. Repeat differentiation with respect to t gives

$$L^k_{\mathbf{f}_0} L_{\mathbf{f}_i} V(\mathbf{x}_0) = 0,\ \ i = 1, \cdots, m,\ \ k \geq 0. \tag{5.7}$$

Because $L_{\mathbf{f}_0} V(\mathbf{x}_0) = 0$,

$$L^k_{\mathbf{f}_0} L_{\mathbf{f}_i} V(\mathbf{x}_0) = L_{ad^k_{\mathbf{f}_0}\mathbf{f}_i} V(\mathbf{x}_0) = 0,\ \ i = 1, \cdots, p,\ \ k \geq 0. \tag{5.8}$$

Therefore, $\dfrac{\partial V}{\partial \mathbf{x}}$ is orthogonal to the whole space defined by condition (5.3), which spans $\mathbb{R}^n$. Thus $\dfrac{\partial V}{\partial \mathbf{x}}$ should be zero, which is contradiction. Hence, $M = \{0\}$ and the theorem is proved. □

Condition (5.3) is reminiscent of the well-known rank condition for accessibility of control-affine nonlinear system (2.9). Note that this condition can be replaced by a weaker condition, given by

$$\left\{\mathbf{x} \in \mathbb{R}^n : L^i_{\mathbf{f}} L_\tau V(\mathbf{x}) = 0,\ \ \forall \tau \in \tilde{D},\ \ i = 0, 1, \ldots\right\} = \{\mathbf{0}\}, \tag{5.9}$$

where $\tilde{D}$ is defined in (5.3).

Theorem 9 proposes a time-varying state feedback control, and shows that adding the suggested transient term does not affect the asymptotic stability of the system. Furthermore, the effect of time-varying term is transient and decays with time, such that $\mathbf{u}(\mathbf{x}, t) \to \mathbf{u}_0(\mathbf{x})$ as $t \to \infty$.

5.2 Optimal Selection of Controller Parameters

The cost function is similar to the cost function introduced in previous chapter which is given by:

$$\min_{\mathbf{x},\mathbf{u}} \quad J = \int_0^\infty \left\{l_1(\mathbf{x}, \mathbf{u}) - l_2(t, \mathbf{x}, \mathbf{x}^1, \cdots, \mathbf{x}^n)\right\} \mathrm{d}t, \tag{5.10}$$

where, $l_1(\mathbf{x}, \mathbf{u}) = \mathbf{x}^T Q \mathbf{x} + \mathbf{u}^T R \mathbf{u}$ and $l_2(\mathbf{x})$ is observability index which is also introduced in Section 4.2 equation (4.11). The only differences here are $\mathbf{u} = -\left[I + S(t)\right] \left(L_G V(\mathbf{x})\right)^T$, and the optimization parameters are α and ω instead of K in Chapter 4.

Here, the recursive gradient-based algorithm, proposed in Algorithm 1, will be use to find a solution of this optimization problem. Here, the gradient vectors are given by:

$$\frac{\partial J}{\partial \alpha} = \left.\frac{\partial x_{n+1}}{\partial \alpha}\right|_{t_f}, \quad \frac{\partial J}{\partial \omega} = \left.\frac{\partial x_{n+1}}{\partial \omega}\right|_{t_f}, \tag{5.11}$$

which can be calculated by the method presented in Chapter 4.

5.3 Nonholonomic Systems

For a nonholonomic control system, the dependence of a stabilizing control law on time is essential, since this type of nonlinear system, given in (5.1), does not satisfy Brockett's necessary condition for smooth feedback stabilization [22]. In [85], an algorithm is introduced to stabilize a class of nonholonomic systems in chained form. The nonholonomic system in chained form (5.1), can be steered to the origin of the system using the following algorithm [85]:

1. Steer ζ_1 and ζ_2 to the origin.

2. For each $\zeta_{k+2}, k \geq 1$, steer ζ_{k+2} to the origin using $u_1 = a\sin(t)$, $u_2 = b\cos(kt)$, where a and b satisfy
$$\zeta_{k+2}(2\pi) - \zeta_{k+2}(0) = \frac{(a/2)^k b}{k!} 2\pi\,. \tag{5.12}$$

This system is controllable using the input vector fields and Lie brackets of the form $ad^k_{\mathbf{f}_1}\mathbf{f}_2$. Corollary 3.1 of [85] proposed that every pair of inputs

$$\begin{aligned} u_1 &= -\zeta_1 - \left(\sum_{j=1}^{n-2} \zeta_{j+2}^2\right)(\sin(t) - \cos(t)) \\ u_2 &= -\zeta_2 - \sum_{j=1}^{n-2} (-1)^j c_j \zeta_{j+2} \cos(jt)\,, \end{aligned} \tag{5.13}$$

with $c_j > 0$, locally asymptotically stabilizes the origin of (5.1). Different types of time-varying oscillatory controls have been constructed in [20, 84, 85, 87].

Here, the objective is to generalize the results of Section 5.1, to include nonholonomic systems by constructing appropriate time-varying stabilizing control inputs. To derive a control law by

Lyapunov design for a system of type (5.1), an invertible state transformation $\mathbf{x} \rightarrow \bar{\mathbf{x}}$ is introduced, where

$$\begin{aligned} \bar{x}_i &= x_i, \;\; i \neq 2 \\ \bar{x}_2 &= x_2 - \sum_{i=1}^{n-2} x_{i+2} \sin(it)\,, \end{aligned} \tag{5.14}$$

and, define new control inputs v_1 and v_2 as follows

$$\begin{aligned} v_1 &= u_1 \\ v_2 &= u_2 - \sum_{i=1}^{n-2} i x_{i+2} \cos(it)\,. \end{aligned} \tag{5.15}$$

Note that the state transformation $\mathbf{x} \rightarrow \bar{\mathbf{x}}$ is simply a time-varying offset and that convergence in $\mathbf{x}$ and $\bar{\mathbf{x}}$ is equivalent, since $\mathbf{x} = 0 \iff \bar{\mathbf{x}} = 0$. The transformed system dynamics is given by

$$\begin{aligned} \dot{\bar{x}}_1 &= v_1 \\ \dot{\bar{x}}_2 &= -\left[\sum_{i=1}^{n-2} \bar{x}_{i+1} \sin(it) + \bar{x}_{i+2} \sin^2(it)\right] v_1 + v_2 \\ \dot{\bar{x}}_3 &= \left[\bar{x}_2 + \sum_{i=1}^{n-2} \bar{x}_{i+2} \sin(it)\right] v_1 \\ \dot{\bar{x}}_4 &= \bar{x}_3 v_1 \\ &\vdots \\ \dot{\bar{x}}_n &= \bar{x}_{n-1} v_1\,, \end{aligned} \tag{5.16}$$

which can be written compactly as $\dot{\bar{\mathbf{x}}} = \bar{\mathbf{f}}_0(\bar{\mathbf{x}}) + \bar{G}(\bar{\mathbf{x}})\mathbf{v} = \bar{\mathbf{f}}_0 + \bar{\mathbf{f}}_1 v_1 + \bar{\mathbf{f}}_2 v_2$, where the drift and control vectors of the transformed system are

$$\bar{\mathbf{f}}_0 = \mathbf{0}, \;\; \bar{\mathbf{f}}_1 = \begin{bmatrix} 1 \\ -\sum_{i=1}^{n-2} \bar{x}_{i+1} \sin(it) + \bar{x}_{i+2} \sin^2(it) \\ \bar{x}_2 + \sum_{i=1}^{n-2} \bar{x}_{i+2} \sin(it) \\ \bar{x}_3 \\ \vdots \\ \bar{x}_{n-1} \end{bmatrix}, \;\; \bar{\mathbf{f}}_2 = \begin{bmatrix} 0 \\ 1 \\ 0 \\ \vdots \\ 0 \end{bmatrix}. \tag{5.17}$$

Theorem 10. *The nonholonomic system in chained form, given by* (5.1)*, is uniformly stable by the time varying state feedback control law*

$$\begin{aligned} u_1(\bar{\mathbf{x}},t) &= -L_{\bar{\mathbf{f}}_1}V(\bar{\mathbf{x}},t)\,, \\ u_2(\bar{\mathbf{x}},t) &= -L_{\bar{\mathbf{f}}_2}V(\bar{\mathbf{x}},t) + \sum_{i=1}^{n-2} i\bar{x}_{i+2}\cos(it)\,, \end{aligned} \tag{5.18}$$

where,

$$V(\bar{\mathbf{x}},t) = \frac{1}{2}\left[\left(\sum_{i=1}^{n-2}\bar{x}_{i+2}\right)^2 + \sum_{i=1}^{n}\bar{x}_i^2\left[e^{-it}(\sin(it)+2)+1\right]^2\right]\,, \tag{5.19}$$

and, $\bar{\mathbf{f}}_1$ *and* $\bar{\mathbf{f}}_2$ *are given in* (5.17)*.*

Proof. Let $W_1(\mathbf{x})$ and $W_2(\mathbf{x})$ be continuously differentiable, positive definite functions given by

$$\begin{aligned} W_1(\bar{\mathbf{x}}) &= \frac{1}{2}\left[\left(\sum_{i=1}^{n-2}\bar{x}_{i+2}\right)^2 + \sum_{i=1}^{n}\bar{x}_i^2\right] \\ W_2(\bar{\mathbf{x}}) &= \frac{1}{2}\left[\left(\sum_{i=1}^{n-2}\bar{x}_{i+2}\right)^2 + \sum_{i=1}^{n}16\bar{x}_i^2\right]\,. \end{aligned} \tag{5.20}$$

Since, $0 < e^{-it} \leq 1$ and $-1 \leq \sin(it) \leq 1$, then

$$\begin{aligned} \left[e^{-it}(\sin(it)+2)+1\right]^2 &\leq 16\,, \\ \left[e^{-it}(\sin(it)+2)+1\right]^2 &\geq 1\,. \end{aligned} \tag{5.21}$$

Therefore, the continuously differentiable function $V(\bar{\mathbf{x}},t)$ satisfies

$$W_1(\bar{\mathbf{x}}) \leq V(\bar{\mathbf{x}},t) \leq W_2(\bar{\mathbf{x}}),\ \ \forall t \geq 0, \tag{5.22}$$

which is the first conditions of Proposition 6. Direct calculation shows that

$$L_{\bar{\mathbf{f}}_0}V(\bar{\mathbf{x}},t) = 0, \tag{5.23}$$

and,

$$\left\{\mathbf{x}\in\mathbb{R}^n : L_{\bar{\mathbf{f}}_i}V(\mathbf{x},t) = 0,\ \ \forall t\geq 0,\ \ i=1,2\right\} = \{\mathbf{0}\}. \tag{5.24}$$

Consider $\mathbf{v} = -\left(L_{\bar{G}}V(\bar{\mathbf{x}},t)\right)^T$, where $\bar{G} = \begin{bmatrix}\bar{\mathbf{f}}_1 & \bar{\mathbf{f}}_2\end{bmatrix}$. Then,

$$\begin{aligned} \dot{V} &= \frac{\partial V}{\partial t} + \frac{\partial V}{\partial \bar{\mathbf{x}}}\dot{\bar{x}} = \frac{\partial V}{\partial t} + \frac{\partial V}{\partial \bar{\mathbf{x}}}\left[\bar{\mathbf{f}}_0 + \bar{G}\mathbf{v}\right] \\ &= \frac{\partial V}{\partial t} - \left(\frac{\partial V}{\partial \bar{\mathbf{x}}}\right)\bar{G}\bar{G}^T\left(\frac{\partial V}{\partial \bar{\mathbf{x}}}\right)^T, \end{aligned} \tag{5.25}$$

where

$$\frac{\partial V}{\partial t} = \sum_{i=1}^{n} \beta_i(t)\bar{x}_i^2 \left[e^{-it}(\sin(it)+2)+1\right], \qquad \beta_i(t) = ie^{-it}\left[\cos(it)-\sin(it)-2\right]. \tag{5.26}$$

Since, $\beta_i(t) < 0, \ \ \forall i \in \mathbb{N}, \ \ \forall t \geq 0$, then $\dfrac{\partial V}{\partial t} < 0$. Therefore,

$$\dot{V} = \frac{\partial V}{\partial t} + \frac{\partial V}{\partial \bar{\mathbf{x}}}\dot{\bar{\mathbf{x}}} \leq 0, \ \ \forall \bar{\mathbf{x}} \neq \mathbf{0}\,. \tag{5.27}$$

Similar to the proof of Theorem 9, it can be shown that $\dot{V} < 0, \ \ \forall \bar{\mathbf{x}} \neq \mathbf{0}$. Based on Proposition 6, the transformed system (5.16) is uniformly stable by the time varying state feedback control law $\mathbf{v} = -\left(L_{\bar{G}}V(\bar{\mathbf{x}},t)\right)^T$. By substituting into (5.15), we can conclude that the nonholonomic system (5.1) is stabilizable by the time-varying state feedback control law (5.18). □

5.4 Illustrative Examples

To demonstrate the results of this chapter, two examples are considered here. The first example is a linear system with nonlinear measurement. We show that a stabilizing control, obtained from a stability analysis of the linear system, makes the system unobservable. By applying the time-varying control, obtained in Section 5.1, the system avoids the unobservable trajectories, while the asymptotic stability behaviour remains unchanged. In the second example, we will consider a nonholonomic system with three states and stability of the system is demonstrated in simulation.

5.4.1 Holonomic Nonlinear System

As the first example, consider a holonomic system given by

$$\dot{x}_1 = u_1\,, \qquad \dot{x}_2 = u_2\,. \tag{5.28}$$

It can be shown that this system is controllable, and

$$\dim \tilde{D} \triangleq \dim \text{span}\,\{\mathbf{f}_1, \mathbf{f}_2\} = 2, \ \ \forall \mathbf{x} \in \mathbb{R}^2 - \{0\}. \tag{5.29}$$

In this case, we have a linear system $\dot{\mathbf{x}} = A\mathbf{x} + B\mathbf{u}$, where, $A = 0, \ \ B = I$. By choosing $Q = R = I$, and solving the algebraic Riccati equation $A^TP + PA - PBR^{-1}B^TP + Q = 0$, we

obtain $P = I$. Thus, the control policy $\mathbf{u}_0 = -R^{-1}B^T P\mathbf{x} = -\mathbf{x}$ asymptotically stabilizes (5.28). Now, assume that the position of vehicle is continuously measured by an omnidirectional camera centred at the origin. Then, the output function can be given as

$$y = \frac{x_1}{x_2}, \tag{5.30}$$

where, $y \in \mathbb{R}$ is a bearing only measurement, which provides information about the direction of the vehicle but not about the distance. In this example, the Lie algebra observability matrix is given by

$$d\mathcal{O} = \frac{\partial}{\partial \mathbf{x}} \begin{bmatrix} y \\ \dot{y} \\ \vdots \end{bmatrix}. \tag{5.31}$$

Recall that the system is locally observable, if the observability matrix, $d\mathcal{O}$, is full rank. In this case, we have

$$\dot{y} = \frac{\dot{x}_1 x_2 - \dot{x}_2 x_1}{x_2^2} = \frac{-x_1 x_2 + x_1 x_2}{x_2^2} = 0. \tag{5.32}$$

All other differential terms are zero ($\ddot{y} = y^{(3)} = \ldots = 0$). Therefore, by applying the control $\mathbf{u}_0 = -\mathbf{x}$, the observability matrix is not full rank, and the system is not observable.

Given the results of Theorem 9, and

$$S(t) = \begin{bmatrix} e^{-t}\sin(\omega t) & 0 \\ 0 & e^{-t}\cos(\omega t) \end{bmatrix}, \tag{5.33}$$

the time-varying oscillatory control is given by

$$\begin{aligned} u_1 &= -\left(1 + e^{-t}\sin(\omega t)\right) x_1\,, \\ u_2 &= -\left(1 + e^{-t}\cos(\omega t)\right) x_2\,. \end{aligned} \tag{5.34}$$

In Fig. 5.1, four sample trajectories from different initial conditions $(\pm 5\,, \pm 5)$ are shown. By applying the modified control given in (5.34), the system still converges to the origin, while the system is observable.

The values of the original stabilizing control, $\mathbf{u}_0 = -\mathbf{x}$ and the time-varying control inputs (5.34) are given in Fig. 5.2. As it can be seen in this figure, the effect of time-varying term in the designed controller becomes negligible, as time increases.

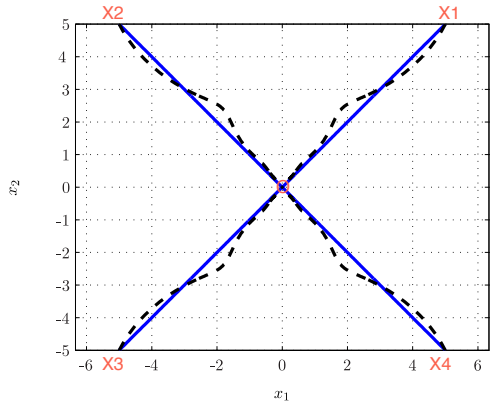

Figure 5.1: Four sample trajectories from four different initial conditions ($X_i, i = 1, ..., 4$) for system (5.28). The red circle indicates the equilibrium point. The solid blue lines indicate trajectories by applying stabilizing control $\mathbf{u}_0 = -\mathbf{x}$, and the dashed black lines indicate observable asymptotically stable trajectories, given in (5.34). The frequency of the modified control is $\omega = 5rad/sec$.

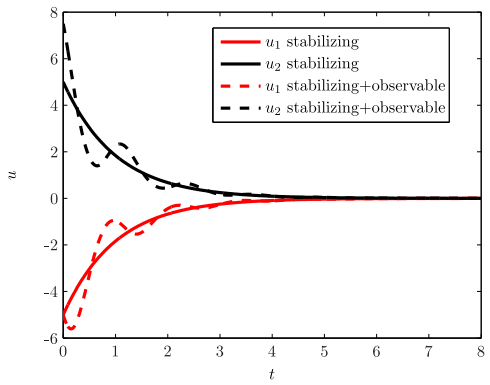

Figure 5.2: Two control policies for system (5.28). The solid lines indicate stabilizing control and the dashed lines indicate time varying oscillatory controls which make the system observable and asymptotically stable.

5.4.2 Nonholonomic Nonlinear Systems

Consider a nonholonomic system in chained form with three states:

$$\begin{aligned} \dot{x}_1 &= u_1 \\ \dot{x}_2 &= u_2 \\ \dot{x}_3 &= x_2 u_1 \,. \end{aligned} \tag{5.35}$$

The output measurement is the nonholonomic state, $y = x_3$. It can be shown that there does not exist any smooth time-invariant state feedback such that all states in (5.35) be steered to the origin. However, it can be shown that there exists a stabilizing control for this system, but the stabilizing control should be time-varying. For this example, the state transformation $\mathbf{x} \rightarrow \bar{\mathbf{x}}$, introduced in Section 5.3, is given by

$$\begin{aligned} \bar{x}_1 &= x_1 \\ \bar{x}_2 &= x_2 - x_3 \sin(t) \\ \bar{x}_3 &= x_3 \,, \end{aligned} \tag{5.36}$$

and the new control inputs v_1 and v_2 are

$$\begin{aligned} v_1 &= u_1 \\ v_2 &= u_2 - x_3 \cos(t) \,. \end{aligned} \tag{5.37}$$

The transformed system dynamics can be written as

$$\begin{aligned} \dot{\bar{x}}_1 &= v_1 \\ \dot{\bar{x}}_2 &= -\left[(\bar{x}_2 + \bar{x}_3 \sin(t)) \sin(t)\right] v_1 + v_2 \\ \dot{\bar{x}}_3 &= (\bar{x}_2 + \bar{x}_3 \sin(t)) v_1 \,. \end{aligned} \tag{5.38}$$

The drift and control vectors of the transformed system are

$$\bar{\mathbf{f}}_0 = \mathbf{0}, \;\; \bar{\mathbf{f}}_1 = \begin{bmatrix} 1 \\ -(\bar{x}_2 + \bar{x}_3 \sin(t)) \sin(t) \\ \bar{x}_2 + \bar{x}_3 \sin(t) \end{bmatrix}, \;\; \bar{\mathbf{f}}_2 = \begin{bmatrix} 0 \\ 1 \\ 0 \end{bmatrix}. \tag{5.39}$$

By choosing positive definite function

$$V(\bar{\mathbf{x}}, t) = \frac{1}{2} \left[\bar{x}_3^2 + \sum_{i=1}^{3} \left(\bar{x}_i \left[e^{-it} (\sin(it) + 2) + 1 \right] \right)^2 \right], \tag{5.40}$$

we have

$$L_{\bar{\mathbf{f}}_0} V(\bar{\mathbf{x}}, t) = 0, \tag{5.41}$$

and,

$$\left\{ \mathbf{x} \in \mathbb{R}^n : L_{\bar{\mathbf{f}}_i} V(\bar{\mathbf{x}}, t) = 0, \;\; i = 1, 2 \right\} = \{\mathbf{0}\}. \tag{5.42}$$

Then, Theorem 10 shows that affine system (5.38) is uniformly stabilizable by the time varying state feedback control law

$$\begin{aligned} v_1 &= -L_{\bar{\mathbf{f}}_1} V(\bar{\mathbf{x}}, t)\,, \\ v_2 &= -L_{\bar{\mathbf{f}}_2} V(\bar{\mathbf{x}}, t)\,. \end{aligned} \tag{5.43}$$

By substituting in (5.37), stabilizing control for system (5.35) is given by

$$\begin{aligned} u_1 &= -L_{\bar{\mathbf{f}}_1} V(\bar{\mathbf{x}}, t)\,, \\ u_2 &= -L_{\bar{\mathbf{f}}_2} V(\bar{\mathbf{x}}, t) + \bar{x}_3 \cos(t)\,. \end{aligned} \tag{5.44}$$

A sample trajectory with this stabilizing control is shown in Fig. 5.3. In Fig. 5.4, it can be seen how the states converge to zero after utilizing the controls (5.44).

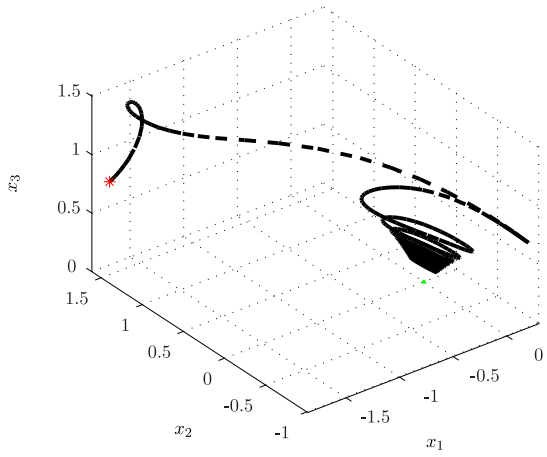

Figure 5.3: A sample trajectory from a random initial condition for system (5.35). The red circle indicates the initial point.

To investigate how these results affect the observability of this system, the observability Gramian for two simulations are compared here. First, a constant control inputs $u_1 = c_1$ and $u_2 = c_2$ are utilized. In the second example, the time-varying oscillatory control, given in (5.44), is applied. Then, the empirical observability Gramian in two cases are computed. A comparison between the determinant of the observability Gramian is given in Fig. 5.5. As it can be seen, by utilizing the constant control, the determinant is very close to zero and therefore the system is not observable.

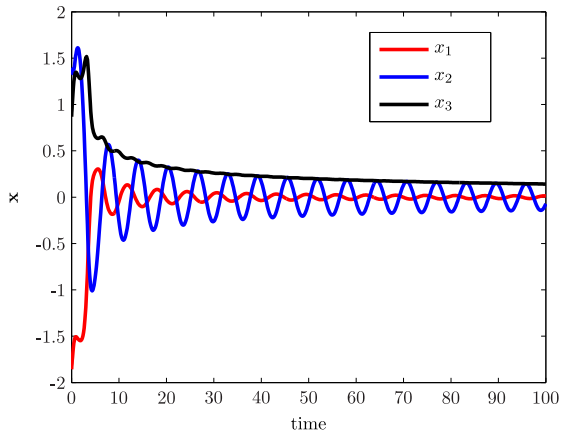

Figure 5.4: States of system (5.35) for the sample trajectory shown in Fig. 5.3.

By utilizing the control given in (5.44), the observability Gramian matrix becomes non-singular, and thus observability improves.

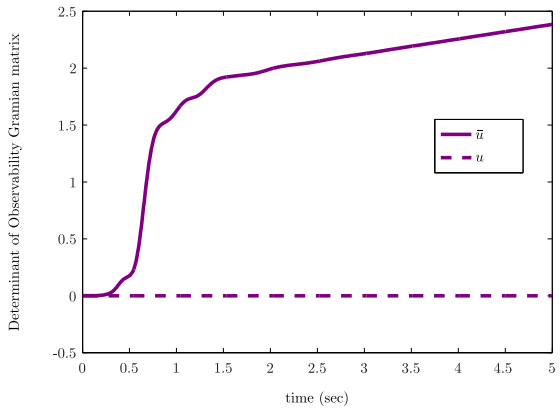

Figure 5.5: A comparison between the observability Gramian of two sample trajectories for system (5.35). The dashed line indicates the determinant of the empirical observability Gramian after utilizing the constant control, $\mathbf{u} = (c_1, c_2)$, and the solid line indicates the determinant of the empirical observability Gramian for the case of the time-varying oscillatory control, $\mathbf{u}(\bar{\mathbf{x}}, t)$ given in (5.44).

Chapter 6

OBSERVABILITY-BASED NETWORK DESIGN

Networked dynamic systems consist of multiple dynamic units that are connected via a network. The network represents communication topology to exchange information between agents to coordinate for reaching a goal. In recent years, the area of networked systems has received extensive attention. We deal with many examples of networked systems in our everyday life; such as social networks and internet network. Analysis of some complex networks such as biological networks, power grids and robotic networks is of increasing interest in recent works of many researchers. Collective behaviour of a large number of agents connected to each other via a limited information sharing among them can be studied from different points of view. In this chapter, observability of a network is the main focus. Observability in a network, which is directly related to the quality and the quantity of information about individual agents in the network, depends on the topology of the network and the number and location of measuring points.

State estimation for multi-agent systems has wide applications especially in sensor networks design and robot networks localization, among many others. Yet, few theoretic results have been obtained to date on the design of a network based on the quality of observability of the networked system. Nevertheless, one may find in the literature that Sharma *et al.* in [88] established a link between nonlinear observability of a group of robots and graph theory. Furthermore, the concept of observability has been used in social networks [89,90], electric power grid management [42,91], and biological systems [47]. Observability analysis for cooperative localization has been an active area of research in both navigation of autonomous underwater vehicles and ground robots navigation.

The necessary conditions for observability using some properties of the graphs, such as connectivity and existing a path between different nodes has been investigated in previous works. For instance, it has been shown in [88] that for complete observability, all the nodes in the graph must have a path to at least two different landmarks of known location. Many different configurations of the robots meet this requirement, but which configuration would maximize the observability criteria

remained unanswered.

Utilizing the concept of observability from control theory, and some tools from graph theory and optimization, the main objective of this chapter is to develop algorithms in networked system design that meet the specified control objectives' guarantees. The main contribution of this chapter can be summarized as design of a network that 1) maximize an observability measure with a small number of sensors, and 2) improve the privacy of network. In the first part of this chapter, the objective is improving the quality of the state estimation of a group of individuals, which exchange information about some of their states (not necessarily the information about all states are propagated). Each agent collects data regarding its own states and shares this information with the rest of the team in its vicinity. The objective of the second part of the chapter is to design an optimal set of weights in the dynamics induced by the communication graph to maximize the privacy of nodes in the network.

6.1 Background and Preliminaries

6.1.1 Representation of A Network as A Graph

The communication between agents in a network is usually represented by an undirected graph $\mathcal{G} = (\mathcal{V}, \mathcal{E}, \mathbf{w})$. Each agent in network is denoted as a node, and edges represent communication links between agents. The number of nodes is N, and the number of edges is M. The node set, $\mathcal{V}$, consists of all nodes in the network. The edge set, $\mathcal{E}$, is comprised of pairs of nodes $\{v_i, v_j\}$, if nodes v_i and v_j are adjacent. Each edge has weight $w_i \in \mathbb{R}_{>0}$. The neighbourhood set $\mathcal{N}(i)$ of node i is composed of all agents in $\mathcal{V}$ adjacent to v_i. The weighting vector, $\mathbf{w} \in \mathbb{R}^M_{>0}$ with dimension M represents the weight of edges. The edges are encoded through the index mapping σ such that $l = \sigma(i, j)$, if and only if edge l connects nodes i and j. The edge weights will be denoted as w_{ij} and w_l , interchangeably. The incidence matrix $E(\mathcal{G})$ is a $N \times M$ matrix. Column $\sigma(i, j)$ of the matrix incidence matrix is $\mathbf{e}_i - \mathbf{e}_j$. The weighted degree δ_i of node v_i is the sum of the weights of the edges connecting node v_i to its neighbours. The weighted degree matrix, Δ_w, is a diagonal matrix with δ_i as its ith diagonal entry. The adjacency matrix is an $N \times N$ symmetric matrix with $\mathcal{A}[i, j] = 1$ when $\{v_i, v_j\} \in \mathcal{E}$, and $\mathcal{A}[i, j] = 0$, otherwise. The weighted adjacency matrix is an $N \times N$ symmetric matrix with $\mathcal{A}[i, j] = w_l$ when $\{v_i, v_j\} \in \mathcal{E}$ and edge l connects them, and $\mathcal{A}[i, j] = 0$ otherwise. The graph Laplacian is defined as $L = \Delta_w - \mathcal{A}_w$, and is a positive semi-definite matrix, which

satisfies $\mathbf{1}^T L = \mathbf{0}$ and $L\mathbf{1} = \mathbf{0}$. Here, $\mathbf{1}$ denotes a vector which all elements are equal to one. An undirected graph is said to be strongly connected if there exists an elementary path between any pair of vertices. To ensure connectivity of a graph the second smallest eigenvalue of the Laplacian of the graph should be positive ($\lambda_2(L) > 0$).

We consider the following operation over matrices: the Hadamard product is a binary operation that takes two matrices of the same dimensions, and produces another matrix where each element $[i, j]$ is the product of elements $[i, j]$ of the original two matrices:

$$(A \circ B)[i, j] = A[i, j] \cdot B[i, j] \,.$$

The Hadamard product is associative and distributive, and unlike the matrix product it is also commutative. The Hadamard product of two positive semi-definite matrices is positive semi-definite.

6.1.2 Consensus Algorithm

Coordination problem of multi-agent systems has received compelling attention from various scientific communities due to its broad applications in different areas, such as satellite formation flying, cooperative unmanned air vehicles, scheduling of automated highway systems, and air traffic control. The goal of consensus algorithm is developing a control policy based on local information which enables the agents to reach an agreement on certain quantities of interest. Another topic that is closely related to the consensus of multi-agent systems is the synchronization of coupled nonlinear oscillators. The consensus protocol is briefly presented as follows.

Consider $x_i(t) \in \mathbb{R}$ to be the ith node's state at time t. The continuous-time weighted consensus protocol is defined as

$$\dot{x}_i(t) = \sum_{\{i,j\} \in \mathcal{E}} w_{ij} \left(x_j(t) - x_i(t) \right) \,.$$

In a compact form with $\mathbf{x}(t) \in \mathbb{R}^N$, the corresponding collective dynamics is represented as $\dot{\mathbf{x}} = -L(\mathbf{w})\mathbf{x}$. So, each agent only requires its relative state with respect to its neighbours. In the case of a connected graph, the dynamics of a network performing consensus algorithm will converge to an agreement on the state [92].

6.1.3 Online Convex Optimization

Online learning has become popular recently for tackling very large scale estimation problems. Their convergence properties are well understood and have been analysed in a number of different frameworks such as by means of game theory [93]. In this framework, a game is defined called *Online Convex Optimization* problem. In this game, a player chooses a point from a convex set. After choosing the point, an adversary reveals a convex loss function, which the online player receives a loss corresponding to the point she chose. And this scenario is repeated for many times. The online convex optimisation problem is a special case of a genera online optimization problems. To measure the performance of the online player in this game, a metric is used which is called *regret*. Regret is the difference between the loss of the online player and the best fixed point in hindsight. The algorithm introduced in [93] is similar to n the well known Newton-Raphson method for offline optimization. This algorithm attains regret which is proportional to the logarithm of the number of iterations when the loss (cost) functions are convex, and is computationally efficient.

Assume an online player iteratively chooses a point from a non-empty, bounded, closed and convex set in Euclidean space denoted by $\mathcal{P}$ for T times. At iteration t, the algorithm takes the history of cost functions, $\{f_1, \cdots, f_{t-1}\}$ as input, and suggests $x_t \in \mathcal{P}$ to the online player to choose. After committing to this choice, a convex cost function $f_t : \mathcal{P} \to \mathbb{R}$ is revealed. The loss associated to the choice of the online player is the value of the cost function at the point she committed to, i.e. $f_t(x_t)$. The objective is to minimize the accumulative penalty. The regret of the online player at the end of the game, i.e. at time T , is defined as the difference between the total cost and the cost of the best single decision, where the best is chosen with the benefit of hindsight. Formally

$$\mathcal{R}_T = E\left[\sum_{t=1}^{T} f_t(x_t)\right] - \min_{x\in\mathcal{P}} \sum_{t=1}^{T} f_t(x)\,. \tag{6.1}$$

Note that regret measures the difference in performance between the online player and a player who is constrained to choose a fixed point over all iterations, but with the benefit of hindsight. Although, it is tempting to compare the online player to an unconstrained player who has the benefit of hindsight (i.e. can dynamically change his point every iteration), but the comparison becomes trivial, and it is not interesting in many applications. The objective of online algorithm is to achieve a guaranteed low regret. Specifically, it is desired the online algorithm guarantees a sub-linear $\mathcal{R}_T$

or $\frac{\mathcal{R}_T}{T} \to 0$. Sub-linear regret guarantees that on average the algorithm performs as well as the best fixed action in hindsight.

6.2 Optimal Sensors Placement

6.2.1 Introduction

In complex large-scale systems, such as a power electric grids or chemical plants, the first step of control systems design is addressing the following question:

Which subset of variables need to be measured to ensure observability?

Here, we provide the solution to the design of sensor placement under the assumption that each sensor measures a single state variable. Notice that this setup has a wide range of applicability since a variety of sensors are designed to measure a specified physical quantity. The objective is to determine the minimal placement of sensors such that the sensors ensure systems observability. In the scenario considered here, the agents communicate with each other within a graph structure to update their data according to either linear or nonlinear dynamics using neighbour node data. All sensors report their measurements to a central unit which is responsible to reconstruct the states estimations of the entire network. The objective is to recover the states of all nodes from the outputs of a small number of sensors over time, which requires that the dynamics of the overall networked system be observable.

6.2.2 System Modelling

We assume a system of N agents each with nonlinear dynamics. We assume that some states of each agent, called synchronized states, are following the consensus algorithm. In our model, control is responsible for the synchronization. Therefore, the dynamics of a single agent, called agent i, is given by

$$\dot{\mathbf{x}}_i = \mathbf{f}(\mathbf{x}_i) + \mathbf{u}_i, \;\; \mathbf{x}_i, \mathbf{u}_i \in \mathbb{R}^n \tag{6.2}$$

where, the control, $\mathbf{u}_i = \begin{bmatrix} u_{i_1} & u_{i_2} & \cdots & u_{i_n} \end{bmatrix}^T$, is given by

$$u_{i_k} = \sum_{j \in \mathcal{N}(i)} w_{ij} \left(x_{j_k} - x_{i_k} \right), \tag{6.3}$$

if x_{i_k} is a synchronized state, and zero, otherwise. Here, x_{i_k} and u_{i_k} are the kth state and the kth control input of node i.

One can define

$$X_i = \begin{bmatrix} x_{1_i} \\ x_{2_i} \\ \vdots \\ x_{N_i} \end{bmatrix}, \quad U_i = \begin{bmatrix} u_{1_i} \\ u_{2_i} \\ \vdots \\ u_{N_i} \end{bmatrix}, \quad i = 1, 2, \cdots, n. \tag{6.4}$$

Then, for a set of known communication weights, control is given by

$$U_i = -L(\mathbf{w})X_i, \tag{6.5}$$

if $X_i \in \mathbb{R}^N$ is the synchronized state of the agents.

Assume state k of each agent i is measured. Thus, measurement of node i is given by

$$y^i = x_{i_k}, \quad i = 1 \dots N. \tag{6.6}$$

Observability criteria has extensively been used to find the best sensor location [7–9]. In these works, a measure of complete observability for linear systems has been used. .

Assume there is a group of agents called measuring nodes from which we want to maximize the information available from states reconstruction of the entire network. Therefore, we have a subset of nodes $\bar{\mathcal{V}} \subset \mathcal{V}$ for which we want to maximize a measure of observability. Define a binary variable $\beta \in \mathbb{R}^N$ such that $\beta_i = 1$ if $i \in \bar{\mathcal{V}}$ and $\beta_i = 0$ otherwise. Then, the measurement is given by

$$\mathbf{y} = \begin{bmatrix} \beta_1 y^1 & \beta_2 y^2 & \cdots & \beta_N y^N \end{bmatrix}^T, \tag{6.7}$$

where, y^i is defined in (6.6).

6.2.3 Optimization Problem

Here, the objective is to determine a set of $r \leq N$ nodes such that if we communicate with them then we would be able to reconstruct the entire state of the network. In order to find these nodes, we maximize the determinant of the observability Gramian by varying the location of measuring nodes in the network. Maximizing the determinant of the observability Gramian corresponds to a maximization of independence between outputs [94]. The problem can be formulated mathematically

as:

$$\underset{\bar{\mathcal{V}}}{\text{maximize}} \quad \det(W_O(\bar{\mathcal{V}})), \tag{6.8}$$

Suppose the observation is partitioned into multiple sub-vectors from a number of individual sensors (similar to (6.7)), then the total observability Gramian is a sum of the separate observability Gramian matrices, having each individual sensor separately [8]. Therefore,

$$W_O = \sum_{i=1}^{N} \beta_i W_{O,i}. \tag{6.9}$$

Knowing this property of observability Gramian matrix, the problem can be rewritten as a minimization problem, which is called *D-optimal design* in [69]:

$$\begin{aligned} \underset{\beta}{\text{minimize}} \quad & \log \left[\det \left(\sum_{i=1}^{N} \beta_i W_{O,i} \right)^{-1} \right] \\ \text{subject to} \quad & \sum_{i=1}^{N} \beta_i \leq r \\ & \beta_i \in \{0, 1\}, \end{aligned} \tag{6.10}$$

where, $W_{O,i}$ is the observability Gramian obtained from measuring node i. This is a boolean non-linear programming problem. Because of the binary constraint, (6.10) is a non-convex problem. A common method for solving these types of optimization problems is computing a lower-bound on the optimal value of the non-convex problem. In general, there are two standard methods to solve these type of non-convex problems.

The first method is relaxation, in which the non-convex constraint is replaced with a looser, but convex constraint. For example, in the case when r is large compared to N, a good approximate solution of (6.10) can be found by ignoring, or relaxing, the constraint that the values of β_i are integers [69].

The next method is Lagrangian relaxation, where we need to solve the convex dual problem. For example, for solving (6.10), the boolean constraint can also be reformulated as $\beta_i(\beta_i - 1) = 0$, which is a quadratic equality constraint. Then we can solve the Lagrange dual of this problem. The optimal value of the relaxed problem provides a lower bound on the optimal value of the original optimization problem.

Here, since each observability Gramian term, $W_{O,i}$, is a positive semi-definite matrix, the *Outer Approximation* technique, given in [95], can be applied to solve this problem. The advantage of this method comparing to two mentioned conventional relaxation methods, is that the algorithm converges to an optimal solution of (6.10) in a finite number of iterations. The convergence proof can be found in [95]. This algorithm uses linearization of the objective function and the constraints at different points to build a mixed integer linear programming relaxation of the problem.

If $F(\beta)$ refers to the cost function given in (6.10), then we have

$$\begin{aligned} F(\beta) &= \log \left[\det \left(\sum_{i=1}^{N} \beta_i W_{O,i} \right)^{-1} \right], \\ \nabla_j F(\beta) &= -\text{trace} \left[\left(\sum_{i=1}^{N} \beta_i W_{O,i} \right)^{-1} W_{O,j} \right]. \end{aligned} \tag{6.11}$$

A lower bound solution of problem (6.10) can be obtained by solving a Mixed Integer Linear Programming as follows. For any given set of points T, we can build a relaxation of (6.10) as:

$$\begin{aligned} \underset{\beta}{\text{minimize}} \quad & \alpha \\ \text{subject to} \quad & \nabla F(\beta - \bar{\beta}) + F(\bar{\beta}) \leq \alpha, \ \ \forall \bar{\beta} \in T \\ & \sum_{i=1}^{N} \beta_i \leq r \\ & \beta \in \{0, 1\}. \end{aligned} \tag{6.12}$$

The relaxation (6.12) results in an iterative algorithm for solving the original problem (6.10). This iterative algorithm basically relies on updating the set of linearization points, T. The algorithm starts with $T = \{\beta^0\}$, where β^0 is a feasible solution of the original problem (6.10), or its continuous relaxed problem. Each iteration starts by solving (6.12) to find a point (α^k, β^k) and a lower bound α^k on the optimal value of (6.10). Now, β^k is added to T. The algorithm stops when the difference between the lower bound linear approximation and the actual value of the cost function at that point becomes negligible. The algorithm is described in Algorithm 2. More details on this algorithm can be found in [95].

$Z^U := +\infty$;

$Z^L := -\infty$;

$\beta^0 :=$ optimal solution of (6.10), replacing the integer constraint with continuous constraint $0 \leq \beta^i \leq 1$;

$k := 1$;

Choose a convergence tolerance ϵ;

while $Z^U - Z^L > \epsilon$ *and* (6.12) *is feasible* **do**

  Let $(\hat{\alpha}, \hat{\beta})$ be the optimal solution of (6.12);

  $\beta^k := \hat{\beta}$;

  $Z^L := \hat{\alpha}$;

  $Z^U := \min\{Z^U, F(\beta^k)\}$;

  $T := T \cup \{\beta^k\}$;

  $k := k + 1$;

end

Algorithm 2: Outer approximation algorithm

6.3 Privacy in Networks

In systems and control literature, different metrics have been used for designing an adaptive mechanisms for networks based on the desired performance in a specific application. Here, we analyze the privacy properties achievable by a network. More precisely, we study privacy and information leakage properties associated with the weighted average consensus protocol on a given inter-agent communication graph and address the following design goal: design a protocol, by proper selection of the weights in the consensus protocol with the privacy guarantee. In order to guarantee privacy, the goal is to design an adaptive network such that if a node has been attacked by a foreigner, then the amount of information of the other agents which is leaked from this node is minimized.

Protocols with privacy guarantees have been previously addressed [39–42], where they commonly consider the injection of random offsets into the states of the agents, and, the offsets are often sampled independently from a zero-mean distribution which will cancel out in average if the number of agents is large enough. Among many research have been done on the problem of network privacy,

the authors of [43] considered the connection between privacy in network and the observability of the network. The privacy guarantees in [43] means that each agent is not able to retrieve the initial states of non-neighbour agents. Since all agents are potentially malicious-curious, thus the optimal solution of [43] is a conservative solution, which results in removing some edges in the network to generate a topology with smallest number of stars.

In networked system design, a decentralized control structure is more desirable than a centralized one. Particularly, in some sensitive applications, agents prefer not to share their data with remote centres because of privacy and secrecy considerations. The authors of [44] argued that the distributed optimization methods improves privacy-preserving properties. Decentralized control theory has attracted several researchers, and several methodologies have been proposed, see for instance [45].

The problem of disturbance rejection and maintaining privacy are duals of each other. Chapman *et al.* in [96] defined the performance of a network based on the capability of a network to dampen external disturbances on the system, and proposed an online distributed algorithm for optimal selection of weighting the network edges. The problem of dynamic weight selection in the current research is favourable in privacy of the network. Although, the performance defined here is different from the one defined in [96], but the setup of these two problems are closely related to each other. For instance, in [96], the impact of the foreign input on the network dynamics is minimized, while in the current dissertation, we are minimizing the states data that can be reconstructed by directly sensing an output of the network which is observing by the foreign observer. In the problem of disturbance rejection, a metric of controllability Gramian has been used, in the problem of privacy guarantee, which is considered here, a metric based on the observability Gramian will be used.

The present research considers the design of the network weights as an online learning problem to achieve maximum privacy in a regret minimization framework, and in particular, does not require any noise injection, or edge removal. Here, it is assumed that the structure of the network has been given, which means it has been given which weights should be non-zero. Therefore, for any $\mathbf{w} > 0$ the network remains connected. We need to design the weights in the network to minimize the amount of information each agent can acquire about other agents in the network. In order to guarantee privacy, the goal is to design an adaptive network such that if a node has been attacked by a foreigner, then the amount information of the other agents leaking from this node is minimized. When information is broadcasting in a network, it is common to assume that communications are

bilateral, i.e., if agent i transmits to agent j then agent j also transmits to agent i. Therefore, the communication graph (or topology) is framed as an undirected graph.

6.3.1 System Modelling

Consider a multi-agent network consisting of N agents and let $\mathcal{G}$ denotes the inter-agent communication graph, where each agent i has the ability to transmit scalar data to its neighbours, denoted by $\mathcal{N}(i) = \{j : (i,j) \in \mathcal{E}\}$. Assume we have a network of individuals performing consensus algorithm. The dynamics of the network is given by:

$$\dot{\mathbf{x}} = \left\{ \sum_{l=1}^{M} \left[-\left(\mathbf{e}_{ij}\right)\left(\mathbf{e}_{ij}\right)^T w_{ij} \right] - I \right\} \mathbf{x}\,, \;\; l = \sigma(i,j)\,. \tag{6.13}$$

The dynamics of the network can be written as

$$\begin{aligned} \dot{\mathbf{x}} &= A(\mathbf{w})\mathbf{x}\,, \\ A(\mathbf{w}) &= A_0 + \sum_{l=1}^{M} A_l w_{ij}\,, \end{aligned} \tag{6.14}$$

where,

$$\begin{aligned} A_0 &= -I, \\ A_l &= -\mathbf{e}_{ij}\mathbf{e}_{ij}^T\,, \;\; l = \sigma(i,j)\,. \end{aligned} \tag{6.15}$$

Lemma 3. *The matrix $A(\mathbf{w})$ is negative definite for all positive weights.*

Proof. For a vector $\mathbf{a} \neq 0$, we have

$$\mathbf{a}^T A(\mathbf{w})\mathbf{a} = -\left(\sum_{l=1}^{M} \left(a_i - a_j\right)^2 w_{ij} + \|\mathbf{a}\|^2 \right)\,. \tag{6.16}$$

Since $w_{ij} > 0$, we have $\mathbf{a}^T A(\mathbf{w})\mathbf{a} \leq 0$, and, $\mathbf{a}^T A(\mathbf{w})\mathbf{a} = 0$ if and only if $\mathbf{a} = \mathbf{0}$. Thus $A(\mathbf{w}) \prec 0$. □

6.3.2 Optimization Problem

Now, assume a foreign agent attacks the network, i.e. he tries to steal information by connecting to an agent in the network, say agent k. Then the data being directly exposed to the hacker is given by:

$$y = x_k\,. \tag{6.17}$$

The objective, here is to minimize the information leaking from this node. Thus, we need to minimize a metric of observability of the network with respect to the measurement given by (6.17). The optimization problem for privacy can be written as

$$\begin{aligned} \underset{\mathbf{w}}{\text{minimize}} \quad & \operatorname{trace}(W_O) \\ \text{subject to} \quad & \dot{\mathbf{x}} = A(\mathbf{w})\mathbf{x} \\ & y = x_k\,, \end{aligned} \tag{6.18}$$

Now, let discretize the time period $[0, t_f]$, such that $0 = t_0 < t_1 < \cdots < t_f$. Thus, trace of the empirical observability gramian is given by

$$\begin{aligned} \operatorname{trace}(W_O) &= \frac{1}{4\epsilon^2}\int_0^{t_f} \sum_{i=1}^{N} \left\| y^{+i}(\tau) - y^{-i}(\tau) \right\|^2 \mathrm{d}\tau \\ &= \sum_t \int_t^{t+\Delta} \frac{1}{4\epsilon^2} \sum_{i=1}^{N} \left\| x_k^{+i}(\tau) - x_k^{-i}(\tau) \right\|^2 \mathrm{d}\tau \\ &= \sum_t \int_t^{t+\Delta} \sum_{i=1}^{N} \left(\mathbf{e}_i^T e^{A\tau} \mathbf{e}_k \right)^2 \mathrm{d}\tau \\ &= \sum_t \int_t^{t+\Delta} \operatorname{trace}\left(\mathbf{e}_k \mathbf{e}_k^T e^{2A\tau} \right) \mathrm{d}\tau \\ &= \sum_t \int_t^{t+\Delta} \left[e^{2A\tau} \right]_{k,k} \mathrm{d}\tau\,. \end{aligned} \tag{6.19}$$

Lemma 4. *The function* $\phi(\mathbf{w}, \tau) = \left[e^{2A(\mathbf{w})\tau} \right]_{k,k}$ *is convex with respect to* $\mathbf{w} > 0$*, for all* $\tau > 0$*.*

Proof. We can verify convexity by considering an arbitrary line, given by $\mathbf{w} = \mathbf{a} + s\mathbf{b}$, where, $\mathbf{a}, \mathbf{b} > \mathbf{0}$. We define $g(s) = \mathbf{e}_k^T e^{2A(s)\tau} \mathbf{e}_k$, and restrict g to the interval of values of s, that $\mathbf{a} + s\mathbf{b} > 0$. Then,

$$2A(s)\tau = 2\tau \left(A_0 + \sum_{l=1}^{M} A_l \mathbf{a}[l] + s \sum_{l=1}^{M} A_l \mathbf{b}[l] \right)\,.$$

For two matrices X and Y which commute, we have

$$\frac{d^2}{ds^2} e^{X+sY} = e^{X+sY} Y^2 = Y e^{X+sY} Y = Y^2 e^{X+sY}\,.$$

Since, A_0 and A_l commute for all $1 \leq l \leq M$, then

$$\frac{d^2}{ds^2} e^{2A(s)\tau} = 4\tau^2 \left(\sum_{l=1}^{M} \mathbf{e}_{ij} \mathbf{e}_{ij}^T \mathbf{b}[l] \right)^2 e^{2A(s)\tau} \geq 0\,.$$

Thus,

$$\frac{d^2 g(s)}{ds^2} = \mathbf{e}_k^T \left(\frac{d^2}{ds^2} e^{2A(s)\tau} \right) \mathbf{e}_k \geq 0 \,.$$

Since $g''(s) \geq 0$, we conclude that the function $\phi(\mathbf{w}, \tau)$ is convex with respect to $\mathbf{w}$. □

At each time t, the cost function, which was shown that is convex, is given by:

$$\begin{aligned} &\text{minimize} \quad f_t(\mathbf{w}) \\ &\text{subject to} \quad \mathbf{w}_{min} \leq \mathbf{w} \leq \mathbf{w}_{max} \,, \end{aligned} \tag{6.20}$$

where

$$f_t(\mathbf{w}) = \int_t^{t+\Delta} \phi(\mathbf{w}, \tau) \mathrm{d}\tau + \gamma \|\mathbf{w}\|^2 \,. \tag{6.21}$$

Theorem 11. *The cost function* (6.21) *is convex.*

Proof. In Lemma 4, we have shown that $\phi(\mathbf{w}, \tau)$ is convex. Since, integral of a convex function is convex, and, $\gamma \|\mathbf{w}\|^2$ is convex, then, the result of the theorem follows. □

Theorem 12. *The cost function* (6.21) *has gradients upper bounded by a number G.*

Proof. First let calculate the derivative of $\phi(\mathbf{w}, \tau)$ with respect to w_{ij}.

$$\begin{aligned} \frac{\partial \phi(\mathbf{w}, \tau)}{\partial w_{ij}} &= \mathbf{e}_k^T \left(2\tau e^{2A(\mathbf{w})\tau} A_l \right) \mathbf{e}_k \\ &= -\mathbf{e}_k^T \left(2\tau e^{2A(\mathbf{w})\tau} \mathbf{e}_{ij} \mathbf{e}_{ij}^T \right) \mathbf{e}_k \\ &= -2\tau \left(\mathbf{e}_k^T e^{A(\mathbf{w})\tau} \mathbf{e}_{ij} \right) \left(\mathbf{e}_{ij}^T e^{A(\mathbf{w})\tau} \mathbf{e}_k \right) \\ &= -2\tau \left(\mathbf{e}_k^T e^{A(\mathbf{w})\tau} \mathbf{e}_{ij} \right)^2 \\ &= -2 \left(\left[\sqrt{\tau} e^{A(\mathbf{w})\tau} \right]_{k,i} - \left[\sqrt{\tau} e^{A(\mathbf{w})\tau} \right]_{k,j} \right)^2 . \end{aligned} \tag{6.22}$$

Thus,

$$\nabla \phi(\mathbf{w}, \tau) = -2\tau \left(E^T e^{A\tau} \mathbf{e}_k \right) \circ \left(E^T e^{A\tau} \mathbf{e}_k \right) \,, \tag{6.23}$$

and,

$$\mathbf{g}_t(\mathbf{w}) = \nabla f_t(\mathbf{w}) = \int_t^{t+\Delta} \nabla \phi(\mathbf{w}, \tau) \mathrm{d}\tau + 2\gamma \mathbf{w} \,. \tag{6.24}$$

Since A is a negative definite matrix $\forall \mathbf{w}$, then $\lambda_i\{A\} < 0$, thus the matrix $\sqrt{\tau} e^{A\tau}$ has finite entries for all $\tau > 0$. Therefore, $\nabla \phi(\mathbf{w}, \tau)$ is bounded, and the integral over a finite period of time,

$\tau \in [t, t+\Delta]$ is bounded. Since, $\mathbf{w} \leq \mathbf{w}_{max}$, one can easily conclude that there always exists an upper-bound for gradient such that

$$\sup_{\mathbf{w}\in\mathcal{P}, t\in[T]} \quad \|\nabla f_t(\mathbf{w})\|_2 \leq G\,. \tag{6.25}$$

□

6.3.3 Regret Minimization Algorithm

Regret is defined as the difference between the cost of the sequence of actions and the performance of the best single action, $\mathbf{w}^*$, taken at every time step, considering $f_t(\mathbf{w})$ is known for all time a priori. The regret of an action sequence $\{\mathbf{w}_t\}$ is

$$\mathcal{R}_T = \sum_{t=1}^{T} \left(f_t(\mathbf{w}_t) - f_t(\mathbf{w}^*)\right)\,. \tag{6.26}$$

In [93] an online algorithm is presented that achieves regret $O(\log(T))$ for an arbitrary sequence of strictly convex functions, with bounded first and second derivatives. The *Online Newton Step* (ONS) algorithm is given in Algorithm 3. This algorithm is straightforward to implement, and the running time is $O(M)$ per iteration given the gradient [93]. To implement this algorithm, the convex set $\mathcal{P}$ should be bounded, such that

$$D = \max_{\mathbf{x},\mathbf{y}\in\mathcal{P},} \|\mathbf{x}-\mathbf{y}\|_2 < \infty\,. \tag{6.27}$$

D is called the diameter of the underlying convex set $\mathcal{P}$.

Proposition 7. *Assume that for all t, the cost function $f_t(\mathbf{w})$ is convex and has the property that $\forall \mathbf{w} \in \mathcal{P} : \|\nabla f(\mathbf{w})\| \leq G$. Then the algorithm Online Newton Step has the following regret bound:*

$$\mathcal{R}_T(ONS) \leq 5\left(\frac{1}{\alpha} + GD\right) n \log T\,. \tag{6.28}$$

Proof. See Theorem 2 of [93]. □

Inputs: convex set $\mathcal{P} \subset \mathbb{R}^M$, initial $\mathbf{w}_1 \in \mathcal{P}$;

$\beta := \min\{\frac{1}{4GD}, \alpha\}$;

$\epsilon = \frac{1}{\beta^2 D^2}$;

In iteration $s = 1$: use point $\mathbf{w}_1 \in \mathcal{P}$;

repeat

  foreach $\{i, j\} \in \mathcal{E}$ **do**

    $l := \sigma(i, j)$;

    $\mathbf{g}_s[l] := -\frac{1}{2}\left(\mathbf{e}_i^T A_s^{-1}\mathbf{e}_k - \mathbf{e}_j^T A_s^{-1}\mathbf{e}_k\right)^2 + \gamma \mathbf{w}_s[l]$;

    $\mathbb{A}_s := \sum_{i=1}^{s} \mathbf{g}_i[l]\mathbf{g}_i[l]^T + \epsilon I_M$;

    $\mathbf{w}_{s+1}[l] = \Pi_{\mathcal{P}}\left(\mathbf{w}_s[l] - \frac{1}{\beta}\mathbb{A}_s^{-1}\mathbf{g}_s[l]\right)$;

    $s := s + 1$;

    Here, $\Pi_{\mathcal{P}}$ denotes the *projection* in the norm induced by $\mathbb{A}_s$,

    $\Pi_{\mathcal{P}}^{\mathbb{A}_s}(\mathbf{y}) = arg\min_{\mathbf{x}\in\mathcal{P}}(\mathbf{y} - \mathbf{x})^T \mathbb{A}_s(\mathbf{y} - \mathbf{x})$;

  end

until *Convergence*;

Algorithm 3: Online Newton Step Algorithm

Chapter 7

APPLICATION I: BIO-INSPIRED VISION-BASED ROBOTS

Many existing navigation systems rely on global positioning measurements obtained from GPS or IMU. Due to the lack of GPS reception in some areas (e.g. indoors, underground, underwater, in space, etc.) and the high weight and price of inertial sensors interest is growing for non-traditional sensors for autonomous vehicles. Because vision-aided navigation systems can provide state estimates for the motion of a vehicle when no external reference, e.g. GPS, is available, and because visual sensors such as cameras are widely used because of their small size, light weight, and low cost [6], then optic flow sensing is an appealing option for navigation through dense unstructured environments. While detecting and avoiding obstacles using state estimation from GPS or Inertial Measurement Units (IMUs) is challenging, we can easily interpret optic flow measurements as proximity indications. Optic flow is an approximation of local motion based on local derivatives in a given sequences of images. Simulation results on a flying platform show that optic flow based navigation (OptiPilot) is able to permit collision-free flight in the vicinity of obstacles [97]. Furthermore, optic flow navigation can estimate the proximity to the obstacles, which is required for obstacle avoidance. The purpose in this chapter is to use the coupling property between actuation and sensing in nonlinear systems to find an acceptable sensor configuration and control policy for a robot which makes it capable of localizing itself inside an unknown unstructured environment, estimating its states, and avoid obstacles.

Flying insects are able to perform quick and highly accurate navigation and avoidance maneuvers in complex environments despite their low weight and small brain size. Insects essentially rely on two sensory modalities: gyroscopic and visual [98]. Halteres of many insects, e.g. flies, act as gyroscopic sensors and are responsible for attitude stabilization. Many insects also have two low resolution compound eyes which are particularly sensitive to image motion (optic flow). Insect-inspired visual flight control simulations have shown the usefulness of the optic flow for designing a lightweight (up to 100 gram) UAV [99]. The focus of the work here is on using vision as a sensory

system.

Two approaches have been considered for use of optic flow sensors, one is to use a small number of higher quality sensors, and the other is to use a large number of cheaper sensors, like many flying insects in which signals from arrays of sensors converge into flight commands. With respect to the use of large numbers of sensors in engineered systems, some work has been done with Wide-Field Integration where the estimation of state values is based on data from all local motion detectors as with lobula plate tangential cells in the visual sensory system of insects [100–102]. Humbert *et al.* provided a quick review of visuomotor system of insects in [103]. Other approaches have focused on the use of a small number of sensors. Beyeler and Zufferey proposed a control strategy using seven optic flow sensors [97], and Verveld *et al.* proposed a sensor configuration using six optic flow sensors [104]. A constraint of optic flow sensors is their limitation to estimating proximity of obstacles in the direction of flight. One solution to this problem is using a forward-pointing distance sensor. Another limitation of this strategy relates to the ability to detect small obstacles, which may not intersect with the viewing direction of the optic flow sensors. One way to resolve this problem is to note that for a constantly maneuvering vehicle, obstacles rarely remain unseen. Here, we will use this idea and consider the implementation of small numbers of rotating optic flow sensors for obstacle detection.

To ensure that the sensor measurements provide enough information for state estimation, the observability of the system dynamics must be evaluated. One of the most common approaches to test observability when dealing with a nonlinear model is to linearize it about a nominal trajectory and implement the conventional linear observability tests. As we will show here, if we linearize our model, in some cases the resulting linearized dynamics will not always be fully observable. However, while the observability matrix of the linearized model suffers from rank deficiency, the nonlinear observability matrix, constructed using Lie algebraic tools [6, 104] is full rank. The linearization may be observable in some cases, but the nonlinear observability analysis can help us to choose appropriate controls to make the system more observable in the sense of improving the condition number of the Jacobian of the observability Lie algebra. We also note that in linear models, observability is a function of sensor properties and the dynamics of the system, while in nonlinear systems, the observability is also a function of the control inputs.

The use of the vision sensor in navigation of robots has been investigated by a fair amount

of work in the literature. But, the problem of state estimation from the measurements and the problem of the design of control policy have been considered separately. Some works have been done regarding the state estimation of a vehicle with a fixed number of sensors and fixed configurations [104, 105], while some other works investigate the control policy [97, 106, 107]. In this chapter, the coupling between actuation and sensing in nonlinear systems for this specific problem is addressed. This chapter aims to extract the estimated states of a three degree of freedom vehicle from a minimal number of optic flow sensors. In our model, we are interested in estimating the position and orientation of the vehicle. The nonlinear observability analysis of the model shows that it is possible to obtain states of the system with a small number of optic flow sensors in different scenarios while avoiding obstacles.

In this chapter, the observability of a ground robot with an arbitrary number of sensors is investigated and the minimum number of optic flow sensors and the sensor configuration necessary to have an observable system are determined. Finally, a control policy which guarantees a conflict free path is introduced.

7.1 Modelling

Optic flow is a vector field of relative velocities of material points in the environment, projected into the tangent space of an imaging surface [101,108]. For a given angular velocity, ω, and translational velocity, $\mathbf{v}$, the spatially discrete optic flow pattern, Ω, can be expressed as

$$\Omega = \omega \times \hat{r} + \mu[\mathbf{v} - \langle \mathbf{v}, \hat{r} \rangle \hat{r}], \tag{7.1}$$

where $\hat{\mathbf{r}} = \frac{\mathbf{r}}{|\mathbf{r}|}$, and $\mathbf{r}$ is the distance from the imaging surface to the nearest object in the environment along the viewing direction of the sensor. The variable $\mu = \frac{1}{|\mathbf{r}|}$ is termed the nearness function. A complete study on optic flow can be found in the work by Zufferey [98].

Here it is assumed that the sensor measurements are de-rotated, meaning that the rotational component of the optic flow has been removed. The flow can be de-rotated by measuring the angular velocity of the vehicle using rate gyroscopes and subtracting it from optic flow measurement, or by actively rotating the sensor to counter the rotation of the body, as insects do [97]. De-rotation has been performed on a robot by computing the optic flow in a narrow window which is centred at the heading direction of the robot. It has been shown by Argyros et al that this method is accurate

enough to estimate the rotational motion component of the optic flow [106]. Here, it is assumed that there is an optic flow sensor pointing the heading direction in order to calculate the rotational component of the optic flow. While other methods might be used to calculate the rotational optic flow, they will not be addressed here. In the rest of this chapter, this sensor will not be counted toward the total number of sensors required for observability.

Assume a robot with an optic flow sensor operating in an environment with an obstacle that can be seen by the sensor. This unknown obstacle could be, e.g., a small part of a wall in a room. In Fig. 7.1 a robot is shown which moves with velocity v and heading angle θ.

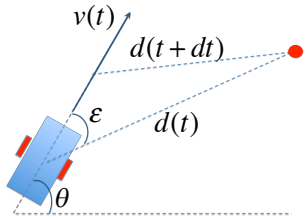

Figure 7.1: Navigation in a unknown environment. The red circle indicates a fixed obstacle.

At time t, the sensor detects an obstacle (red circle) at distance d. For a very small period of time, dt, one could assume that the sensor is still able to see the obstacle at time $t + dt$. Then we have

$$\dot{d} = \lim_{dt \to 0} \frac{d(t+dt) - d(t)}{dt} \approx \frac{v \cos\theta}{\cos(\theta + \epsilon)}. \tag{7.2}$$

In the system considered here, motion is assumed to be restricted to the horizontal plane. There are two control inputs, forward velocity (v) and the angular velocity ($\dot{\theta}$). Taking $\mathbf{x} = (d, \theta)$ as the kinematic variables, the state space equations are

$$\frac{d}{dt}\mathbf{x} = \begin{bmatrix} \frac{u_1 \cos\theta}{\cos(\theta+\epsilon)} \\ u_2 \end{bmatrix} = \begin{bmatrix} \frac{\cos\theta}{\cos(\theta+\epsilon)} \\ 0 \end{bmatrix} u_1 + \begin{bmatrix} 0 \\ 1 \end{bmatrix} u_2, \quad \mathbf{z} = \begin{bmatrix} \Omega_1 \\ \Omega_2 \\ \vdots \\ \Omega_m \end{bmatrix} + \mathbf{w}, \tag{7.3}$$

with nonlinear measurement functions $\Omega_i, i = 1, \ldots, m$, where m is the number of sensors, and Ω_i

can be given as:

$$\Omega_i = \frac{u_1 \sin \epsilon_i}{d_i}, \tag{7.4}$$

and $\mathbf{w}$ is measurement noise which is zero-mean white noise that satisfy $E\{ww^T\} = R$. Note that the dynamics of the system and the output of the sensors are both nonlinear.

Based on the assumption of motion in horizontal plane, two following scenarios are considered:

- Scenario I: multiple fixed sensors
- Scenario II: single rotating sensor

7.1.1 Scenario I: Fixed Sensors

Motion in a corridor and design of a controller for obstacle avoidance using optic flow sensors has been considered in a few prior studies [100, 102, 106, 109]. This scenario is an essential step toward navigating between obstacles in a cluttered environment. Here, we assume that a robot is following a corridor-like path with predefined direction or inside a planar closed space that the robot can freely move in every direction. In this scenario, the purpose is to estimate the position and orientation of the robot.

We assume that there are i_R sensors on the right side of the robot, i_L sensors on the left, and $i_R = i_L$. The configuration is symmetric, and no sensor points forward ($\epsilon = 0$) or backward ($\epsilon = \pi$) of the robot. Considering (7.4), the sensor output at these two locations is zero. Also, recall that all sensor measurements are assumed to be de-rotated. This configuration is shown in Fig. 7.2.

The number of sensors required to determine the position of the robot depends on the complexity of the environment in which the robot is moving and the number of objects required to be detected, e.g., obtaining full position data (forward and lateral positions) of a robot in a simple rectangular-shape room with known geometry requires at least three sensors.

7.1.2 Scenario II: Rotating Sensor

By increasing the complexity of the robot's path or adding more items (obstacles) in the room, we will need more sensors. Visual sensory system of insects works in a similar way to achieve a robust solution. They employ a large number of spatially distributed sensors. Instead of increasing the

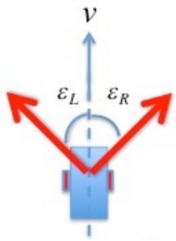

Figure 7.2: The configuration of the sensory system for scenario 7.1.1. The arrows indicate the viewing directions of the sensors. Each sensor contains information about the surroundings along its direction.

number of sensors with the increasing number of obstacles, the idea of active sensing is used in which a small number of rotating sensors are used. In this scenario, a robot which is moving among some obstacles using only one sensor is considered. In this model, the sensor is rotating with a specified angular velocity. The angular velocity of the sensor is determined by a constant value ω_s , and the viewing angle of the sensor is $\epsilon(t) = \omega_s t + \epsilon(t_0)$. It will be shown in Section 7.2.2 that full state estimation is possible with one rotating sensor.

7.2 Observability Analysis

Based on the discussion presented in previous chapters, if we can find n linearly independent vectors within the state dependent matrix dO for a given point, then the system is locally observable at that point. In case we need a specific vector field $\mathbf{f}$ to make the matrix full rank, we need to ensure that the corresponding inputs are present. For example if we need $[\mathbf{f}_0, \mathbf{f}_i]$ to make dO full rank, we should have non-zero u_i input, or if we have $[\mathbf{f}_i, \mathbf{f}_j]$ as one of the rows of dO, we need a motion that results from combination of u_i and u_j. Sinusoids are a common input to generate this kind of motion [23, 59]. If the matrix is full rank for all states, then the system is observable.

7.2.1 Scenario I: Fixed Sensors

To begin exploration of estimation with multiple fixed sensors, first, assume a robot with one sensor (ϵ_1). The state vector in this case is $\mathbf{x} = (d_1, \theta)^T$, where d_1 is the distance of the sensor to the

closest object in the environment located in the viewing direction of the sensor. The number of states is $n = 2$, and the output is $z_1 = \Omega_1$. In this case, the linearized model of (7.3) about some chosen nominal trajectory is not full rank. Since $\mathbf{f}_0 = \mathbf{0}$ in (7.3), the linearized observability matrix given by (2.7) for zero inputs is

$$O(t) = H(t) = \mathbf{0}. \tag{7.5}$$

The rank of this linearized observability matrix is zero, which corresponds to unobservability of the linearized model. To investigate the observability of this system, we need to apply nonlinear observability tools as follows.

Theorem 13. *Given system* (7.3) *with an arbitrary number of sensors. The system is locally observable if* $\epsilon_i \neq 0$ *for all sensors, and a control policy with* $u_1 \neq 0$ *or* $[\mathbf{f}_1, \mathbf{f}_2] \neq 0$.

Proof. The control vector fields ($\mathbf{f}_1$ and $\mathbf{f}_2$) and their Lie bracket ($[\mathbf{f}_1, \mathbf{f}_2]$) are:

$$\begin{aligned} \mathbf{f}_1 &= \begin{bmatrix} \frac{\cos\theta}{\cos(\theta+\epsilon_1)} \\ 0 \end{bmatrix} = \begin{bmatrix} g_0(\epsilon_1;\theta) \\ 0 \end{bmatrix}, \quad \mathbf{f}_2 = \begin{bmatrix} 0 \\ 1 \end{bmatrix} \\ [\mathbf{f}_1, \mathbf{f}_2] &\equiv \frac{\partial \mathbf{f}_2}{\partial \mathbf{x}}\mathbf{f}_1 - \frac{\partial \mathbf{f}_1}{\partial \mathbf{x}}\mathbf{f}_2 = \begin{bmatrix} -\frac{\partial}{\partial\theta}\left(\frac{\cos\theta}{\cos(\theta+\epsilon_1)}\right) \\ 0 \end{bmatrix} = \begin{bmatrix} g_1(\epsilon_1;\theta) \\ 0 \end{bmatrix}. \end{aligned} \tag{7.6}$$

The Lie algebra observability matrix, $\mathcal{O}$, has the terms

$$\mathcal{O} = \begin{bmatrix} z_1 \\ \frac{\partial z_1}{\partial \mathbf{x}}\mathbf{f}_1 \\ \frac{\partial z_1}{\partial \mathbf{x}}[\mathbf{f}_1, \mathbf{f}_2] \end{bmatrix}, \tag{7.7}$$

where

$$\frac{\partial z_1}{\partial \mathbf{x}} = \begin{bmatrix} \frac{-u_1 \sin\epsilon_1}{d_1^2} & 0 \end{bmatrix} = \begin{bmatrix} g_2(\epsilon_1; d_1) & 0 \end{bmatrix}. \tag{7.8}$$

The Jacobian matrix, $d\mathcal{O}$, can be constructed as:

$$d\mathcal{O} = \begin{bmatrix} g_2(\epsilon_1;d_1) & 0 \\ g_0(\epsilon_1;\theta)g_2'(\epsilon_1;d_1) & g_2(\epsilon_1;d_1)g_0'(\epsilon_1;\theta) \\ g_1(\epsilon_1;\theta)g_2'(\epsilon_1;d_1) & g_2(\epsilon_1;d_1)g_1'(\epsilon_1;\theta) \end{bmatrix}. \tag{7.9}$$

One can easily conclude that $d\mathcal{O}$ is full rank if $u_1 \neq 0$ or $[\mathbf{f}_1, \mathbf{f}_2] \neq 0$. As long as the robot moves in a way that the Lie bracket term is non-zero, full state estimation is possible.

If $\epsilon_1 = 0$, then $z_1 = 0$ and the system becomes unobservable. This situation happens when the robot moves exactly toward to or away from an obstacle. In this case, the system is not locally observable, and the distance d cannot be estimated.

Now, we add another sensor, ϵ_2. The new state vector is $\mathbf{x} = (d_1, \theta, d_2)$, where d_i is the distance of the sensor i to the closest object in the environment located in the viewing direction of that sensor. The number of states is now $n = 3$, and the output is $\mathbf{z} = (z_1, z_2) = (\Omega_1, \Omega_2)$. The vector fields $\mathbf{f}_1$, $\mathbf{f}_2$, and $[\mathbf{f}_1, \mathbf{f}_2]$ become

$$\mathbf{f}_1 = \begin{bmatrix} g_0(\epsilon_1;\theta) \\ 0 \\ g_0(\epsilon_2;\theta) \end{bmatrix}, \quad \mathbf{f}_2 = \begin{bmatrix} 0 \\ 1 \\ 0 \end{bmatrix}, \quad [\mathbf{f}_1, \mathbf{f}_2] = \begin{bmatrix} g_1(\epsilon_1;\theta) \\ 0 \\ g_1(\epsilon_2;\theta) \end{bmatrix}. \tag{7.10}$$

The Lie algebra observability matrix, $\mathcal{O}_2$, is given by:

$$\mathcal{O}_2 = \begin{bmatrix} \mathcal{O} \\ z_2 \end{bmatrix}, \tag{7.11}$$

where $\mathcal{O}$ is the Lie algebra matrix in (7.7). Therefore, the Jacobian matrix, $d\mathcal{O}_2$, is

$$d\mathcal{O}_2 = \begin{bmatrix} g_2(\epsilon_1;d_1) & 0 & 0 \\ g_0(\epsilon_1;\theta)g_2'(\epsilon_1;d_1) & g_2(\epsilon_1;d_1)g_0'(\epsilon_1;\theta) & 0 \\ g_1(\epsilon_1;\theta)g_2'(\epsilon_1;d_1) & g_2(\epsilon_1;d_1)g_1'(\epsilon_1;\theta) & 0 \\ 0 & 0 & g_2(\epsilon_2;d_2) \end{bmatrix}. \tag{7.12}$$

It can be seen that $d\mathcal{O}_2$ is full rank under the same condition as the matrix $d\mathcal{O}$ being full rank, and $\epsilon_2 \neq 0$. This result clearly extends to the addition of an arbitrary number of sensors. Therefore, the system is observable with any number of sensors if $u_1 \neq 0$ or $[\mathbf{f}_1, \mathbf{f}_2] \neq 0$.

□

It can be seen that if $u_1 \neq 0$ but $u_2 = \dot{\theta} = 0$, then the Lie bracket term vanishes, and the system is still observable. We will show in Section 7.3 that implementing the control inputs suggested by the nonlinear Lie algebra observability analysis, a control which generates a non-zero Lie bracket term, can sometimes improve the quality of observability of the states.

Note that nothing here is dependent on having a symmetric sensors configuration. For the sake of simplicity in obtaining optic flow based control policy (which will be presented in the next section), we assume that we have the same number of sensors on each side of the vehicle.

Practically, more than one sensor is needed for a robot which is capable of navigating in an unknown environment based on the level of complexity of the specific mission designed for the robot. To obtain an admissible placement of the sensors to improve the quality of navigation in a planar room, the determinant of the Lie algebra observability matrix has been evaluated for different values of ϵ_{L_i} and ϵ_{R_i} (Fig. 7.2) and different number of sensors on the left and right sides of the robot. To find admissible values for ϵ_L and ϵ_R among all candidates, a set of Monte Carlo simulations has been performed. The result of this simulation shows that one admissible configuration is a symmetric configuration with two sensors at each side.

7.2.2 Scenario II: Rotating Sensor

Assume a robot with one rotating sensor is moving in a known square room similar to Fig. 7.3.

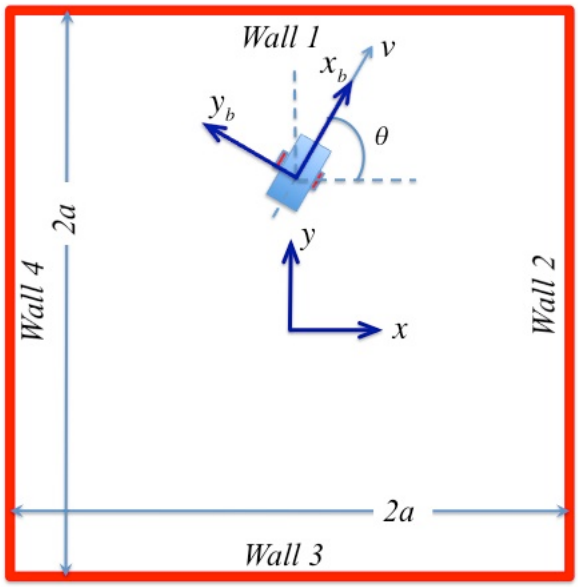

Figure 7.3: The robot in a 2-D room with a single sensor represents scenario II.

To show that the system in this specific example is observable, the definition of the modified observability matrix [110–112] can be used.

Definition 2. *The nonlinear system given by* (7.3) *with* $m = 1$ *satisfies the modified nonlinear observability rank condition if for any sequence of indices* $\tau_i \in \mathbb{N}_0,\ \ i = 1, 2,\ \tau_1 < \tau_2$ *the modified*

nonlinear observability matrix

$$\mathbb{O} = \begin{bmatrix} \frac{\partial z}{\partial \mathbf{x}}(\mathbf{x}_{k+\tau_1}) \frac{\partial \mathbf{f}}{\partial \mathbf{x}}(\mathbf{x}_{k+\tau_1-1}) \dots \frac{\partial \mathbf{f}}{\partial \mathbf{x}}(\mathbf{x}_k) \\ \frac{\partial z}{\partial \mathbf{x}}(\mathbf{x}_{k+\tau_2}) \frac{\partial \mathbf{f}}{\partial \mathbf{x}}(\mathbf{x}_{k+\tau_2-1}) \dots \frac{\partial \mathbf{f}}{\partial \mathbf{x}}(\mathbf{x}_k) \end{bmatrix} \tag{7.13}$$

has full rank $n = 2$ *at* $\mathbf{x}_k$.

Theorem 14. *The nonlinear system given by* (7.3) *with* $m = 1$ *moving in a 2-D square room satisfies the modified nonlinear observability rank condition if* $\omega_s \neq 0$.

Proof. The validity of this theorem using the definition of modified observability matrix, can be found in related work of the author of this dissertation [113]. □

Based upon Theorem 14, the angular velocity of the sensor ω_s should be non-zero for this specific example. The proof of observability in general is given as follows.

The state vector in the case of a single rotating sensor is $\mathbf{x} = (\epsilon, d, \theta)$ with the equation (7.3) augmented with $\dot{\epsilon} = u_3$. Note that ϵ, which was a parameter in section 7.2.1, is now a state. The vector fields $\mathbf{f}_1$, $\mathbf{f}_2$, $\mathbf{f}_3$, $[\mathbf{f}_1, \mathbf{f}_2]$ and $[\mathbf{f}_1, \mathbf{f}_3]$ are

$$\begin{gathered} \mathbf{f}_1 = \begin{bmatrix} 0 \\ g_0(\epsilon, \theta) \\ 0 \end{bmatrix} \quad \mathbf{f}_2 = \begin{bmatrix} 0 \\ 0 \\ 1 \end{bmatrix} \quad \mathbf{f}_3 = \begin{bmatrix} 1 \\ 0 \\ 0 \end{bmatrix} \\ [\mathbf{f}_1, \mathbf{f}_2] = \begin{bmatrix} 0 \\ g_1(\epsilon, \theta) \\ 0 \end{bmatrix} \quad [\mathbf{f}_1, \mathbf{f}_3] = \begin{bmatrix} 0 \\ g_3(\epsilon, \theta) \\ 0 \end{bmatrix}, \end{gathered} \tag{7.14}$$

where

$$g_3(\epsilon, \theta) = -\frac{\partial}{\partial \epsilon} \left(\frac{\cos \theta}{\cos (\theta + \epsilon)} \right). \tag{7.15}$$

The observability Lie algebra has the terms:

$$\mathcal{O} = \begin{bmatrix} z \\ L_{\mathbf{f}_1} z \\ L_{\mathbf{f}_3} z \\ L_{[\mathbf{f}_1, \mathbf{f}_2]} z \\ L_{[\mathbf{f}_1, \mathbf{f}_3]} z \end{bmatrix}, \tag{7.16}$$

and one can show that the Jacobian matrix is full rank if any pair of the corresponding control inputs in the set $\{\mathbf{f}_1, \mathbf{f}_3, [\mathbf{f}_1, \mathbf{f}_2], [\mathbf{f}_1, \mathbf{f}_3]\}$ are non-zero. It can be seen that even in the case of $\dot{\epsilon} = 0$ (non rotating sensor), the system could be observable if the applied control policy for the robot involves $u_1 \neq 0$ and non-zero Lie bracket term $[\mathbf{f}_1, \mathbf{f}_2]$. It is also clear that in all cases, we need vector field $\mathbf{f}_1$ for observability. In fact, the robot should continuously move in order to be observable.

7.3 State Estimation

To demonstrate state reconstruction, an Unscented Kalman Filter (UKF) is used. Compared to Extended Kalman filter [6, 105, 114], the UKF makes fewer assumptions on the form of the noise, and typically performs better in the presence of nonlinearities. The references [55, 104] include a complete description of the UKF algorithm.

In this section, an oscillatory sinusoidal control will be used whenever generation of a non-zero Lie bracket vector field is needed. This control policy is a common choice for generating the Lie bracket term which is sometimes necessary to make the nonlinear system observable [59].

To demonstrate how the position and orientation of a robot can be obtained using an optic flow sensor, an estimator is simulated for a hypothetical scenario. Here, an infinite-length tunnel is assumed. Mission of the robot is moving along this tunnel. A schematic view of this tunnel along with the simulated trajectory of the system can be seen in Fig. 7.4. Applied controls in this scenario are

$$u_1 = 0.05 \cos \omega t, \quad u_2 = 0.01 \sin \omega t. \tag{7.17}$$

It is clear that because of symmetry, the position of the robot along this tunnel cannot be obtained by having information of relative distances. The error in the UKF for estimating the position and the orientation and the 95% confidence measure can be seen in Fig. 7.5. The estimator is only capable of estimating vertical position, and the initial error in the horizontal position remains unchanged.

In the next simulation, the effect of the control input on the quality of observability is considered. As it was shown in Section 7.2.1, the system is observable if $u_1 \neq 0$ with no use of control input u_2. This simulation will demonstrate the effect of control inputs on improving the quality of the observability. The condition number of the observability matrix (the square root of the ratio of the

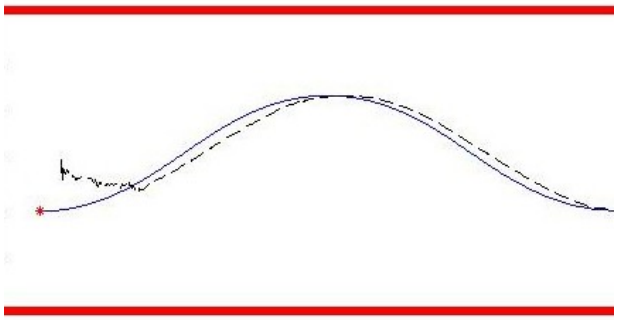

Figure 7.4: Simulated trajectory of a robot in a tunnel. The trajectory above represents the motion using controls (7.17) while moving along an infinite-length tunnel with fixed walls. The true and estimated trajectories are indicated by the blue line and black dashed line. The walls of the tunnel are indicated by red lines.

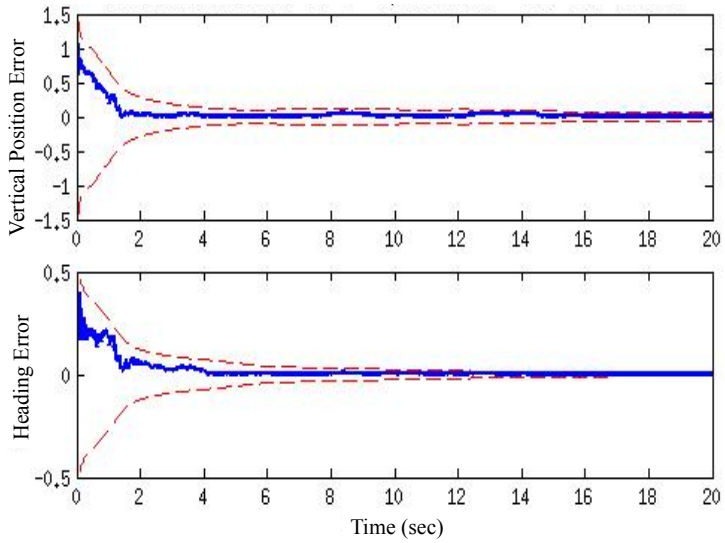

Figure 7.5: State error of the Unscented Kalman Filter. The blue line indicates the error and the red lines indicate 3σ bounds. The measurement noise is zero-mean Gaussian white noise with covariance equal to 10^{-2}.

largest eigenvalue of that matrix to its smallest) is used as a criterion to measure the observability of the system. A smaller value of the condition number (close to one) generally implies increased observability of a system. In this example, random initial and final points inside the room have been chosen. Two control policies are considered. First, the robot moves from the initial to the final point with constant velocity along a straight line ($u_2 = 0$). The second policy is given by:

$$u_1 = 0.1 \cos \omega t, \quad u_2 = \frac{\pi}{8} \sin \omega t. \tag{7.18}$$

The random linear and oscillatory trajectories have been shown in Fig. 7.6. In Fig. 7.7, the condition number of the observability matrix for the two control policies are compared. As can be seen in this figure, the condition numbers of the straight line control policies are larger than for the oscillatory motion for all cases. These results demonstrate the subtle effect that controller design can have for nonlinear systems.

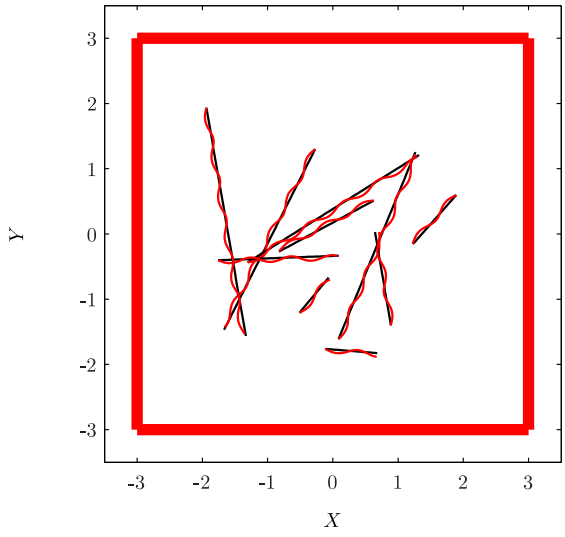

Figure 7.6: Ten randomly chosen linear/oscillatory trajectories inside the square room.

7.4 Conflict Resolution

Navigation in some unknown environments is a major role for the autonomous use of a robot. Optic flow sensors have been used for safely maneuvering through indoor corridors [98, 106, 107]. Our

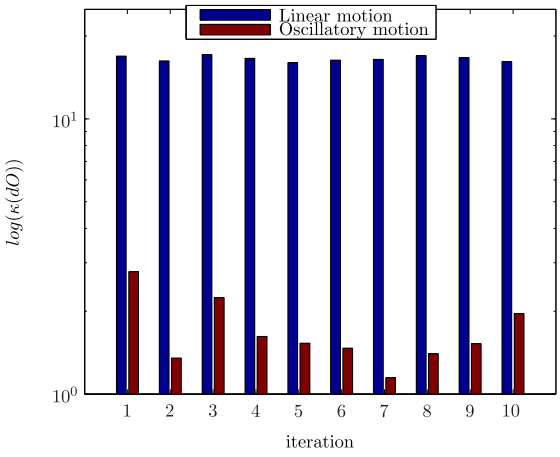

Figure 7.7: The condition number of the Lie algebra observability matrix for the sample trajectories shown in Fig. 7.6.

purpose here is designing control algorithms to enable an autonomous robot to be able to move inside an unknown area, and also to have the capability to estimate its location and orientation to localize itself or generate a map from its environment.

The sensors have different effects based on their viewing direction. Since the robot does not need to avoid obstacles that are behind it, the sensors with viewing direction corresponding to behind the vehicle ($\frac{\pi}{2} < \epsilon_L, |\epsilon_R| < \pi$ in Fig. 7.2) should be less effective for conflict resolution than the sensors in front of the robot. Beyeler et. al suggest that the area around $\epsilon_L, \epsilon_R = \pm\frac{\pi}{4}$ is the best and most reliable area which should be covered by optic flow sensors [97].

7.4.1 Fixed Sensors Scenario

In this section, a feedback control policy based on fixed sensor orientations is presented. Using this control policy, robots are capable of autonomously navigating in different closed environments filled with obstacles. This policy, which is based upon the weighted sum of the sensor measurements, is

described as follows:

$$\begin{aligned} u_1 &= k_1 \cos \omega t \\ u_2 &= k_2 \left(\sum_{i=1}^{i_R} \Omega_{R_i} \cos\left(\frac{\epsilon_{R_i}}{2}\right) - \sum_{i=1}^{i_L} \Omega_{L_i} \cos\left(\frac{\epsilon_{L_i}}{2}\right) \right) + k_3 \sin \omega t, \end{aligned} \tag{7.19}$$

where $k_1, k_2, k_3 \in \mathbb{R}_{>0}$ are constant, and i_R and i_L are the number of sensors on the right and left of the robot respectively. The term corresponding to k_2 in (7.19) determines whether the robot is closer to obstacles to the left or to the right side of its heading direction. If there is an obstacle on the left, then $\Omega_L > 0$, and a negative $\dot{\theta}$ command is produced which is a turn right command. On the other hand, an obstacle on the right side of the vehicle results in a left turn. The weighting factors $0 < \cos\left(\frac{\epsilon}{2}\right) < 1$ give higher weight to the forward pointing sensors rather than backward pointing sensors. The weighting factors for the forward pointing sensors are in the interval of $\left[\frac{\sqrt{2}}{2}, 1\right)$, while the weighting factors for the backward pointing ones are in the interval of $\left(0, \frac{\sqrt{2}}{2}\right]$.

In the following simulation, this control policy is applied. In Fig. 7.8, a simulated trajectory is shown. It can be seen in this figure that by applying the feedback methodology described above, the robot is capable of navigating inside a 2-D environment and clearly avoids collision with the walls. The error for estimating the position, heading, and the 95% confidence measure can be seen in Fig. 7.9.

7.4.2 Rotating Sensor Scenario

Because the sensor is itself not fixed in the case of rotating sensor, the conflict avoidance control does not require oscillatory terms for observability (section 7.2.2). The control policy in this case is given as:

$$\begin{aligned} u_1(t) &= U_0 \\ u_2(t) &= -k_2 \Big[\sum_{\tau=t-T}^{\tau=t} \Omega(\mathbf{x}(\tau)) \cos\left(\frac{\epsilon(\tau)}{2}\right) \Big] \\ u_3(3) &= \omega_s. \end{aligned} \tag{7.20}$$

In the control policy given by (7.20), the controls u_1 and u_3 are non-zero. As was discussed in section 7.2.2, one of the sufficient conditions for observability is active sensing along vector fields $\mathbf{f}_1$ and $\mathbf{f}_3$. Therefore, the control policy (7.20) satisfies the observability condition.

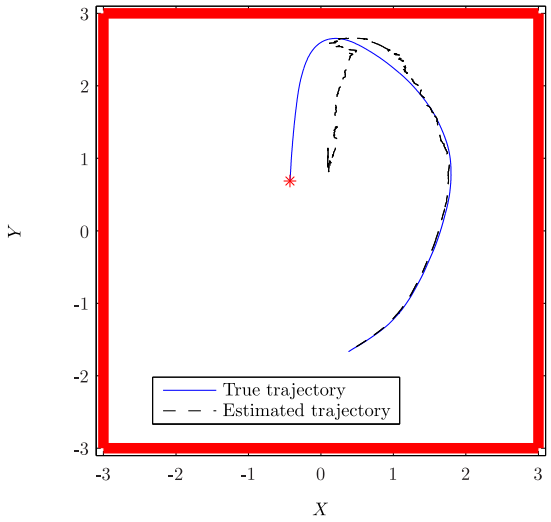

Figure 7.8: Simulated trajectory of the vehicle in a room. The true trajectory and estimated trajectory are indicated by blue line and black dashed line respectively. The walls are indicated by red lines. The red star shows the initial point.

On the other hand, since in this case the sensor measurement of only one sensor is available at each time step, we need to use the sensor measurements over a time interval $[t-T, t]$ for a constant T, which can be chosen as $T = N\Delta t$, where Δt is the time step between measurement arrival and $N \in \mathbb{N}$. The values of ω_s and T should be chosen such that by choosing $N \approx 4$ or 5, the value of $T\omega_s$, which is the viewing angle swept by the sensor in T seconds, covers an acceptable area around the robot.

By employing these controls, an example of corridor navigation is solved. The resulting trajectory is shown in Fig. 7.10. As can be seen, the robot is also capable of navigating autonomously in a corridor-like environment.

Based on the discussions of observability analysis and conflict resolution in this chapter, it was shown that a robot is capable of navigating in an unknown environment, avoiding obstacles, and estimating its states. If the data d, θ, and ϵ are available as the robot moves, an estimation of the map of the area around the robot becomes possible.

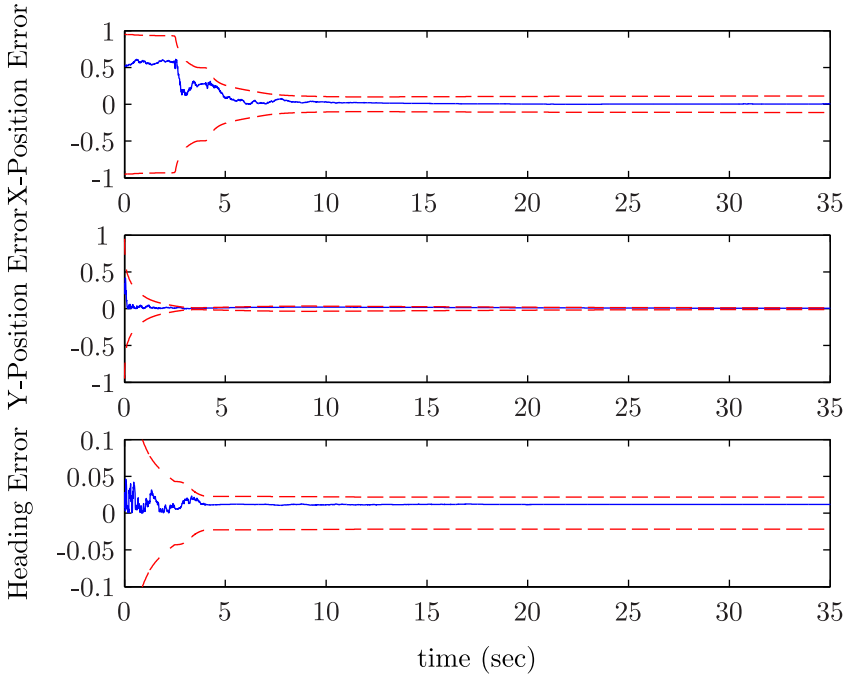

Figure 7.9: State error of and 3σ bounds. The measurement noise is zero-mean Gaussian white noise with covariance equal to 10^{-2}.

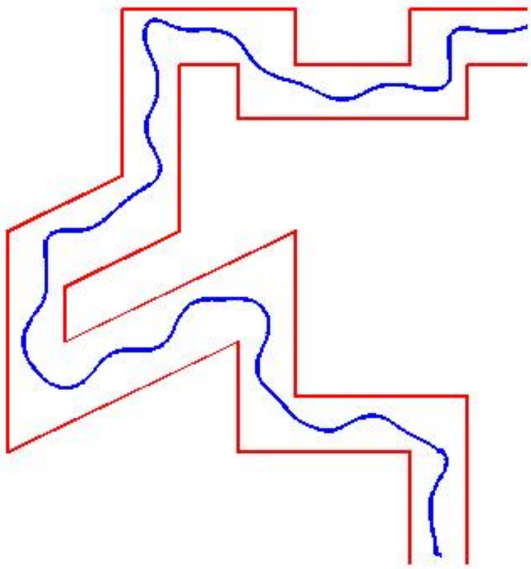

Figure 7.10: Navigation in a corridor, while avoiding the walls.

Chapter 8

APPLICATION II: OPTIMAL SENSOR ALLOCATION IN BIOLOGICAL NETWORKS

Analysing complex networks, such as the Internet, social networks, and biological networks has been the subject of increasing research attention in recent years. A key characteristic of system analysis is being able to determine information about the system state using measurement data. This observability analysis, as applied to a network, aims to predict the behaviour of each individual in the network based on a set of measured properties and on the local rules governing individual vertices. Observability-based design of a multi-agent network can be found in some recent works such as [26, 43]. In these works, the objective is to find the structure of the communication graph to guarantee observability (unobservability) in [26] ([43]). The authors of these works studied the effect of different topologies of the communication graph and the communication weights between nodes in a network on the rank of the observability matrix.

Social networks have the longest history in the field of study of real-world networks where studying interactions in human behaviour has received significant attention. For instance, it is of interest to consider the process of decision-making in a group of people [89] or to study the process of creating different colonies in a human group based on the level of trust between the individuals in that group [90]. In these studies, data collection is usually carried out by querying a subset of participants in the network directly using questionnaires or interviews. Such methods are labour-intensive, and the size of the network that can be observed is limited. Therefore the problem of optimal choice of nodes to be observed is critical. Another application of high impact is electric power grid management. An electric power grid is a network of interconnected high-voltage transmission lines spanning a country or a portion of a country. Identification of abnormal patterns of behaviour in power distribution networks is very important and has been the subject of many studies recently, e.g. [91] and [42]. Finally, some biological systems can be represented as networks. Genetic regulatory networks, blood vessel networks, and neural networks are classes of biological

network systems have been receiving recent attention in the research literature.

The focus of this chapter is studying two examples of biological network:

- The first example is a virus spreading network. The purpose here is to detect the spread of an epidemic disease in an arbitrary community by observing the infected/healthy status of a few number of people in that community. The problem of containing virus spreading processes in a network has been studied in the literature, e.g. [47]. This modelling is an important step toward understanding the behaviour of spreading a disease in a community. However, given an arbitrary network, it remains a challenge to determine the requirements that make the entire network observable.

- The second example is a model of genetic system, and was invented by Brian Goodwin in 1965 [48]. This model describes the negative feedback oscillation on gene expression. In our three-dimensional model, the state variables are related with mRNA concentration, the protein concentration, and the inhibitor concentration of transcription. Basically, mRNA produces a protein, which, in turn, activates a transcriptional inhibitor. An advantage of this model is its simplicity that allows for analytical understanding of the biochemical mechanism, whereas other biological models of cellular behaviour usually exhibit high complexity which make them hard to implement. The observability analysis of a single Goodwin oscillator has been investigated previously. It has been proven that the system is fully observable from mRNA concentration measurements [37, 115]. This is an important step toward understanding this biochemical oscillator. However, given a network of oscillators coupled through inter-cellular interactions, it remains a challenge to determine the requirements that make the entire network observable. In this research, we consider a network of synchronized Goodwin oscillators [10, 116, 117], and find the best selection of nodes which yield the state information of the entire network. In these systems it is always necessary to know about unmeasured internal information from external measurements [37]. The problem of observability analysis is critical, because some states are very hard to measure directly. For example, protein concentrations are impossible to measure. Instead, some other states of the system, for example mRNA levels, can be measured, in order to obtain a whole understanding of the biological process.

In both cases mentioned above, we desire to maximize the amount of information we can gather about all the agents in the network by communicating with a small number of agents. Specifically, we would like to maximize the observability of the overall network by sharing limited information between the agents. Network observability is a property of a network in which we can infer all state information about all the agents in the network by knowing the structure of information sharing via a communication graph, i.e., we should be able to recover the whole state of the system by having partial information from some nodes of the network.

8.1 Virus Spreading Model in Networks

Here, we formulate our problem using the setting proposed in [118] for virus spread in any network with N nodes. This approach is one of the most popular epidemic models and is called the Susceptible-Infected-Susceptible (SIS) model [119]. In this model, each node in the network is either infected or healthy. An infected node, i, can infect its neighbours with an infection rate, β_i, and it is cured with curing rate, δ_i. As a node is cured and healthy, it is again prone to the virus. The spread is modelled by an undirected network specified by a symmetric adjacency matrix, $\mathcal{A}$. The state of each node i is described by the binary random variable $X_i(t) \in \{H, I\}$, i.e. the node at time t in the network has two states: infected with probability $Pr[X_i(t) = I]$ and healthy with probability $Pr[X_i(t) = H]$. The evolution of the states is described by a Markov Process. The two possible state transitions of node i are:

(1) Assume node i is healthy at time t, i.e. $X_i(t) = H$. This node can switch to infected state over small time $\Delta t > 0$ with probability:

$$Pr[X_i(t + \Delta t) = I | X_i(t) = H] = \sum_{j \in \mathcal{N}_i} \mathcal{A}[i, j]\beta_i X_j(t)\Delta t + o(\Delta t). \tag{8.1}$$

(2) Assume node i is infected at time t, i.e. $X_i(t) = I$. The probability of being recovered after small time $\Delta t > 0$ is:

$$Pr[X_i(t + \Delta t) = H | X_i(t) = I] = \delta_i \Delta t + o(\Delta t). \tag{8.2}$$

Denoting $x_i(t) = Pr[X_i(t) = I]$ and considering that $Pr[X_i(t) = H] = 1 - x_i(t)$, the Markov differential equation for node i turns out to be nonlinear, given by

$$\dot{x}_i(t) = f_i(\mathbf{x}) = \beta_i \sum_{j=1}^{N} \mathcal{A}_{ij} x_j(t) - x_i(t) \left(\beta_i \sum_{j=1}^{N} \mathcal{A}[i,j] x_j(t) + \delta_i \right). \tag{8.3}$$

By defining $\mathbf{x} = \begin{bmatrix} x_1 & x_2 & \cdots & x_N \end{bmatrix}^T$, the differential equation (8.3) can be written in matrix form as

$$\dot{\mathbf{x}}(t) = \mathbf{f}(\mathbf{x}) = (B\mathcal{A} - D)\,\mathbf{x}(t) - \left(\sum_{j=1}^{N} e_j e_j^T \mathbf{x}(t) e_j^T \right) B\mathcal{A}\mathbf{x}(t)\,, \tag{8.4}$$

where $B = \text{ diag}(\beta_j)$ and $D = \text{ diag}(\delta_j)$. Here, it is assumed that $\lambda_1 (B\mathcal{A} - D) < 0$, where $\lambda_1(\cdot)$ is the largest eigenvalue. It is proved in [120] that the linear dynamics system $\dot{\mathbf{x}}(t) = (B\mathcal{A} - D)\,\mathbf{x}(t)$ is an upper bound for the nonlinear dynamics system (8.4). Therefore, the disease-free equilibrium ($\mathbf{x} = 0$) is stable.

The model of virus spreading is a nonlinear dynamics system. In this chapter, the empirical approach is used to compute the observability Gramian. The empirical observability Gramian, considering $y^k = x_k$, is an $N \times N$ matrix, $W_{O,k}$, whose (i,j) component is

$$\frac{1}{4\epsilon^2} \int_0^{t_f} \left(x_k^{+i}(t) - x_k^{-i}(t) \right)^T \left(x_k^{+j}(t) - x_k^{-j}(t) \right) \mathrm{d}t. \tag{8.5}$$

In this case, the initial condition of the system should be perturbed in all directions of the states. In the case of a network with a large number of nodes, we need to solve the nonlinear differential equation (8.4) $2N$ times. When the number of nodes is large, the computation of the empirical observability Gramian for all N nodes is computationally expensive. To detect an epidemic, we just need to know the state of a subset of nodes in the network, termed the *test set*. Here, we randomly select $s \leq N$ nodes, and perturb the initial condition in these s directions. Then the observability Gramian, W_O, is an $s \times s$ matrix.

The infection rate of node i, β_i, and the recovery rate of node i, δ_i, can be changed by allocating preventative resources such as vaccinations and antidotes on this node. As the value of either infection rate or recovery rate changes, the observability Gramian matrices should be updated accordingly.

The observability Gramian of a linear system, W,

$$\dot{\mathbf{x}} = A\mathbf{x} \quad \mathbf{y} = C\mathbf{x} \tag{8.6}$$

is obtained by solving for W in

$$A^T W + W A + C^T C = 0\,. \tag{8.7}$$

Therefore,

$$A^T \left(\frac{\partial W}{\partial \chi}\right) + \left(\frac{\partial W}{\partial \chi}\right) A + \left[\left(\frac{\partial A}{\partial \chi}\right)^T W + W \left(\frac{\partial A}{\partial \chi}\right)\right] = 0\,, \tag{8.8}$$

where χ is a variable of the dynamic system (A), and does not affect the observation (C). This equation can be solved to obtain $\left(\frac{\partial W}{\partial \chi}\right)$.

Theorem 15. *Consider the adjacency matrix, $\mathcal{A}$, of a connected graph, and two sets of positive numbers $\{\beta_i\}_{i=1}^N$ and $\{\delta_i\}_{i=1}^N$. Assume $\tilde{\mathbf{x}}$ represents the infected/healthy status of a network at an arbitrary time τ. Define $\tilde{\beta}_i = (1-\tilde{x}_i)\,\beta_i$ and $\tilde{B} = diag(\tilde{\beta}_i)$. Then the nonlinear system* (8.4) *for any $\mathbf{x}$ close to $\tilde{\mathbf{x}}$ can be approximated as $\dot{\mathbf{x}}(t) = \left(\tilde{B}\mathcal{A} - D\right)\mathbf{x}(t)$.*

Proof. Using the Tylor expansion of $f_i(\mathbf{x})$ in (8.3), the linear approximation in the vicinity of $\tilde{\mathbf{x}}$ is given by

$$\begin{aligned} f_i(\mathbf{x}) &= f_i(\tilde{\mathbf{x}}) + \sum_{j=1}^{N} \left.\frac{\partial f_i}{\partial x_j}\right|_{\tilde{\mathbf{x}}} (x_j - \tilde{x}_j) + \varsigma_i \\ &= \beta_i(1-\tilde{x}_i)\sum_{j=1}^{N} \mathcal{A}[i,j]x_j - \delta_i x_i + \varsigma_i \\ &= \tilde{\beta}_i \sum_{j=1}^{N} \mathcal{A}[i,j]x_j - \delta_i x_i + \varsigma_i\,, \end{aligned} \tag{8.9}$$

where

$$\begin{aligned} \varsigma_i &= \frac{-\beta_i}{2}\left(\mathbf{x}-\tilde{\mathbf{x}}\right)^T \mathbf{e}_i \mathbf{a}_i^T \left(\mathbf{x}-\tilde{\mathbf{x}}\right) \\ &= \frac{-\beta_i}{2}\left(x_i - \tilde{x}_i\right)\sum_{j=1}^{N} \mathcal{A}[i,j]\left(x_j - \tilde{x}_j\right)\,, \end{aligned} \tag{8.10}$$

where $\mathbf{a}_i = \mathcal{A}\mathbf{e}_i$. If $(\mathbf{x}-\tilde{\mathbf{x}}) \to \mathbf{0}$, then $\varsigma_i \to 0$, and the dynamic system can be written in matrix form as

$$\dot{\mathbf{x}}(t) \approx \left(\tilde{B}\mathcal{A} - D\right)\mathbf{x}(t)\,, \tag{8.11}$$

which proves the theorem. □

Theorem 16. *Consider the adjacency matrix, $\mathcal{A}$, of a connected graph, and two sets of positive numbers $\{\beta_i\}_{i=1}^N$ and $\{\delta_i\}_{i=1}^N$ such that $\lambda_1\left(B\mathcal{A}-D\right) \prec 0$. Define the approximation error of* (8.11)*, ς, as*

$$\varsigma = |\mathbf{f}(\mathbf{x}) - \left(\tilde{B}\mathcal{A}-D\right)\mathbf{x}(t)|_1 = |\begin{bmatrix}\varsigma_1\\ \vdots \\ \varsigma_N\end{bmatrix}|_1 . \tag{8.12}$$

Then, $\varsigma < \frac{1}{2} max\{\delta_i\}_{i=1}^N \|\tilde{\Delta}\|^2$, where $\tilde{\Delta} = \begin{bmatrix}|x_1-\tilde{x}_1|\\ \vdots \\ |x_N-\tilde{x}_N|\end{bmatrix}$.

Proof. Based on the definition of the approximation error, ς, we have

$$\begin{aligned}\varsigma = \sum_{i=1}^N |\varsigma_i| &\leq \frac{1}{2}\sum_{i=1}^N \beta_i\tilde{\Delta}_i \sum_{j=1}^N \mathcal{A}[i,j]\tilde{\Delta}_j = \frac{1}{2}\tilde{\Delta}^T B\mathcal{A}\tilde{\Delta} \\ &\leq \frac{1}{2}\lambda_1(B\mathcal{A})\|\tilde{\Delta}\|^2 .\end{aligned} \tag{8.13}$$

Recall that we assumed $\lambda_1\left(B\mathcal{A}-D\right) < 0$. Thus,

$$\lambda_1(B\mathcal{A}) < \max\{\delta_i\}_{i=1}^N . \tag{8.14}$$

Therefore $\varsigma < \frac{1}{2}\max\{\delta_i\}_{i=1}^N \|\tilde{\Delta}\|^2$.

□

Theorem 17. *Consider the adjacency matrix $\mathcal{A}$ of a connected graph, and two sets of positive numbers $\{\beta_i\}_{i=1}^N$ and $\{\delta_i\}_{i=1}^N$ such that $\lambda_1\left(B\mathcal{A}-D\right) < 0$. Then the linearized dynamic system $\dot{\mathbf{x}}(t) = \left(\tilde{B}\mathcal{A}-D\right)\mathbf{x}(t)$ is asymptotically stable.*

Proof. Using the definition of $\tilde{B} = \text{diag}\left((1-\tilde{x}_i)\,\beta_i\right)$, the dynamics of node i is given by

$$\dot{x}_i(t) = \beta_i \sum_{j=1}^N \mathcal{A}[i,j]x_j(t) - \delta_i x_i(t) - \beta_i\tilde{x}_i \sum_{j=1}^N \mathcal{A}[i,j]x_j(t) . \tag{8.15}$$

Since $\beta_i, \tilde{x}_i, x_j(t), \mathcal{A}[i,j] \geq 0$, then

$$\dot{x}_i(t) \leq \beta_i \sum_{j=1}^N \mathcal{A}[i,j]x_j(t) - \delta_i x_i(t) . \tag{8.16}$$

Since $\lambda_1 \left(B\mathcal{A} - D \right) < 0$, then the system

$$\dot{\hat{x}}_i(t) = \beta_i \sum_{j=1}^{N} \mathcal{A}[i,j]\hat{x}_j(t) - \delta_i \hat{x}_i(t) \tag{8.17}$$

is asymptotically stable. Given that $\dot{x}_i(t) \leq \dot{\hat{x}}_i(t)\,, \forall t$, we can conclude that the linearized dynamics system, $\dot{\mathbf{x}}(t) = \left(\tilde{B}\mathcal{A} - D \right) \mathbf{x}(t)$, should also be asymptotically stable. □

To study the effect of a change in infection and recovery rates of a node (i.e. , β_k or δ_k) on the observability Gramian, assume a change occurs at time $t = \tau$ where $\mathbf{x}(\tau) = \tilde{\mathbf{x}}$. Now, by using the result of Theorem 15, the dynamics of the system can be written as

$$\dot{\mathbf{x}}(t) \approx \left(\tilde{B}\mathcal{A} - D \right) \mathbf{x}(t) = \tilde{A}\mathbf{x}(t)\,. \tag{8.18}$$

Proposition 8. *Given a positive semi-definite matrix, W, and the adjacency matrix, $\mathcal{A}$, of a connected graph, then the Lyapunov equation*

$$\tilde{A}^T \left(\frac{\partial W}{\partial \chi} \right) + \left(\frac{\partial W}{\partial \chi} \right) \tilde{A} + \left[\left(\frac{\partial \tilde{A}}{\partial \chi} \right)^T W + W \left(\frac{\partial \tilde{A}}{\partial \chi} \right) \right] = 0\,, \tag{8.19}$$

where $\tilde{A}$ was defined in (8.18)*, has exactly one solution for* $\left(\frac{\partial W}{\partial \chi} \right)$.

Proof. The proof is directly derived from the result of Theorem 17, which demonstrates that $\tilde{A}$ is stable. Since $\tilde{A}$ is stable, we know that the Lyapunov operator defined by $\mathcal{L}(P) = \tilde{A}^T P + P\tilde{A}$ is non-singular and for a symmetric matrix matrix, Q, the equation $\mathcal{L}(P) + Q = 0$ has exactly one solution for P. Since $\left[\left(\frac{\partial \tilde{A}}{\partial \chi} \right)^T W + W \left(\frac{\partial \tilde{A}}{\partial \chi} \right) \right]$ is a symmetric matrix, thus the Lyapunov equation (8.19) has a unique solution for $\left(\frac{\partial W}{\partial \chi} \right)$. □

Now, assume $W_O(\beta^0, \delta^0)$ is the empirical observability Gramian obtained from (8.5) for the initial values of infection and recovery rates, $\{\beta_i^0\}_{i=1}^N$ and $\{\delta_i^0\}_{i=1}^N$ respectively. Considering $\tilde{A} = \left(\tilde{B}\mathcal{A} - D \right)$, then

$$\frac{\partial \tilde{A}}{\partial \beta_k} = (1 - \tilde{x}_k)\, \mathbf{e}_k \mathbf{e}_k^T \mathcal{A}\,, \tag{8.20}$$

and

$$\frac{\partial \tilde{A}}{\partial \delta_k} = -\mathbf{e}_k \mathbf{e}_k^T\,. \tag{8.21}$$

In the case of a change in the infection rate of node k (e.g. , because of vaccination of node k), such that $\beta_k = \beta_k^0 + \Delta\beta_k$, we do not need to re-calculate the empirical observability Gramian, W_O. The updated observability Gramian, $W_O(\beta_k)$, is given by

$$W_O(\beta_k) \approx W_O(\beta^0, \delta^0) + \left(\frac{\partial W_O}{\partial \beta_k}\right) \Delta\beta_k \,. \tag{8.22}$$

To compute $\left(\frac{\partial W_O}{\partial \beta_k}\right)$, we can substitute $\chi = \beta_k$ in (8.19) and use (8.20) to obtain the following Lyapunov equation

$$\begin{aligned} &\left(\mathcal{A}\tilde{B} - D\right)\left(\frac{\partial W_O}{\partial \beta_k}\right) + \left(\frac{\partial W_O}{\partial \beta_k}\right)\left(\tilde{B}\mathcal{A} - D\right) \\ &+ (1 - \tilde{x}_k)\left[\mathbf{a}_k \mathbf{e}_k^T W_O + W_O \mathbf{e}_k \mathbf{a}_k^T\right] = 0 \,. \end{aligned} \tag{8.23}$$

Similarly, if there is a change in the recovery rate of node k (e.g. , because of allocating antidotes on node k), such that $\delta_k = \delta_k^0 + \Delta\delta_k$, the updated observability Gramian, $W_O(\delta_k)$, is given by

$$W_O(\delta_k) \approx W_O(\beta^0, \delta^0) + \left(\frac{\partial W_O}{\partial \delta_k}\right) \Delta\delta_k \,. \tag{8.24}$$

In this case, to compute $\left(\frac{\partial W_O}{\partial \delta_k}\right)$, we can substitute $\chi = \delta_k$ in (8.19) and use (8.21) to obtain the following Lyapunov equation

$$\begin{aligned} &\left(\mathcal{A}\tilde{B} - D\right)\left(\frac{\partial W_O}{\partial \delta_k}\right) + \left(\frac{\partial W_O}{\partial \delta_k}\right)\left(\tilde{B}\mathcal{A} - D\right) \\ &- \left[\mathbf{e}_k \mathbf{e}_k^T W_O + W_O \mathbf{e}_k \mathbf{e}_k^T\right] = 0 \,. \end{aligned} \tag{8.25}$$

As was proposed in Proposition 8, there is exactly one solution of Lyapunov equations (8.23) and (8.25), which are used to obtain the updated observability Gramian matrix in the case of a change in the infection rates and recovery rates.

Here, simulation results are presented that demonstrate the effect of graph configurations and demonstrate the corresponding theoretical analysis presented in Section 6.2. It is worthy to note here that the value optimal function in (6.10) depends on the value of r. If r is small compared to N, the optimal solution of (6.10) is too large. If the optimal solution is large, we conclude that the determinant of the observability Gramian of the network with observing nodes obtained from the optimization problem is very small, which corresponds to a practically unobservable condition. Therefore, first we need to find the minimum number of observing nodes required for observability. Here, to find a minimum number of observing nodes, we set an upper-bound accepted value for the

cost function, such that the solution of (6.10) is acceptable only if the solution is less that the upper-bound accepted value. Here, the upper-bound accepted value is set to zero, which is equivalent to $\det(W_O) \geq 1$.

Consider a fairly small group of people having interaction with each other. This group is modelled by an undirected graph of 15 nodes (Fig. 8.1). The nodes in the graph could be students of a class in an elementary school, and the edges denote the friendship between the children in this class. This graph could also be cities in a specific region which are connected through air transportation.

The initial healthy/infected status of each node and the infection and recovery rates are chosen randomly. Here, the purpose is to find a small number of observing nodes, if possible, such that we obtain the health data of the entire group. We first try to find a single observing node to obtain the status of the entire network. In the first example (Fig. 8.1a), we have a dense structure. This structure is an example of a network with many interactions between them. By solving the optimization problem, one can find that by observing node 6, the network becomes observable. Now, consider a network with much less interaction between the nodes (Fig. 8.1b). The calculation shows that in this case we are not able to attain the state information of the entire network by observing only a single node. In the case of sparse structure with one observing node, the observability Gramian is close to be singular, $\det(W_O) \approx 0$. Therefore, the network is not observable. By increasing the number of observing nodes to $r = 2$, the solution of the optimization problem becomes feasible, and hence, the network becomes observable.

8.2 Genetic System Model

Focus of this section is on a network of Goodwin oscillators. Consider a network of N identical oscillators, which they are connected by diffusive coupling. Each oscillator of the network is a third order, dimensionless Goodwin oscillator model [48]. The equations of motion for the i^{th} oscillator are given as:

$$\begin{aligned} \dot{\mathbf{x}}_i &= \begin{bmatrix} -b_1 x_{i_1} + f(x_{i_3}) \\ -b_2 x_{i_2} + b_2 x_{i_1} + u_i \\ -b_3 x_{i_3} + b_3 x_{i_2} \end{bmatrix}, \\ f(x) &= \frac{1}{1+x^p}, \end{aligned} \tag{8.26}$$

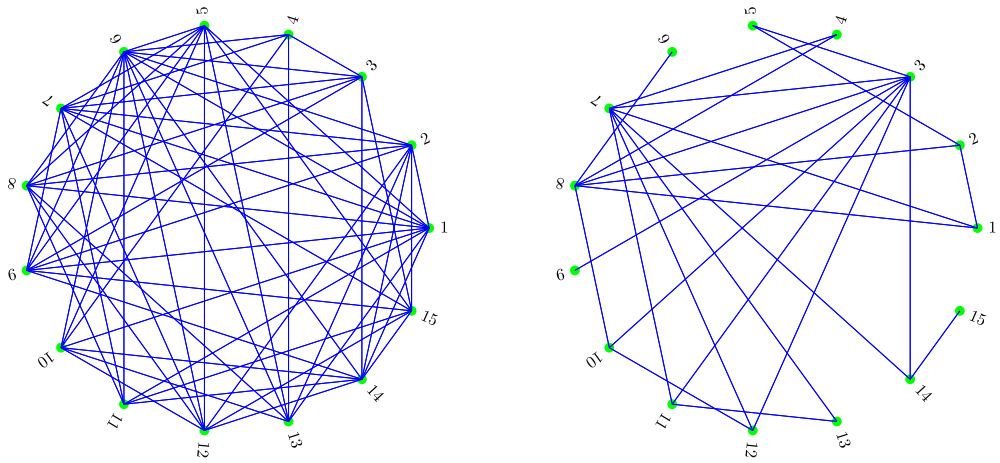

(a) dense graph

(b) sparse graph

Figure 8.1: Two different graph topologies of a network of 15 nodes: (a) dense and (b) sparse structures.

where, the diffusion term $u_i = \sum_{(i,j)\in E} w_{ij}\,(x_{j_2} - x_{i_2})$ is the control input. This interaction rule corresponds to the consensus protocol explained above. In (8.26), x_{i_1}, x_{i_2}, and x_{i_3} are concentrations of mRNA, protein, and end product, respectively. The variable p is called the cooperativity coefficient and governs the rate at which the end product (x_{i_3}) inhibits the formation of mRNA. To simplify the example, we shall assume that $b_1 = b_2 = b_3 = 1$. In this case, the dynamical system has a steady state at the point $x_1 = x_2 = x_3 = \zeta$, where ζ is the positive solution of $\dfrac{1}{1+\zeta^p} = \zeta$. It has been shown in [121] that this equilibrium is locally asymptotically stable if and only if $p(1-\zeta) < 8$. Taking $p = 3$, gives us the equilibrium point $x_1 = x_2 = x_3 = 0.7245$, which also satisfies the local asymptotic stability condition. Note that for computing the empirical observability Gramian, the perturbation of the states should be chosen such that the system stays in the region of attraction of this equilibrium point.

Since protein is usually diffusible and involved in inter-cellular signalling [116], in (8.26), the inter-cellular coupling is modelled by the diffusion of x_2. A schematic diagram in Fig. 8.2 shows the interconnection structure of an example of a network of three Goodwin oscillators. In this figure,

w_{ij} denotes the coupling strength between nodes i and j. If $w_{ij} = 0$, then there is no interaction between oscillators i and j. In the example shown in Fig. 8.2, $w_{12} = 0$, which means there is no interaction between nodes 1 and 2.

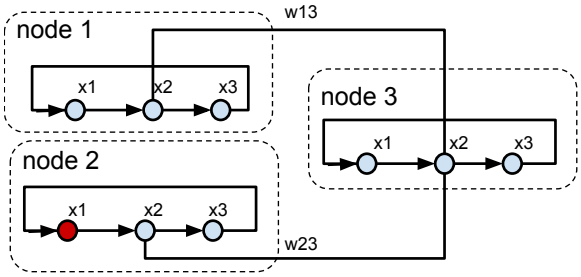

Figure 8.2: Structure of a network consists of three Goodwin oscillators. Each node is a nonlinear system with three states. The edge connecting two separate nodes in the figure shows the difussion of protein concentration (x_2) between those nodes. The red circle denotes the location of the measurment, which is state x_1 of node 2. The nodes composing in the network are assumed to be identical.

For convenience, define

$$X_i = \begin{bmatrix} x_{1_i} \\ x_{2_i} \\ \vdots \\ x_{N_i} \end{bmatrix}, \quad i = 1, 2, 3, \quad \mathbf{f}(X_3) = \begin{bmatrix} f(x_{1_3}) \\ f(x_{2_3}) \\ \vdots \\ f(x_{N_3}) \end{bmatrix}. \tag{8.27}$$

Then, (8.26) can be rewritten as

$$\begin{aligned} \dot{X} = \begin{bmatrix} \dot{X}_1 \\ \dot{X}_2 \\ \dot{X}_3 \end{bmatrix} &= \begin{bmatrix} -X_1 + \mathbf{f}(X_3) \\ -X_2 + X_1 - L(\mathbf{w})X_2 \\ -X_3 + X_2 \end{bmatrix}, \\ \mathbf{y} &= \begin{bmatrix} \beta_1 I_N^1 X_1 & \beta_2 I_N^2 X_1 & \cdots & \beta_N I_N^N X_1 \end{bmatrix}^T \end{aligned} \tag{8.28}$$

where, $L(\mathbf{w})$ is the Laplacian matrix of the graph of interaction between oscillators.

In order to demonstrate the effect of communication graph topology and number of observing nodes on the observability of network, in Table 8.1, the values of the cost function in (6.10), for

networks of five Goodwin oscillators in different graph formations are given. The cost is calculated for different numbers of observing nodes, r, in each configuration. In this example, all non-zero weights are set to one. As the number of communication edges between the nodes of the network decreases, or the network becomes sparser, the network becomes less observable and in fact practically unobservable. In these cases, we need to increase the number of measuring nodes to have an acceptable measure of observability. The last two configurations in Table 8.1, show that a network with fewer interactions between the nodes (sparser network) might have better performance than a denser network regarding the observability of the network, if the measuring nodes are chosen wisely.

In order to find a minimum number of observing nodes, we can set a minimum value for the cost function. For example, one can impose a condition on the solution of optimization problem such that $\det(W_O) \geq 1$, and increase the number of observing nodes to meet the condition. For the third configuration in Table 8.1 (ring configuration graph), we need at least three observing nodes to satisfy this condition, while for the first case (complete graph), one observing node would be sufficient for having an acceptable observability measure.

Configuration	Measure of Unobservability		
	$r = 1$	$r = 2$	$r = 3$
	-0.7	-11.1	-55.4
	5.0	-4.1	-38.6
	27.7	5.4	-32.4
	14.4	9.6	-15.8

Table 8.1: The values of observability-based cost function for different diffusive graph topologies for different values of measuring nodes.

Chapter 9

CONCLUSION AND FUTURE WORK

This dissertation began with obtaining sufficient conditions for observability, which is non-singularity of the observability matrix. After presenting some preliminaries related to the different methods of evaluating the observability of a linear and nonlinear systems in Chapter 2, a class of second-order nonlinear systems which are affine with respect to the controls was considered in Chapter 3. In this chapter the problem of constructing a control policy to guarantee observability of the system had been considered, and admissible controls in the sense of full states observability of the system were computed using three methods: non-zero determinant of $d\mathcal{O}'$, minimizing the condition number of $d\mathcal{O}'$ and generating an orthogonal $d\mathcal{O}'$ matrix.

Although the observability matrix is an effective tool for examining the observability of a system, it only provides a binary answer to the question of the system observability. An alternative tool that can be used to quantify the performance of the system in the sense of observability is the observability Gramian matrix. Different metrics of this positive definite matrix, such as minimum singular value, determinant, and trace have been used. However, the computation of the observability Gramian matrix for a nonlinear system is expensive, if possible. The empirical observability Gramian is not only computationally expensive to compute, but also difficult to evaluate for some real world systems, such as biological systems. Based on the current definition of the empirical observability Gramian, we need to perturb the initial condition in each direction of the state space, while the value of the initial condition in all other directions remain unchanged. In some cases, we are not able to change one state of a system independently from others. Furthermore, when we are dealing with a system with an unknown model, often a big pool of data is given to us and we do not have access to the response signal as a result of initial condition perturbations in all directions. The idea, here, is considering the initial condition as a random variable with covariance related to ϵ, which is the size of perturbation in the current definition of the empirical observability Gramian. Then, we can compute the observability Gramian based on the expected value of the output energy.

We believe that this new definition could be applied on many more real world problems, and also provides more information. For example, it could give us information on finding the samples which improve the accuracy of the computation of the observability Gramian matrix. Implementation of this idea is left for the future studies.

In Chapter 4 obtaining an optimal control of a nonlinear system in control-affine form based on the nonlinear observability criteria was considered. An algorithm to optimize a non-quadratic cost function was proposed which contained two parts: l_1 determined asymptotic behaviour of the system, and l_2 was a transient term. The cost function was a combination of quadratic and non-quadratic terms and came from our intent to maximize the observability of the nonlinear system. The transient term was responsible for maximizing a notion of observability. We introduced observability index, which gives an approximation of the trace of the empirical observability gramian for our nonlinear dynamics system. A gradient-based recursive algorithm was used to obtain an optimal controller. Similar to many nonlinear optimization problems, a big problem of this approach is that a global optimization is not generally guaranteed for nonlinear systems. In addition, stability of the system was investigated, and it was shown that under some conditions on the terminal cost, the stability of the closed loop system is guaranteed. Here, the controller was assumed to be linear state feedback, which is not necessarily the optimal control for all types of nonlinear systems. One approach toward this problem is relaxing the condition of control in linear form to a more general class of function. This results in solving the optimization problem for a higher number of parameters, and increases the computational price of the optimization problem. The next approach is solving the HJB equation for the specific class of cost functions given in Chapter 4. Even for this specific form, finding an analytical solution for the HJB equation is not feasible, and we need to solve the optimal control problem using a numerical method.

Furthermore, there are some restrictions for nonlinear systems to be stabilized by smooth feedback control [24, 25]. There are some nonlinear systems which are not stabilizable by time invariant state feedback control. For example, there are some restrictions on the existence of the time invariant smooth feedback controller for nonholonomic systems. Either discontinuous or time varying oscillatory control is a way to stabilize these kinds of nonlinear systems. In Chapter 5 time varying oscillatory feedback control was considered to increase the chance of stabilization for a larger group of nonlinear systems while improving the observability of the system. This chapter had been

concerned with the joint tasks of stabilizing a control-affine nonlinear system while enabling us to improve some other aspects of the system. A method was constructed by superimposing a transient time-varying oscillatory term on a stabilizing controller. Using a Lyapunov-based method, it was shown that the addition of this transient term does not affect the asymptotic stability of the classes of nonlinear systems being considered. Furthermore, these results were extended to application in a class of chained form nonholonomic systems.

An application of the results obtained in Chapters 3-5 was demonstrated in Chapter 7. In this chapter, the effect of control input on improving the observability was investigated for an example of robot navigation using optic flow sensory system. The controller is assumed to be state feedback. Inspired by the optic flow sensing used by insects, the main focus of this chapter was to study the navigation problem of an autonomous robot when no inertial measurements are available, and the robot is equipped with optic flow sensors. The observability properties of an autonomous robot using a small number of optic flow sensors were investigated. Specifically, two scenarios were considered: multiple fixed sensors and a single rotating sensor. The use of sinusoidal inputs superimposed over a nominal trajectory was shown to not only improve observability but to also allow some freedom in shaping a trajectory based on the presence of obstacles. By varying the amplitude, phase, and number of cycles of the input sinusoids, different trajectories can be generated. It is believed that flying insects use a very similar method to avoid obstacles and navigate through dense environments, without any need for direct distance calculation. A control policy was introduced in the case of a fixed sensor configuration as well as a rotating sensor configuration based on the weighting summation method. An Unscented Kalman Filter was used as an estimation tool to evaluate the performance of the estimator for the proposed control policy. The construction of feedback controls based on state estimation with the methods discussed here as well as construction of multi-sensor fusion (e.g. sensing from inertial as well as optic flow data) we leave for future work.

The next step of the dissertation was considering the observability of a network instead of the observability of a single agent. The observability of a network of agents was considered in Chapter 6. One of the main contributions of this chapter was an algorithm for obtaining the optimal node selection for maximizing an index of observability for a network of dynamical systems. The observability index was the determinant of the inverse of the observability Gramian. An optimization problem

was proposed for obtaining an optimal node selection that provides the full state observability of a network. The optimization problem was a mixed integer nonlinear programming problem. The outer approximation algorithm was used as a relaxation method for solving a convex optimization problem with integer non-convex constrains. The results of this chapter is applicable to similar problems, such as the problem of spreading of an idea or rumour through a social network like Twitter and the problem of spreading a computer virus through the World Wide Web. Initial results indicated that if the structure of interactions between nodes and the weights of interaction between nodes are known, then by directly observing a few number of nodes in a complex network, we are able to estimate the states of the entire nodes. However, the problem of state estimation with unknown interaction weights is still a challenging problem. This analysis is an important problem when we are dealing with complex real world situations with unknown interactions (for example trusting interaction between people in a group) or when we have control over changes in the weights.

The next problem considered in Chapter 6 was the privacy of a network. The privacy of network was posed as a convex optimization problem. An online learning algorithm was used to find an optimal set of weights that guarantee sub-linear regret. The main contribution of this part was presenting the problem of privacy maximization in a network as a regret minimization problem.

Two applications of the results obtained in Chapter 6 were presented in Chapter 8. The first application was on a model of Goodwin oscillators. The results showed that it is possible to reconstruct all states (diffusive and non-diffusive states) of the Goodwin oscillators by measuring the mRNA concentration of a limited number of nodes. The second application was on a model of virus spreading processes of a disease in an arbitrary network. The results showed that it is possible to reconstruct the state of all the nodes by observing a select number of nodes.

BIBLIOGRAPHY

[1] A. Levine and K. Narendra, "Control of nonlinear dynamical systems using neural networks, part II: Observability, identification, and control," *IEEE Trans. Neural Networks*, vol. 7, no. 1, pp. 30–42, 1996.

[2] P. Muller and H. Weber, "Analysis and optimization of certain qualities of controllability and observability for linear dynamical systems," *Automatica*, vol. 8, no. 3, pp. 237–246, 1972.

[3] J. Hedrick and A. Girard, "Lecture notes in control of nonlinear dynamic systems: Theory and applications," 2005.

[4] R. W. Brockett, "Nonlinear systems and differential geometry," *Proceedings of the IEEE*, vol. 64, no. 1, pp. 61–72, 1976.

[5] R. Hermann and A. J. Krener, "Nonlinear controllability and observability," *IEEE Transactions on Automatic Control*, vol. 22, no. 5, pp. 728–740, 1977.

[6] F. M. Mirzaei and S. I. Roumeliotis, "A Kalman filter-based algorithm for IMU-camera calibration: Observability analysis and performance evaluation," *IEEE Transactions on Robotics*, vol. 24, no. 5, pp. 1143–1156, 2008.

[7] A. K. Singh and J. Hahn, "Determining optimal sensor locations for state and parameter estimation for stable nonlinear systems," *Industrial & Engineering Chemistry Research*, vol. 44, no. 15, pp. 5645–5659, 2005.

[8] A. J. Krener and K. Ide, "Measures of unobservability," in *Proceedings of the 48th Conference on Decision and Control, held jointly with the 2009 28th Chinese Control Conference*, pp. 6401–6406, 2009.

[9] M. Serpas, G. Hackebeil, C. Laird, and J. Hahn, "Sensor location for nonlinear dynamic systems via observability analysis and max-det optimization," *Computers & Chemical Engineering*, vol. 48, pp. 105–112, 2013.

[10] C. De Persis and B. Jayawardhana, "On the internal model principle in the coordination of nonlinear systems," *IEEE Transactions on Control of Network Systems*, vol. 1, pp. 272–282, Sept 2014.

[11] A. Alaeddini and K. A. Morgansen, "Trajectory design for a nonlinear system to insure observability," in *European Control Conference*, pp. 2520–2525, IEEE, 2014.

[12] F. Lorussi, A. Marigo, and A. Bicchi, "Optimal exploratory paths for a mobile rover," in *International Conference on Robotics and Automation*, vol. 2, pp. 2078–2083, 2001.

[13] H. Yu, R. Sharma, R. W. Beard, and C. N. Taylor, "Observability-based local path planning and collision avoidance for micro air vehicles using bearing-only measurements," in *American Control Conference*, pp. 4649–4654, 2011.

[14] L. DeVries, S. J. Majumdar, and D. A. Paley, "Observability-based optimization of coordinated sampling trajectories for recursive estimation of a strong, spatially varying flowfield," *Journal of Intelligent & Robotic Systems*, vol. 70, no. 1-4, pp. 527–544, 2013.

[15] B. T. Hinson, M. K. Binder, and K. A. Morgansen, "Path planning to optimize observability in a planar uniform flow field," in *American Control Conference*, pp. 1392–1399, 2013.

[16] A. Alessandretti, A. P. Aguiar, and C. N. Jones, "Optimization based control for target estimation and tracking via highly observable trajectories," in *Proceedings of the 11th Portuguese Conference on Automatic Control*, pp. 495–504, 2015.

[17] F. A. Fontes, "A general framework to design stabilizing nonlinear model predictive controllers," *Systems & Control Letters*, vol. 42, no. 2, pp. 127–143, 2001.

[18] A. Narang-Siddarth and J. Valasek, "A constructive stabilization approach for open-loop unstable non-affine systems," in *American Control Conference*, pp. 5685–5689, June 2013.

[19] T. Çimen and S. P. Banks, "Global optimal feedback control for general nonlinear systems with nonquadratic performance criteria," *Systems & Control Letters*, vol. 53, no. 5, pp. 327–346, 2004.

[20] J.-M. Coron and J.-B. Pomet, "A remark on the design of time-varying stabilizing feedback laws for controllable systems without drift," in *IFAC Symposia Series*, pp. 397–397, 1993.

[21] J.-B. Pomet, "Explicit design of time-varying stabilizing control laws for a class of controllable systems without drift," *Systems & control letters*, vol. 18, no. 2, pp. 147–158, 1992.

[22] R. Brockett, "Asymptotic stability and feedback stabilization," *Differential Geometric Control Theory*, pp. 181–208, 1983.

[23] R. M. Murray and S. S. Sastry, "Nonholonomic motion planning: Steering using sinusoids," *IEEE Transactions on Automatic Control*, vol. 38, no. 5, pp. 700–716, 1993.

[24] W. Lin, "Feedback stabilization of general nonlinear control system: A passive system approach," *Systems & Control Letters*, vol. 25, pp. 41–52, 1995.

[25] V. N. Phat, "Global stabilization for linear continuous time-varying systems," *Applied Mathematics and Computation*, vol. 175, no. 2, pp. 1730–1743, 2006.

[26] S. Pequito, F. Rego, S. Kar, A. P. Aguiar, A. Pascoal, and C. Jones, "Optimal design of observable multi-agent networks: A structural system approach," in *European Control Conference*, pp. 1536–1541, 2014.

[27] A. Y. Kibangou and C. Commault, "Observability in connected strongly regular graphs and distance regular graphs," *IEEE Transactions on Control of Network Systems*, vol. 1, no. 4, pp. 360–369, 2014.

[28] S. S. Kia, J. Cortés, and S. Martinez, "Dynamic average consensus under limited control authority and privacy requirements," *International Journal of Robust and Nonlinear Control*, vol. 25, no. 13, pp. 1941–1966, 2015.

[29] A. Alaeddini and K. A. Morgansen, "Optimal disease outbreak in a community," in *American Control Conference*, 2016.

[30] G. L. Mariottini, G. Pappas, D. Prattichizzo, and K. Daniilidis, "Vision-based localization of leader-follower formations," in *44th IEEE Conference on Decision and Control, European Control Conference*, pp. 635–640, IEEE, 2005.

[31] X. S. Zhou and S. I. Roumeliotis, "Robot-to-robot relative pose estimation from range measurements," *IEEE Transactions on Robotics*, vol. 24, no. 6, pp. 1379–1393, 2008.

[32] G. P. Huang, N. Trawny, A. I. Mourikis, and S. I. Roumeliotis, "Observability-based consistent ekf estimators for multi-robot cooperative localization," *Autonomous Robots*, vol. 30, no. 1, pp. 99–122, 2011.

[33] R. Sharma, R. W. Beard, C. N. Taylor, and S. Quebe, "Graph-based observability analysis of bearing-only cooperative localization," *IEEE Transactions on Robotics*, vol. 28, no. 2, pp. 522–529, 2012.

[34] D. Golovin and A. Krause, "Adaptive submodularity: Theory and applications in active learning and stochastic optimization," *Journal of Artificial Intelligence Research*, pp. 427–486, 2011.

[35] F. Wu, "Real-time network security monitoring, assessment and optimization," *International Journal of Electrical Power & Energy Systems*, vol. 10, no. 2, pp. 83–100, 1988.

[36] W. Kang and L. Xu, "Computational analysis of control systems using dynamic optimization," *arXiv preprint arXiv:0906.0215*, 2009.

[37] O.-T. Chis, J. R. Banga, and E. Balsa-Canto, "Structural identifiability of systems biology models: a critical comparison of methods," *PloS one*, vol. 6, no. 11, p. e27755, 2011.

[38] A. J. Whalen, S. N. Brennan, T. D. Sauer, and S. J. Schiff, "Observability of neuronal network motifs," in *46th Annual Conference on Information Sciences and Systems (CISS)*, pp. 1–5, IEEE, 2012.

[39] M. Kefayati, M. S. Talebi, B. H. Khalaj, and H. R. Rabiee, "Secure consensus averaging in sensor networks using random offsets," in *IEEE International Conference on Telecommunications and Malaysia International Conference on Communications*, pp. 556–560, IEEE, 2007.

[40] Z. Huang, S. Mitra, and G. Dullerud, "Differentially private iterative synchronous consensus," in *Proceedings of the 2012 ACM workshop on Privacy in the electronic society*, pp. 81–90, ACM, 2012.

[41] N. E. Manitara and C. N. Hadjicostis, "Privacy-preserving asymptotic average consensus," in *European Control Conference (ECC)*, pp. 760–765, IEEE, 2013.

[42] J. Giraldo, A. Cárdenas, E. Mojica-Nava, N. Quijano, and R. Dong, "Delay and sampling independence of a consensus algorithm and its application to smart grid privacy," in *IEEE 53rd Annual Conference on Decision and Control*, pp. 1389–1394, 2014.

[43] S. Pequito, S. Kar, S. Sundaram, and A. P. Aguiar, "Design of communication networks for distributed computation with privacy guarantees," in *Proceedings of the 53th IEEE Conference on Decision and Control*, pp. 1370–1376, 2014.

[44] F. Yan, S. Sundaram, S. Vishwanathan, and Y. Qi, "Distributed autonomous online learning: Regrets and intrinsic privacy-preserving properties," *IEEE Transactions on Knowledge and Data Engineering*, vol. 25, no. 11, pp. 2483–2493, 2013.

[45] N. R. Sandell Jr, P. Varaiya, M. Athans, and M. G. Safonov, "Survey of decentralized control methods for large scale systems," *IEEE Transactions on Automatic Control*, vol. 23, no. 2, pp. 108–128, 1978.

[46] M. Ji and M. Egerstedt, "Observability and estimation in distributed sensor networks," in *46th IEEE conference on decision and control*, pp. 4221–4226, 2007.

[47] V. M. Preciado, M. Zargham, C. Enyioha, A. Jadbabaie, and G. J. Pappas, "Optimal resource allocation for network protection against spreading processes," *IEEE Transactions on Control of Network Systems*, vol. 1, no. 1, pp. 99–108, 2014.

[48] B. C. Goodwin, "Oscillatory behavior in enzymatic control processes," *Advances in enzyme regulation*, vol. 3, pp. 425–437, 1965.

[49] H. Nijmeijer and A. Van der Schaft, *Nonlinear dynamical control systems*. Springer, 1990.

[50] C.-T. Chen, *Linear system theory and design*. Oxford University Press, Inc., 1995.

[51] H. Nijmeijer, "Observability of autonomous discrete time non-linear systems: a geometric approach," *International Journal of Control*, vol. 36, no. 5, pp. 867–874, 1982.

[52] Y. Wang and E. D. Sontag, "On two definitions of observation spaces," *Systems & Control letters*, vol. 13, no. 4, pp. 279–289, 1989.

[53] M. R. James, "Controllability and observability of nonlinear systems.," tech. rep., Mathematics Department and Systems Research Center, University of Maryland, 1987.

[54] U. Vaidya, "Observability Gramian for nonlinear systems," in *Proceedings of the 46th IEEE Conference on Decision and Control*, pp. 3357–3362, 2007.

[55] D. Simon, *Optimal state estimation: Kalman, H_∞, and nonlinear approaches*. John Wiley & Sons, 2006.

[56] J. M. Scherpen, "Balancing for nonlinear systems," *Systems & Control Letters*, vol. 21, no. 2, pp. 143–153, 1993.

[57] C. Rowley, "Model reduction for fluids, using balanced proper orthogonal decomposition," *International Journal of Bifurcation and Chaos*, vol. 15, no. 03, pp. 997–1013, 2005.

[58] S. Lall, J. E. Marsden, and S. Glavaški, "A subspace approach to balanced truncation for model reduction of nonlinear control systems," *International journal of robust and nonlinear control*, vol. 12, no. 6, pp. 519–535, 2002.

[59] R. M. Murray and S. S. Sastry, "Steering nonholonomic systems using sinusoids," in *Proceedings of the 29th IEEE Conference on Decision and Control*, pp. 2097–2101, 1990.

[60] B. Wittenmark, "Adaptive dual control methods: An overview," in *IFAC Symposium on Adaptive System in Control and Signal Processing*, pp. 67–72, 1995.

[61] J. P. Gauthier and G. Bornard, "Observability for any u(t) of a class of nonlinear systems," *IEEE Transactions on Automatic Control*, vol. 26, no. 4, pp. 922–926, 1981.

[62] A. Alaeddini and K. A. Morgansen, "Autonomous state estimation using optic flow sensing," in *American Control Conference*, pp. 585–590, 2013.

[63] A. Isidori, *Nonlinear control systems*, vol. 1. Springer, 1995.

[64] H. J. Sussmann and W. Liu, "Limits of highly oscillatory controls and the approximation of general paths by admissible trajectories," in *Proceedings of the 30th IEEE Conference on Decision and Control*, pp. 437–442, 1991.

[65] E. Sontag and H. Sussmann, "Remarks on continuous feedback," in *Proceedings of the 19th IEEE Conference on Decision and Control including the Symposium on Adaptive Processes*, vol. 19, pp. 916–921, 1980.

[66] E. D. Sontag and Y. Wang, "I/O equations for nonlinear systems and observation spaces," in *Proceedings of the 30th IEEE Conference on Decision and Control*, pp. 720–725, 1991.

[67] M. Anguelova, *Nonlinear Observability and identifiability: General Theory and a Case Study of a Kinetic Model for S. cerevisiae*. PhD thesis, Chalmers University of Technology, April 2004.

[68] N. Barth, "The Gramian and k-volume in n-space: Some classical results in linear algebra," *Journal of Young Investigators*, vol. 2, 1999.

[69] S. Boyd and L. Vandenberghe, *Convex optimization*. Cambridge university press, 2004.

[70] B. T. Hinson and K. A. Morgansen, "Observability optimization for the nonholonomic integrator," in *American Control Conference*, pp. 4257–4262, 2013.

[71] S. Beeler, H. Tran, and H. Banks, "Feedback control methodologies for nonlinear systems," *Journal of Optimization Theory and Applications*, vol. 107, no. 1, pp. 1–33, 2000.

[72] Y. Chen, T. Edgar, and V. Manousiouthakis, "On infinite-time nonlinear quadratic optimal control," in *Proceedings of the 42nd IEEE Conference on Decision and Control*, vol. 1, pp. 221–226 Vol.1, Dec 2003.

[73] P. Esfahani, F. Farokhi, and M. Karimi-Ghartemani, "Optimal state-feedback design for nonlinear feedback-linearisable systems," *Control Theory & Applications, IET*, vol. 5, no. 2, pp. 323–333, 2011.

[74] W. Kang and L. Xu, "A quantitative measure of observability and controllability," in *Proceedings of the 48th IEEE Conference on Decision and Control, held jointly with the 2009 28th Chinese Control Conference.*, pp. 6413–6418, 2009.

[75] D. Aeyels, R. Sepulchre, and J. Peuteman, "Asymptotic stability for time-variant systems and observability: uniform and nonuniform criteria," *Mathematics of Control, Signals and Systems*, vol. 11, no. 1, pp. 1–27, 1998.

[76] R. Tedrake, "Underactuated robotics: Algorithms for walking, running, swimming, flying, and manipulation (course notes for mit 6.832)," *Downloaded in Fall*, 2014.

[77] S. Wright and J. Nocedal, *Numerical optimization*, vol. 2. Springer New York, 1999.

[78] A. Alessandretti, A. P. Aguiar, and C. N. Jones, "A model predictive control scheme with additional performance index for transient behavior," in *Proceedings of the 52nd Conference on Decision and Control*, pp. 5090–5095, 2013.

[79] R. Tedrake, I. R. Manchester, M. Tobenkin, and J. W. Roberts, "Lqr-trees: Feedback motion planning via sums-of-squares verification," *The International Journal of Robotics Research*, 2010.

[80] J. D. Quenzer and K. A. Morgansen, "Observability based control in range-only underwater vehicle localization," in *American Control Conference*, pp. 4702–4707, 2014.

[81] P. Baccou and B. Jouvencel, "Homing and navigation using one transponder for auv, post-processing comparisons results with long base-line navigation," in *International Conference on Robotics and Automation*, vol. 4, pp. 4004–4009, 2002.

[82] M. B. Larsen, "Synthetic long baseline navigation of underwater vehicles," in *OCEANS 2000 MTS/IEEE Conference and Exhibition*, vol. 3, pp. 2043–2050, 2000.

[83] S. Hammel and V. Aidala, "Observability requirements for three-dimensional tracking via angle measurements," *IEEE Transactions on Aerospace Electronic Systems*, vol. 21, pp. 200–207, 1985.

[84] I. Kolmanovsky and N. H. McClamroch, "Developments in nonholonomic control problems," *Control Systems, IEEE*, vol. 15, no. 6, pp. 20–36, 1995.

[85] A. R. Teel, R. M. Murray, and G. Walsh, "Nonholonomic control systems: From steering to stabilization with sinusoids," in *Proceedings of the 31st IEEE Conference on Decision and Control*, pp. 1603–1609, 1992.

[86] H. K. Khalil and J. Grizzle, *Nonlinear systems*, vol. 3. Prentice hall Upper Saddle River, 2002.

[87] J. Godhavn and O. Egeland, "A lyapunov approach to exponential stabilization of nonholonomic systems in power form," *Transactions on Automatic Control*, vol. 42, no. 7, pp. 1028–1032, 1997.

[88] R. Sharma, "Observability based control for cooperative localization," in *International Conference on Unmanned Aircraft Systems*, pp. 134–139, 2014.

[89] V. Srivastava and N. E. Leonard, "Collective decision-making in ideal networks: The speed-accuracy tradeoff," *IEEE Transactions on Control of Network Systems*, vol. 1, no. 1, pp. 121–132, 2014.

[90] W. Xia, M. Cao, and K. Johansson, "Structural balance and opinion separation in trust-mistrust social networks," *IEEE Transactions on Control of Network Systems*, 2015.

[91] K. Manandhar, X. Cao, F. Hu, and Y. Liu, "Detection of faults and attacks including false data injection attack in smart grid using kalman filter," *IEEE Transactions on Control of Network Systems*, vol. 1, no. 4, pp. 370–379, 2014.

[92] R. Olfati-Saber, A. Fax, and R. M. Murray, "Consensus and cooperation in networked multi-agent systems," *Proceedings of the IEEE*, vol. 95, no. 1, pp. 215–233, 2007.

[93] E. Hazan, A. Agarwal, and S. Kale, "Logarithmic regret algorithms for online convex optimization," *Machine Learning*, vol. 69, no. 2-3, pp. 169–192, 2007.

[94] A. V. Wouwer, N. Point, S. Porteman, and M. Remy, "An approach to the selection of optimal sensor locations in distributed parameter systems," *Journal of process control*, vol. 10, no. 4, pp. 291–300, 2000.

[95] P. Bonami, L. T. Biegler, A. R. Conn, G. Cornuéjols, I. E. Grossmann, C. D. Laird, J. Lee, A. Lodi, F. Margot, N. Sawaya, *et al.*, "An algorithmic framework for convex mixed integer nonlinear programs," *Discrete Optimization*, vol. 5, no. 2, pp. 186–204, 2008.

[96] A. Chapman, E. Schoof, and M. Mesbahi, "Distributed online topology design for network-level disturbance rejection," in *52nd Annual Conference on Decision and Control*, pp. 817–822, IEEE, 2013.

[97] A. Beyeler, J.-C. Zufferey, and D. Floreano, "Vision-based control of near-obstacle flight," *Autonomous robots*, vol. 27, no. 3, pp. 201–219, 2009.

[98] J.-C. Zufferey, *Bio-inspired vision-based flying robots*. PhD thesis, EPFL, 2005.

[99] F. Ruffier and N. Franceschini, "Optic flow regulation: the key to aircraft automatic guidance," *Robotics and Autonomous Systems*, vol. 50, no. 4, pp. 177 – 194, 2005. Biomimetic Robotics {ISR} Biomimetic Robotics.

[100] J. Humbert, R. Murray, and M. Dickinson, "A control-oriented analysis of bio-inspired visuomotor convergence," in *Proceedings of the 44th IEEE Conference on Decision and Control, and European Control Conference*, pp. 245–250, Dec 2005.

[101] A. M. Hyslop and J. S. Humbert, "Autonomous navigation in three-dimensional urban environments using wide-field integration of optic flow," *Journal of guidance, control, and dynamics*, vol. 33, no. 1, pp. 147–159, 2010.

[102] J. Conroy, G. Gremillion, B. Ranganathan, and J. S. Humbert, "Implementation of wide-field integration of optic flow for autonomous quadrotor navigation," *Autonomous Robots*, vol. 27, pp. 189–198, 2009.

[103] J. S. Humbert, A. Hyslop, and M. Chinn, "Experimental validation of wide-field integration methods for autonomous navigation," in *IEEE/RSJ International Conference on Intelligent Robots and Systems*, pp. 2144–2149, 2007.

[104] M. Verveld, Q.-P. Chu, C. Wagter, and J. Mulder, "Optic flow based state estimation for an indoor micro air vehicle," in *AIAA Guidance, Navigation and Control Conference, Toronto, Canada*, 2010.

[105] T. P. Webb, R. J. Prazenica, A. J. Kurdila, and R. Lind, "Vision-based state estimation for autonomous micro air vehicles," *Journal of guidance, control, and dynamics*, vol. 30, no. 3, pp. 816–826, 2007.

[106] A. A. Argyros, D. P. Tsakiris, and C. Groyer, "Biomimetic centering behavior [mobile robots with panoramic sensors]," *Robotics & Automation Magazine, IEEE*, vol. 11, no. 4, pp. 21–30, 2004.

[107] S. Zingg, D. Scaramuzza, S. Weiss, and R. Siegwart, "Mav navigation through indoor corridors using optical flow," in *International Conference on Robotics and Automation*, pp. 3361–3368, 2010.

[108] A. Hyslop, H. G. Krapp, and J. S. Humbert, "Control theoretic interpretation of directional motion preferences in optic flow processing interneurons," *Biological cybernetics*, vol. 103, no. 5, pp. 353–364, 2010.

[109] S. Fuller and R. Murray, "A hovercraft robot that uses insect-inspired visual autocorrelation for motion control in a corridor," in *IEEE International Conference on Robotics and Biomimetics*, pp. 1474–1481, Dec 2011.

[110] S. Kluge, K. Reif, and M. Brokate, "Stochastic stability of the extended kalman filter with intermittent observations," *IEEE Transactions on Automatic Control*, vol. 55, no. 2, pp. 514–518, 2010.

[111] X. Liu and A. Goldsmith, "Kalman filtering with partial observation losses," in *Proceedings of the 43rd IEEE Conference on Decision and Control*, vol. 4, pp. 4180–4186, 2004.

[112] B. Sinopoli, L. Schenato, M. Franceschetti, K. Poolla, M. I. Jordan, and S. S. Sastry, "Kalman filtering with intermittent observations," *IEEE Transactions on Automatic Control*, vol. 49, no. 9, pp. 1453–1464, 2004.

[113] A. Alaeddini and K. Morgansen, "Bioinspired navigation for a nonholonomic mobile robot," *Journal of Aerospace Information Systems*, pp. 1–11, 2015.

[114] Y. Ma, J. Kosecka, and S. S. Sastry, "Vision guided navigation for a nonholonomic mobile robot," *IEEE Transactions on Robotics and Automation*, vol. 15, no. 3, pp. 521–536, 1999.

[115] R. Aguilar-López, M. I. Neria-González, R. Martínez-Guerra, and J. L. Mata-Machuca, "Nonlinear estimation in a class of gene transcription process," *Applied Mathematics and Computation*, vol. 226, pp. 131–144, 2014.

[116] Y. Wang, Y. Hori, S. Hara, and F. Doyle, "The collective oscillation period of inter-coupled goodwin oscillators," in *51st Annual Conference on Decision and Control (CDC)*, pp. 1627–1632, Dec 2012.

[117] H. Bai and S. Y. Shafi, "Output synchronization of nonlinear systems under input disturbances," in *21st International Symposium on Mathematical Theory of Networks and Systems*, pp. 506–512, July 2014.

[118] P. Van Mieghem and J. Omic, "In-homogeneous virus spread in networks," *arXiv preprint arXiv:1306.2588*, 2013.

[119] R. M. Anderson, R. M. May, and B. Anderson, *Infectious diseases of humans: dynamics and control*, vol. 28. Wiley Online Library, 1992.

[120] V. M. Preciado, M. Zargham, C. Enyioha, A. Jadbabaie, and G. Pappas, "Optimal vaccine allocation to control epidemic outbreaks in arbitrary networks," in *IEEE 52nd Annual Conference on Decision and Control*, pp. 7486–7491, 2013.

[121] G.-B. Stan, A. Hamadeh, R. Sepulchre, and J. Gonçalves, "Output synchronization in networks of cyclic biochemical oscillators," in *American Control Conference*, pp. 3973–3978, 2007.

[122] H. K. Mathews and L. C. Kammer, "Reliability-driven sensor selection via observability indices," in *American Control Conference*, pp. 3715–3720, 2007.

[123] K. Schittkowski, "On the convergence of a sequential quadratic programming method with an augmented lagrangian line search function 2," *Optimization*, vol. 14, no. 2, pp. 197–216, 1983.

[124] J. Hahn and T. F. Edgar, "An improved method for nonlinear model reduction using balancing of empirical gramians," *Computers & chemical engineering*, vol. 26, no. 10, pp. 1379–1397, 2002.